A HISTOPATHOLOGICAL STUDY ON SELECTED BACTERIAL VASCULAR DISEASES WITH EMPHASIS ON ULTRASTRUCTURE

by

FREDERICK MICHAEL WALLIS
M.Sc. Agric. (Natal)

Submitted in partial fulfilment of the requirements
for the Degree of

Doctor of Philosophy

in the

Department of Plant Pathology and Microbiology
Faculty of Agriculture
University of Natal
Pietermaritzburg

December, 1975

DECLARATION

I HEREBY CERTIFY THAT THIS RESEARCH IS THE RESULT OF MY OWN INVESTIGATION.

F.M. Wallis

F.M. WALLIS

CONTENTS

ACKNOWLEDGEMENTS

I wish to express my sincere thanks to Professor Susarah J. Truter, Head of the Department of Plant Pathology and Microbiology, for her continued interest and encouragement during this investigation and for her critical appraisal of the draft manuscript.

I also wish to record my gratitude to many other staff members of the University of Natal, in particular the following:
Mr M.M. Martin, Dr J.J. Joubert, Professor M.A. Loos and particularly Dr F.H.J. Rijkenberg, for providing a critical dialogue from which many useful suggestions and valuable ideas arose.
Miss I.F. Schlösser for her technical assistance.
Mrs M.G. Gilliland and others at the electron microscope unit for often making the facilities available to me after normal shut-down time.

I gratefully acknowledge the advice and help received from Mr J. Schoonraad, Department of Agricultural Technical Services, in the reproduction of the Plates.
Mrs B. de Smidt is thanked for typing the draft manuscript.

Finally, I would like to express my deepest gratitude to my parents and especially to my wife, Pat and son, Christopher, for their many self-sacrifices, constant encouragement, and understanding throughout the course of this investigation.

CHAPTER 1

ULTRASTRUCTURAL HISTOPATHOLOGY OF CABBAGE LEAVES INFECTED WITH *XANTHOMONAS CAMPESTRIS* *)

INTRODUCTION

Although electron microscopic techniques have been used to study host-parasite relationships in some bacterial diseases of plants (27, 30, 75) the author is unaware of any report, other than the preliminary work of Buddenhagen and Takata (11), on the ultrastructure of host-parasite interactions involving vascular bacterial pathogens. At the light microscope level black rot disease of cabbage and other cruciferous plants, caused by the vascular bacterial parasite *Xanthomonas campestris* (Pammel) Dows., has been extensively investigated (14, 22, 77, 97, 105, 112, 113, 120). It was generally thought that the characteristic vessel plugging associated with this disease is due primarily to masses of bacterial cells, their extracellular polysaccharides, and wound gums and tyloses formed by the host in response to infection. The results of an *in vitro* investigation (121) indicated that bacterial extracellular polysaccharides constitute the major plugging material.

The present study reports the results of an ultrastructural examination of black rot infected cabbage leaves and attempts to elucidate the origin and nature of the plugging materials.

---

*) An article based on part of this chapter has appeared in *Physiological Plant Pathology* 3, 371 - 378.

MATERIALS AND METHODS

Cabbage (*Brassica oleracea* var. *capitata* L. "Surehead") and cauliflower (*B. oleracea* var. *botrytis* L. "Southern Cross") seedlings were grown in the greenhouse and inoculated with *X. campestris* when the first leaves were approximately 3 cm across. Eleven isolates of the pathogen, obtained from naturally infected cabbage and cauliflower plants growing in various parts of Natal, were used as inoculum. All the cultures were isolated and maintained on YDC medium (16).

Cultures were grown for 24 h at 28 °C and then stored at 4 °C until required. Regular microscopic examination of Gram-stained preparations was conducted to check the purity of the cultures. When inoculum was required, subcultures were grown on YDC for 24 h at 28 °C, the cells harvested, suspended in sterile distilled water and centrifuged at 6000 g for 10 min. The pellets were washed twice, resuspended in sterile distilled water and the suspension adjusted photometrically to 10^6 cells/ml.

Two methods of inoculation were tested. In the first, 0,1-ml aliquots of bacterial suspension were introduced into guttation drops at the margins of young cabbage seedling leaves. The second method entailed applying the inoculum to wounds made in pre-selected tertiary veins of cabbage leaves surface-sterilized with a 1:10 sodium hypochlorite solution. Wounding was effected by drawing a burred dissecting needle across the veins in such a way that only slight damage to the tissue occurred. As controls, cabbage seedlings of comparable size were similarly inoculated with sterile distilled water. After inoculation seedlings were kept for 2 h at 100% RH and then for 8 h at approximately 75% RH. The seedlings were then transferred to the greenhouse and grown under continuous supplementary light (2500 to 2900 lx) at 25 $\pm$ 2 °C.

When vein blackening, the first visible symptom of disease, was observed, the infected and control leaves were removed and placed in 6% glutaraldehyde. Veinlet pieces approximately 0,5 cm in length were then excised from blackened and from control veinlets with the point of inoculation occupying a central position. Subsequently each was cut through the point of inoculation into two approximately equal portions in order to investigate bacterial spread along the vein in both directions.

These pieces were vacuum infiltrated with 6% glutaraldehyde in 0,05 M-sodium cacodylate, pH 7,2-7,4, for 6 h at 22 °C. After three 30-min washes in 0,05 M-sodium cacodylate buffer the material was postfixed for 4 h in 2% osmium tetroxide in 0,05 M-sodium cacodylate. Following two 30-min washes in 0,05 M-sodium cacodylate buffer the tissue was dehydrated in a cold ethanol series, passed through epoxypropane and embedded in Ladd's Araldite. Longitudinal and transverse sections were cut with glass knives on a Porter-Blum MT-1 ultramicrotome, stained with uranyl acetate (50 min) and Reynolds' (95) lead citrate (15 to 20 min) and examined in a Hitachi HU-11E electron microscope. Unless otherwise stated this procedure was followed in all subsequent preparations for electron microscopy.

Since the presence of bacterial extracellular slime, and released vessel-wall components or their breakdown products, could be anticipated in infected xylem vessels, these substances were examined in the electron microscope. Three methods were used to investigate the ultrastructure of bacterial extracellular material:-

(i) Cultures of <u>X. campestris</u> were grown on YDC + ½% glucose for 36 h at 28 °C, harvested, suspended in sterile distilled water, centrifuged at 42 500 g for 1 h and the resultant pellet prepared for electron microscopy.

(ii) 75-guttation fluid from young cabbage plants was placed in a 200 ml Erlenmeyer flask and inoculated with 5-ml of a light suspension of 18 h YDC-grown X. campestris cells in guttation fluid. The culture was shaker incubated at 28 °C at 250 rev/min. A sample was removed each day over a period of 15 days and its draining time measured in an Ostwald viscometer. A 20% sucrose solution was used for comparison. All measurements were made at 25 °C. The viscosity of the inoculated guttation fluid at the times of sampling was calculated by means of the relationship : $\eta_1 = \frac{t_1 \times \eta_2}{t_2}$, where η_1 is the viscosity of the culture medium; t_1 the mean draining time for 5 replicate runs of the bacterial suspension; t_2 the mean draining time for 5 replicate runs of the sucrose solution; and η_2 the known viscosity (1, 7040 centipoise) of a 20% sucrose solution at 25 °C. After the 5 replicate draining times were measured for each sample it was stored at 4 °C. Subsequently the sample with the highest viscosity was centrifuged at 60 000 g in a Beckman Model L2-65B ultracentrifuge. The supernatant was carefully decanted and the pellet prepared for electron microscopy. The supernatant was then centrifuged at 100 000 g and the small pellet obtained prepared for electron microscopy.

(iii) Drops of natural guttation fluid lightly inoculated with X. campestris, in a manner similar to that described under (ii) above, were placed on 3 collodion-coated specimen grids and incubated at 28 °C for 24, 48 and 96 h respectively. Thereafter the excess fluid was drawn off, the grids negatively stained with 2% uranyl acetate for 2 min, washed gently, and allowed to dry. The dry grids were examined in the electron microscope.

The cell wall components investigated were lignin, pectin, and delignified holocellulose, all isolated from leaf-veins of healthy cabbage plants comparable in size and grown under conditions identical to those infected with X. campestris. To retain, as far as possible, the natural state of these substances no attempt was made to isolate them in pure form. Lignin was prepared from tertiary leaf veins by extraction with cold 72% H_2SO_4 followed by repeated washing with sterile distilled water. The pectinic and cellulosic fractions were prepared according to the method used by Jermyn and Isherwood (55).

To investigate the possible contribution of vessel wall breakdown products to vessel plugging, the lignic, pectinic and cellulosic materials were suspended separately in filter-sterilized guttation fluid. In addition commercial carboxymethyl cellulose (CMC) [Type 7HOF, obtained from Hercules Inc., Wilmington, Delaware], was similarly suspended. Drops of these suspensions were placed separately on each of 3 collodion-coated specimen grids and inoculated with a light suspension of YDC-grown X. campestris cells in guttation fluid. A single grid of each substance was placed in each of 3 sterile moistened Petri dishes which were then incubated at 28 °C for 24, 48 and 96 h respectively. After incubation the grids were prepared for electron microscopy as described under (iii) above.

RESULTS

Hydathode inoculations were not successful and lesion development did not occur unless the leaves were wounded during the inoculation procedure. Direct veinlet inoculations were generally effective and resulted in the typical disease symptoms of vein blackening, followed by a progressive chlorosis and desiccation of interveinal areas delimited by the blackened veins. None of the isolates of X. campestris tested produced any cytological differences

in host response following inoculation. Since cabbage and cauliflower were so similar in their response to infection only cabbage seedlings were used in the ultrastructural investigation.

The bacteria spread in both directions through the xylem vessels from the point of inoculation. During the initial stages of infection the pathogen is confined to the xylem vessels [Plates 1(a) and 2]. The bacteria are unevenly distributed among the vessels and also within individual vessels, and are generally orientated with their long axes parallel to the long axes of the vessels [Plate 1(a)]. Bacteria aggregate in the interspiral regions where they possibly multiply, and it is in these areas that the first indications of vessel wall degradation appear [Plates 1(a), 1(b) and 3]. Eventually complete dissolution of primary wall material is effected between adjacent vessels and bacteria pass through the resultant openings [Plates 1(a) and 1(b)].

In the outermost vessels of the bundle, adjacent to the surrounding parenchyma, the bacteria also aggregate between the spiral thickenings (Plate 2). In these vessels primary wall breakdown appears to be initially restricted. However, continued aggregation of bacteria, and associated partial wall dissolution, eventually causes the weakened wall to protrude into the lumen of the adjoining parenchyma cell. Where it bounds these protrusions the wall is considerably thinner than where it subtends the spiral attachment.

The cytoplasmic contents of parenchyma cells adjacent to infected vessels degenerate; the protoplasm becomes electron-opaque and withdraws from the cell wall [Plates 1(a) and 2]. The cause of this condition was not established; it is, however, certainly due to infection and does not result from any preparative procedure, since it was not observed in healthy material (Plates 4 and 5).

Within invaded vessels electron-opaque granules, of various shapes

and sizes, are embedded in a fibrillar substance (Plates 3 and 6). An interesting, and possibly significant, observation is that larger amounts of what appears to be capsular material surrounds those bacteria in close proximity to the vessel walls than surrounds those occupying a more central position in the lumina of the vessels. This phenomenon is particularly evident in vessels adjoining parenchyma cells (Plate 2).

Constitutive enzymes, that hydrolyze the primary walls of tracheary elements but appear to have little effect on lignified secondary walls, have been reported in healthy oat coleoptiles (85). In the present study a similar phenomenon was observed in the xylem vessels of healthy cabbage seedling leaves (Plates 4 and 5). Enzyme activity on the primary wall is restricted or retarded at the point of spiral attachment and the lignified spiral remains attached, even when an advanced stage of interspiral primary wall breakdown is reached (Plates 4 and 5). This indicates possible structural or compositional specialization of the primary wall at the point of attachment. There is almost complete dissolution of primary walls between some contiguous vessels (Plate 4) but where a vessel element and parenchyma cell abut breakdown is limited to the vessel wall (Plates 4 and 5).

By contrast X. campestris-infected vessels, in addition to showing natural wall dissolution also show, at an early stage, breakdown of the electron-transparent primary wall layer where spiral thickening and primary wall connect (Plates 3 and 6). This is probably due to a combination of bacterial enzyme action and mechanical pressure, exerted by the increasing mass of bacterial cells, in the spaces between spiral attachments and eventually results in separation of the spiral thickening from the primary wall (Plate 6). Observations based on many hundreds of sections indicate that vessel walls in healthy

tertiary veinlets, in spite of extensive dissolution due to natural hydrolysis, retain their contours with little indication of rupturing (Plates 4 and 5). On the other hand the primary walls of vessels undergoing bacterial enzymolysis, although retaining initially a certain degree of structural integrity, eventually show severe disruption (Plates 3 and 6). Separation of the spiral thickening and primary wall in infected vessels is accompanied by a "shredding" of the exposed layers of the primary wall with resultant release of fibrillar material, into the lumina of the vessels (Plates 3 and 6). This substance, which is seen stretched between the separating spiral and primary wall in Plate 6, has a beaded fine structure (Plate 6, inset). Shredding or loosening of primary wall material occurs also in the interspiral regions, resulting in swelling and release of additional masses of fibrillar material (Plates 3 and 6). Similar fibrils are seen surrounding the bacteria within the lumina of invaded xylem vessels (Plate 2, inset, and Plate 3). The density of this material is positively correlated with the concentration of bacteria in the vessels [Plate 1(a)].

As the bacteria spread and multiply in the xylem elements a substance with a reticulate structure accumulates and eventually partially or completely occludes the vessels [Plates 7(a), 7(b), 8 and 9]. Surprisingly it is those vessels in which the parasite is not seen that are completely plugged [Plates 7(a) and 9], whereas those containing bacteria are only partly occluded [Plates 7(a) and 8].

Neither the bacterial extracellular material produced on YDC medium [Method (i)] nor the cellular and extracellular fractions isolated from natural guttation fluid [Method (ii)] at the time of maximum viscosity (Plates 10 and 11), showed any ultrastructural resemblance to either type of plugging material observed in the xylem vessels of infected cabbage leaves [Plates 12(a) and 12(b)].

Likewise the bacterial extracellular material observed in natural guttation fluid incubated on grids Method (iii) /Plate 12(c)/ showed no ultrastructural similarity to either type of vessel plugging material /Plates 12(a) and 12(b)/.

Interesting results were obtained in the experiments conducted with amended guttation fluid. The lignin-amended guttation fluid contained small amounts of material /Plate 12(d) - arrows/ which in structure very closely resembles the beaded fibrillar plugging material /Plate 12(a) - arrows/. The pectin appears to have gelled to some extent /Plate 12(e)/ but nevertheless shows some ultrastructural similarity to the plugging material seen in Plate 12(b), insofar as both display a reticulate-type structure. This structural feature was also observed in the CMC-amended guttation fluid /Plate 12(f)/; however, the reticulations were not as well defined.

Many very thin thread-like structures /Plate 12(g) - arrows/, interspersed with aggregations of some unidentified amorphous material /Plate 12(g) - double-headed arrows/, were observed in the inoculated cellulose-amended guttation fluid following bacterial growth. These threads are much finer than the individual threads that constitute the beaded fibrillar material seen in plugged vessels /Plate 12(a)/ but their dimensions correspond to some of the thread-like structures observed in the reticulate-type plugging material /Plate 12(b) - arrows/.

DISCUSSION

The observed bidirectional spread of X. campestris cells in the xylem vessels from the point of inoculation and their initial restriction to the xylem elements are typical of many diseases caused by vascular bacterial pathogens (83), and has previously been reported in the black rot disease of crucifers (77, 105, 120). Likewise the observed dissolution of primary wall material between spiral

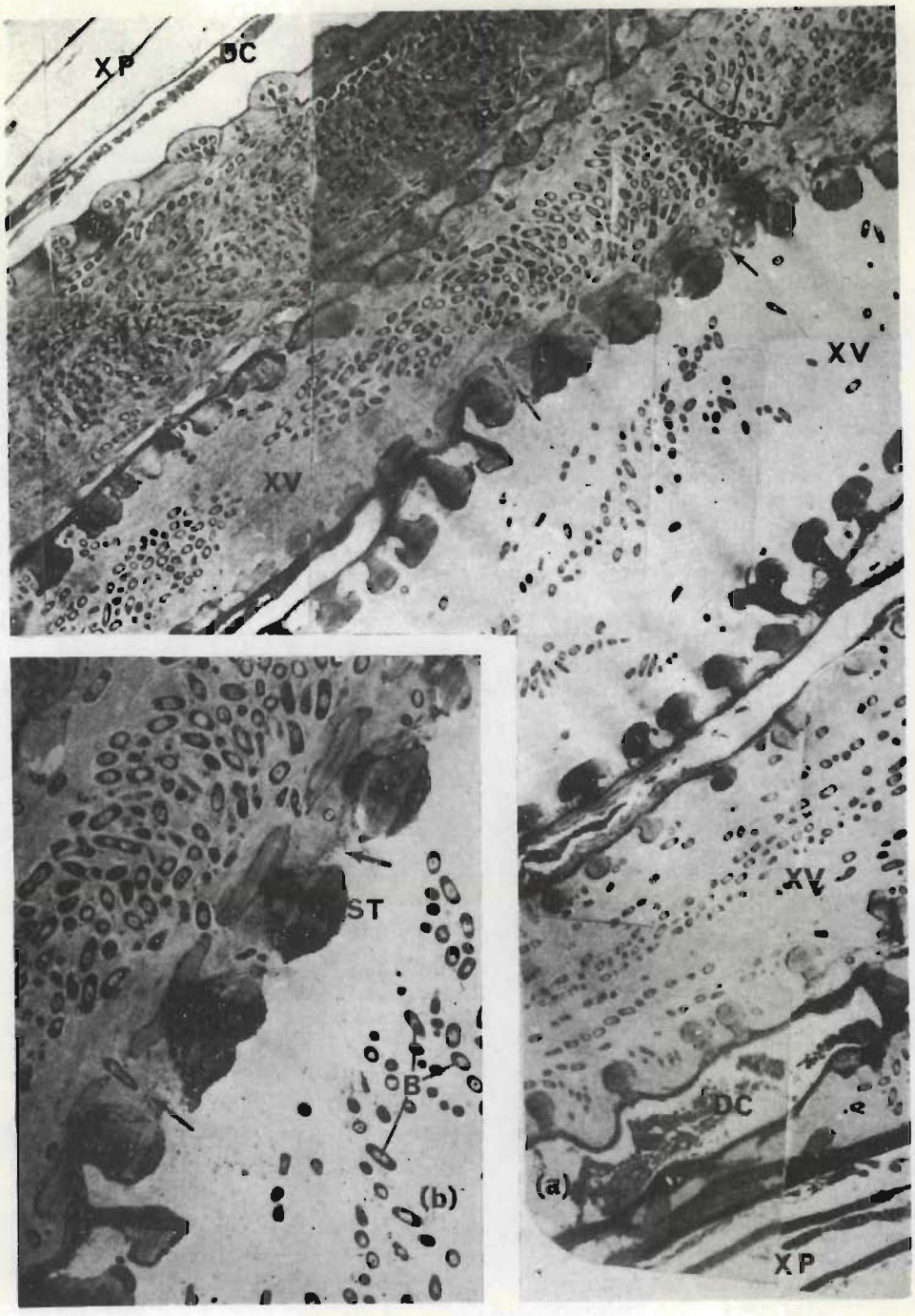

PLATE 1. (a) Montage of longitudinal section through infected vascular bundle showing uneven distribution of bacteria (B) within and between vessels, XV. Note bacteria-free xylem parenchyma (XP) containing degenerating cytoplasm, DC. (× 2650.) (b) Detail of area in (a) showing spiral thickenings, ST; degraded primary wall and bacterial passage between contiguous vessels (arrows). (× 6000.)

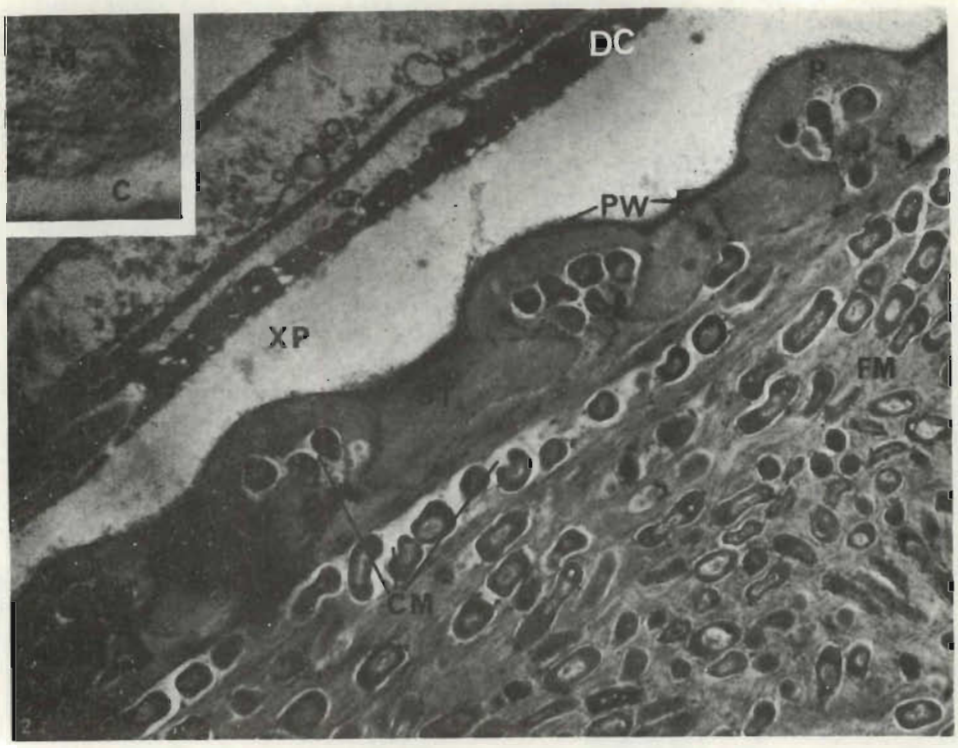

PLATE 2. Bacteria aggregating in interspiral regions in outer vessel of bundle. Primary wall (PW) breakdown is restricted and protuberances (P) form between the spiral thickenings (ST) and bulge into xylem parenchyma cell (XP) which contains disrupted cytoplasm, DC. Large amounts of capsular material (CM) surround bacteria in close proximity to the vessel wall. Note fibrillar material (FM) amongst bacteria. (×8400.) Inset. Part of bacterial capsule (C) and detail of fibrillar material (FM) showing beaded fine structure. (×183 000.)

PLATE 3. Electron-opaque granules (arrows) embedded in a matrix of released fibrillar material (FM) both arising from bacterial action on the primary wall (PW) which has begun to swell and shred (broken arrow). The middle lamella (ML) is discontinuous. (×20 500.)

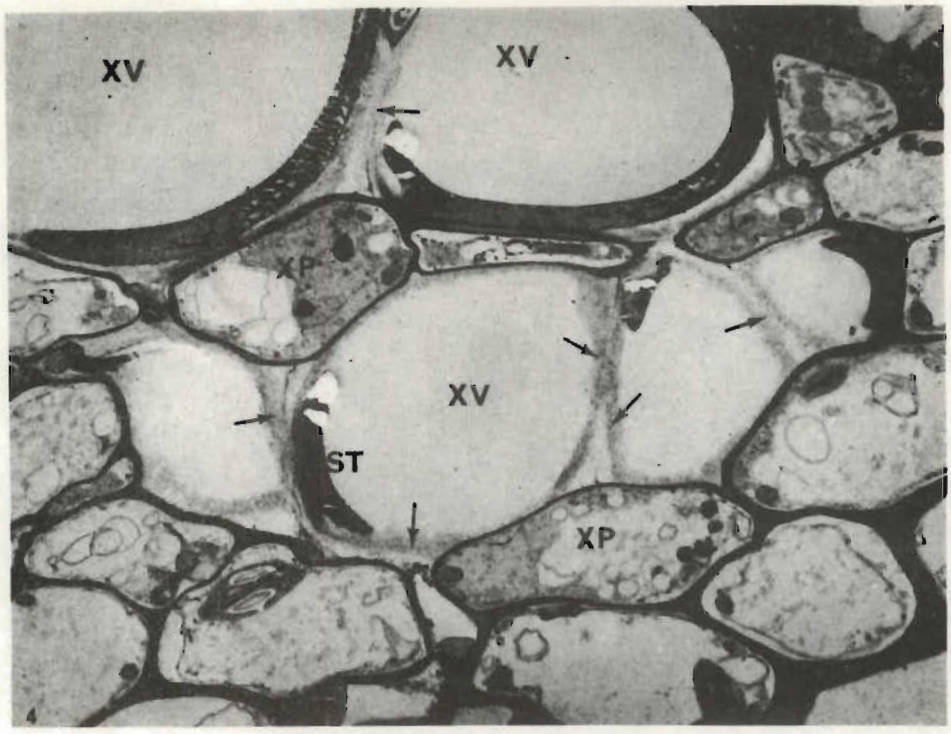

PLATE 4. Healthy tissue showing natural hydrolysis (arrows) of primary wall of vessels, XV. Surrounding xylem parenchyma (XP) appear normal. (× 5000.)

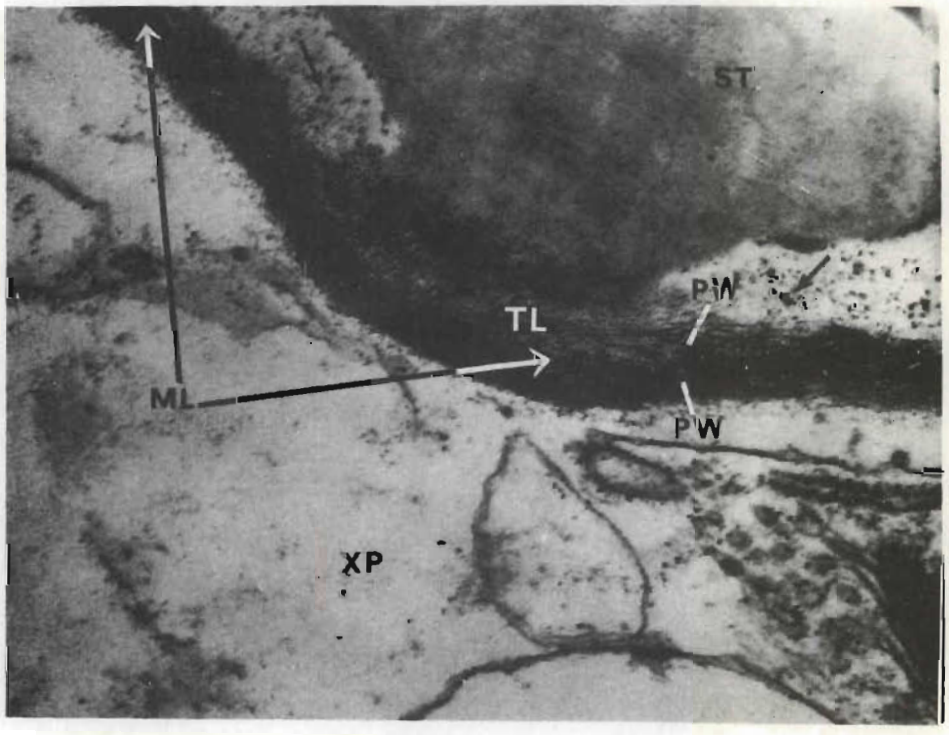

PLATE 5. Healthy tissue showing electron-opaque granules (arrows) arising from natural enzyme action on the primary wall (PW). At point where spiral thickening (ST) and primary wall attach (TL) the vessel primary wall is not degraded. On parenchyma side of middle lamella (ML) the primary wall remains intact. (× 58 500.)

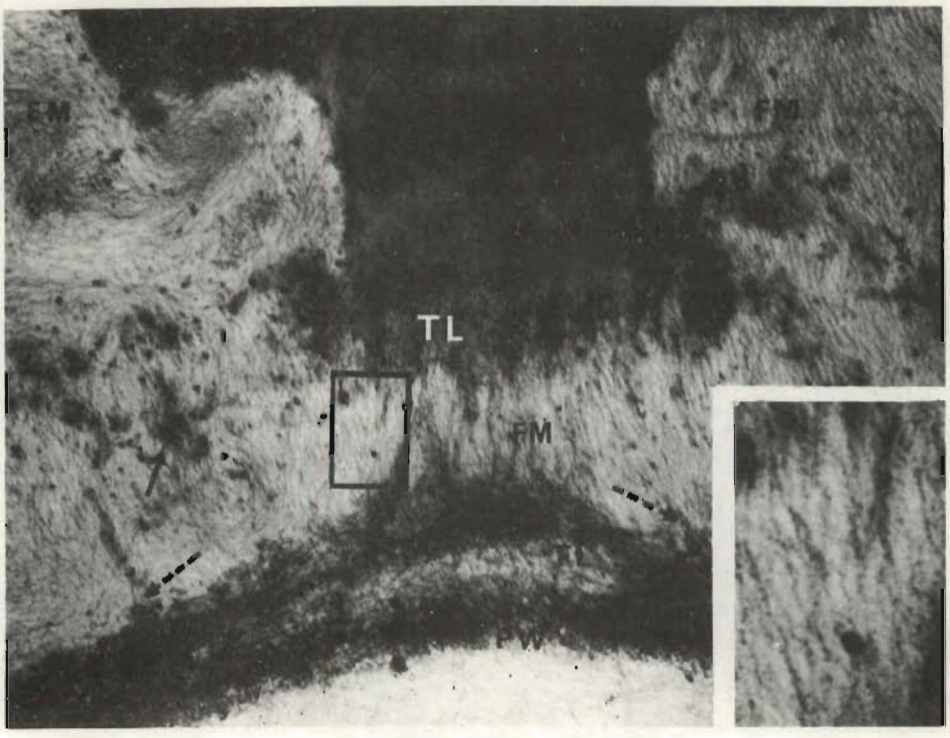

PLATE 6. Late stage in separation of primary wall and spiral thickening (ST) in infected tissue. Note degradation of primary wall at point of attachment (TL) and shredding of exposed primary wall layers (broken arrows) with concomitant release of masses of fibrillar material (FM) and granules (arrows). (× 60 000.) Inset. Detail of boxed area showing granules and beaded fine structure of fibrillar material (× 185 000.)

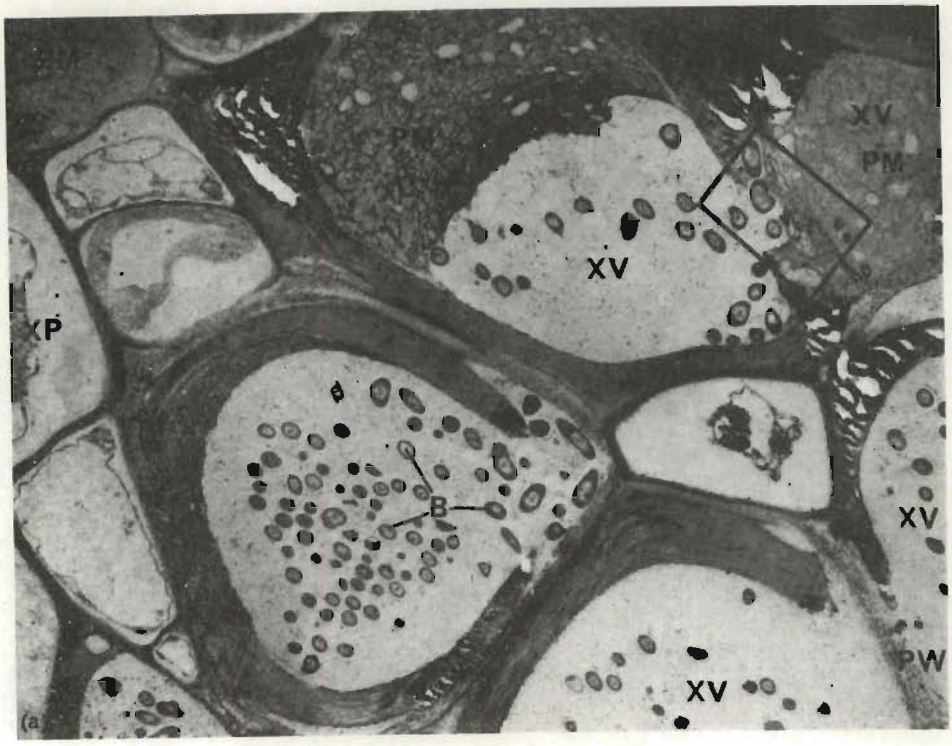

PLATE 7. (a) Infected tissue showing bacteria-containing and apparently bacteria-free vessels completely or partially occluded with reticulate plugging material (PM). Primary wall (PW) degradation and disruption of cytoplasm have occurred in vessels and xylem parenchyma (XP) respectively. (×5000.) (b) Detail of boxed area indicated in Plate 7(a) showing advanced stage of primary wall (PW) dissolution. Note presence of granules (arrows) and continuity between plugging material (PM) and primary wall (PW) residue. (×35 000.)

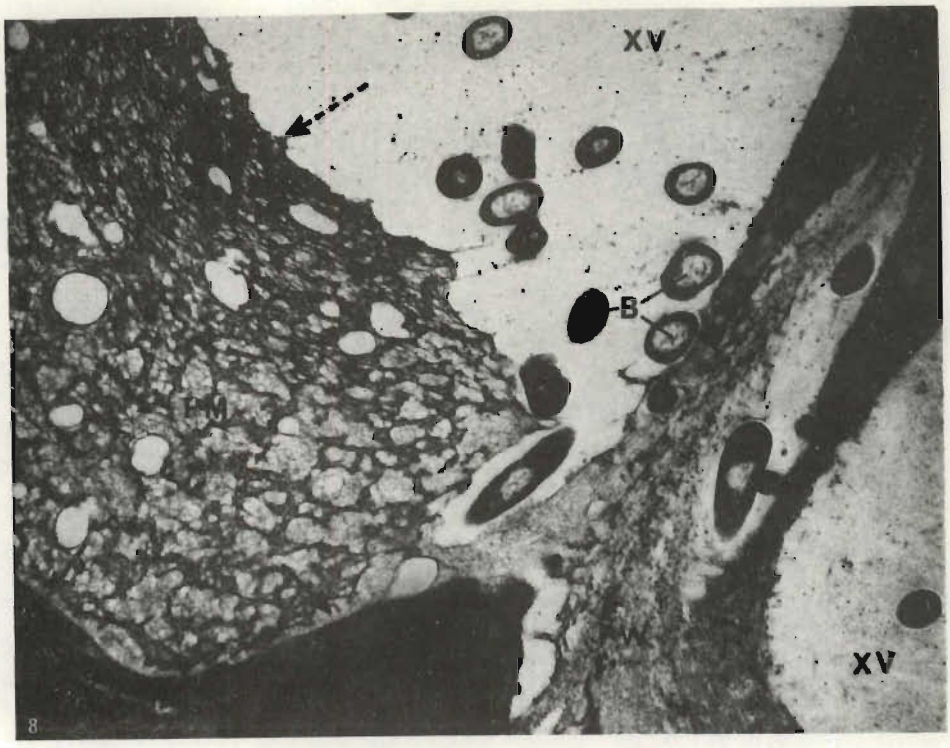

PLATE 8. Plugging material (PM) in invaded vessel. Bacterial action on the electron-transparent layer of this material (solid arrows) causes detachment of plug from vessel wall with resultant contraction (broken arrow) of the plugging material. Primary wall has begun to disintegrate. (× 16 800.)

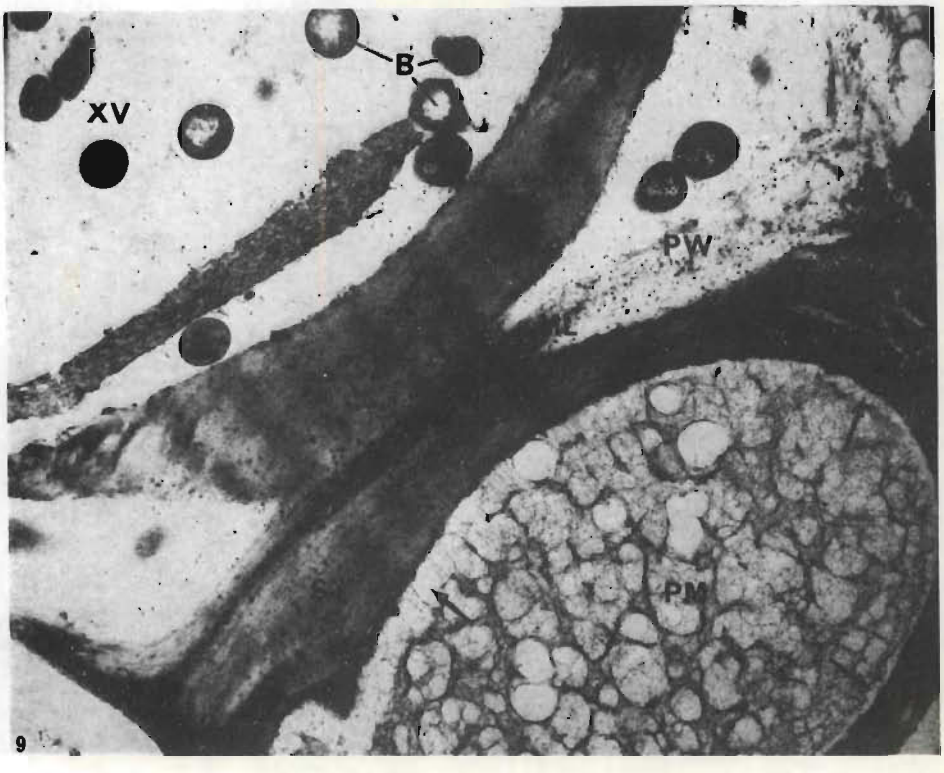

PLATE 9. Plugging material (PM) with electron-transparent outer layer (arrows) intact, completely occluding a bacterium-free vessel. Degradation of middle lamella (ML), and primary wall (PW) of the contiguous vessel is well advanced. (× 15 250.)

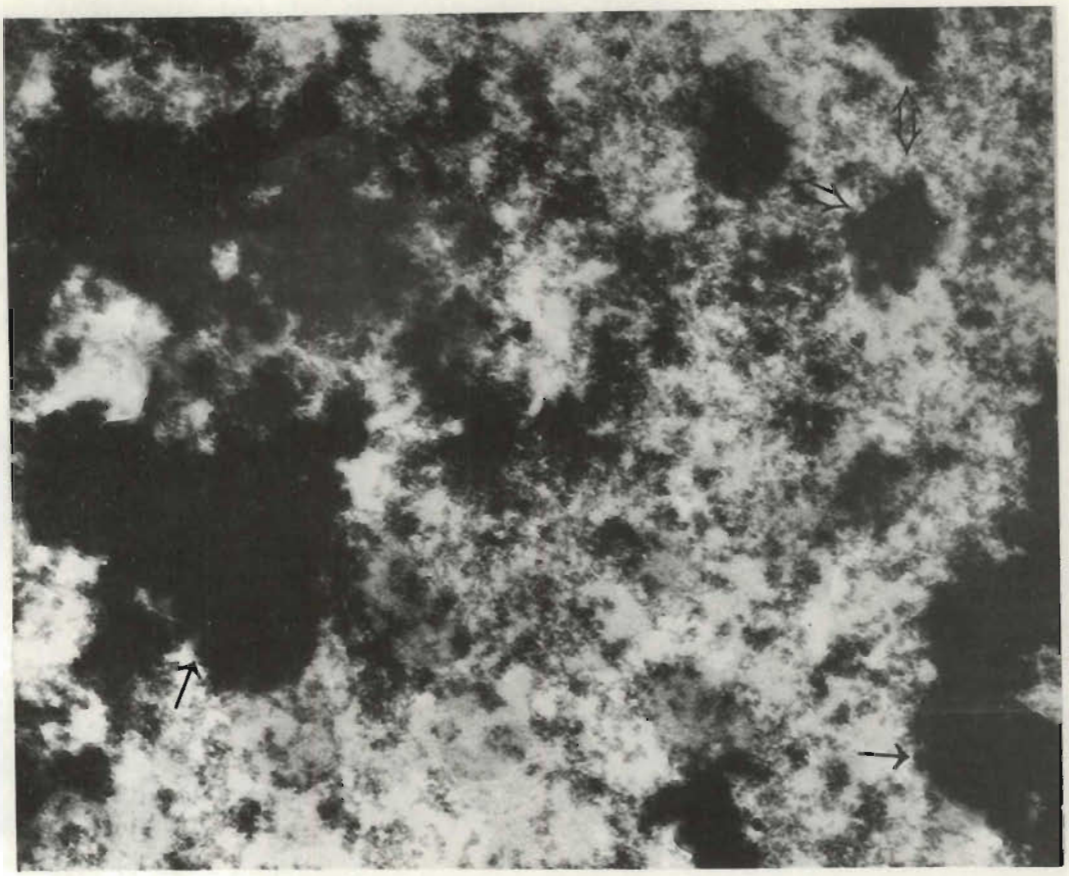

PLATE 10. Negatively stained whole bacterial cells (arrows), large cell fragments (double arrows) and extracellular material obtained from X. campestris-inoculated guttation fluid by ultracentrifugation at 60 000 g (x 62 500.)

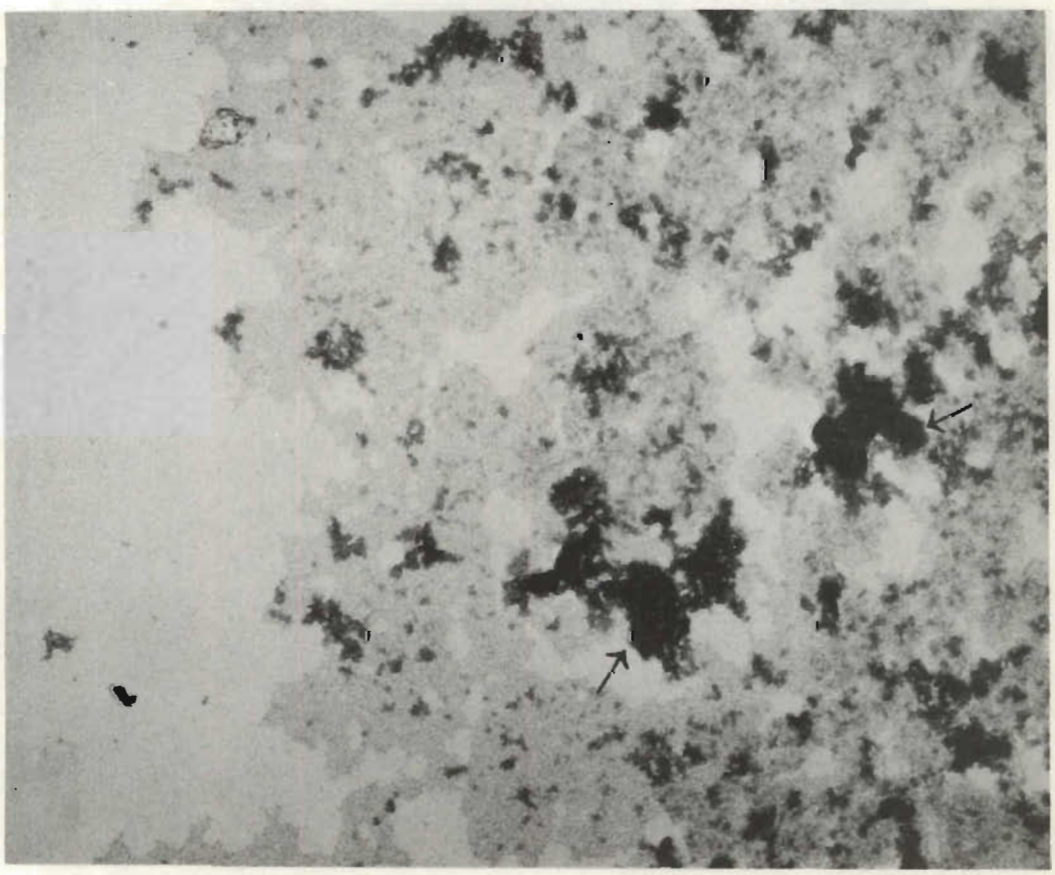

PLATE 11. Negatively stained small cell fragments (arrows) and bacterial cellular and extracellular material fractionated from X. campestris-inoculated guttation fluid by ultracentrifugation at 100 000 g (x 163 200.)

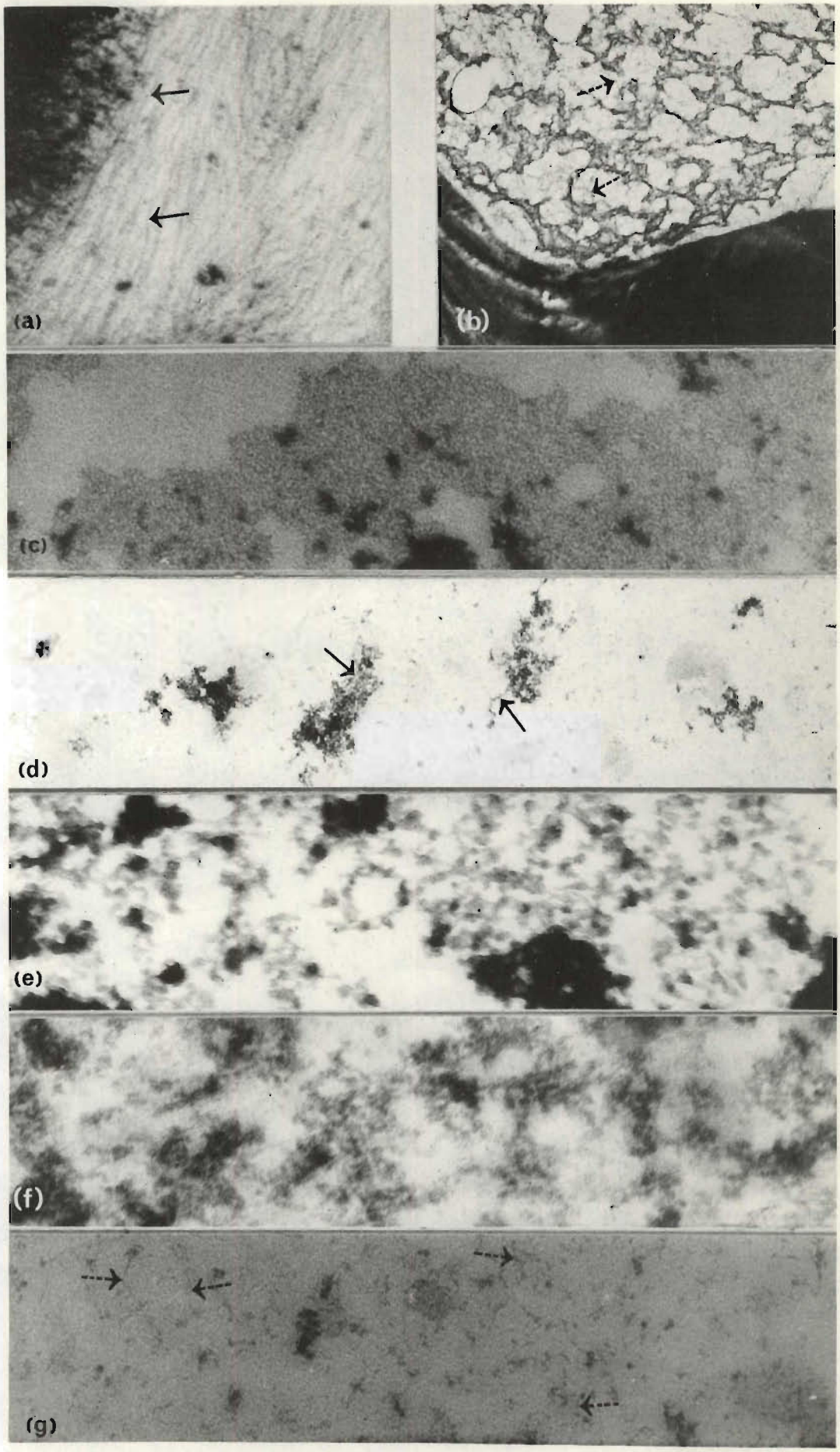

PLATE 12. Comparison of beaded fibrillar (a) (x 148 500) and reticulate (b) (x 24 600) plugging material in X. campestris-invaded xylem vessels, and the materials present after growth of the pathogen in guttation fluid, either unamended (c) or amended with lignin (d), pectin (e), CMC (f), and cellulose (g). Electronmicrographs 12 (c) to 12 (g) all of negatively stained material, (x 148 500). Similar type arrows indicate substances with similar structural features.

thickening of adjacent vessels, and passage of bacteria between vessels [Plate 1(b)], support the results obtained by Pine, Grogan and Hewitt (91) in light microscopic studies on tomatoes infected with Corynebacterium michiganense. Protuberances formed by the bulging of the wall of the outermost vessels of bundles into the lumina of surrounding parenchyma cells have also been observed by Nelson and Dickey (82) in light microscopic studies on carnations infected with Pseudomonas caryophylli. These authors reported that eventual rupture of the protuberances allows bacteria to enter the parenchyma tissue. Although not observed, a similar process may be operative in cabbage black rot. Thus, although belonging to various genera, many of the vascular bacterial pathogens appear to be very similar in their invasion of, and pathogenicity in, their respective host plants.

The finding that hydathode inoculations were unsuccessful unless accompanied by wounding supports the observation of Sutton and Williams (120). Klement (63) has shown that Pseudomonas tabaci, a leaf-spot bacterium, multiplies rapidly in intercellular fluid extracted from tobacco. Preliminary experiments in the present investigation showed that although X. campestris remained viable in natural guttation fluid collected from large mature healthy cabbage plants, multiplication was limited. The inoculum used in these experiments was obtained from a culture which had been growing for several weeks on YDC medium. In subsequent experiments guttation fluid from much younger plants growing in a different field, was found to support rapid multiplication of the bacterium when a culture newly isolated from infected cabbage was used as inoculum. These conflicting results are possibly due to differences in either the age of the cultures used or to the nature of the guttation fluid tested. It has been reported that the chemical composition of the soil in which the plants are grown may influence the ability of their guttation fluid to support growth of X. campestris

(129), and that the solutes in guttation fluid may vary from day to day (17).

According to Husain and Kelman (53) vascular parasites acquire nutrients, in part, from the cell walls of invaded conducting tissue; initially, however, tissue degradation may be so limited as to escape detection by light microscopy. In the present study tissue breakdown was observed at an early stage of infection. In order to utilize cell wall materials for metabolic purposes the parasite must produce pectinolytic, cellulolytic, hemicellulolytic or ligninolytic enzymes. X. campestris is known to produce considerable amounts of polygalacturonase and pectinmethylesterase (33, 34, 108) and polygalacturonic acid transeliminase (81) in liquid culture. The production of protopectinase has been reported as a variable attribute of this organism (24), and cellulase activity has been demonstrated both in vitro (34, 64, 65) and in vivo (33). In the latter paper evidence was provided of C_1 cellulolytic enzyme activity which caused a marked decrease in total cellulose in diseased cauliflower leaf tissue. It was also possible to distinguish decreases in α-cellulose and a concomitant increase in β- and γ-cellulose in such tissue. The parasite thus is potentially well equipped to degrade plant cell walls. The pH optima for many of these enzymes correspond to the pH 7,05 of the cabbage guttation fluid used in the present study.

The larger amounts of capsular material seen surrounding bacteria in close contact with vessel walls (Plate 2) may indicate a higher metabolic activity of those organisms in close proximity to sources of metabolizable substances of may result from the effects of laminar flow.

The chemical nature of the irregularly shaped electron-opaque granules observed scattered in the lumina of invaded vessels (Plates 3 and 6) is uncertain. It appears that these substances are released

following bacterial enzyme action on the primary wall of invaded vessels. Since similar granules are seen in electronmicrographs of lignin chemically isolated from healthy cabbage leaf-veins it may be assumed that the granules constitute a lignic component of the vessel wall. They are to be seen also within vessel walls dissolving as a result of the action of constitutive hydrolytic enzymes in both healthy (Plates 4 and 5) and diseased /Plate 7(a)/ leaf-veins. It seems, therefore, that in the cellulosic residue of naturally hydrolysed walls described by O'Brien and Thimann (85) a granular lignic component is retained.

One of the most contentious issues in vascular phytobacteriological histopathology concerns the origin and composition of the plugging materials found in the vessel elements of infected plants. Various theories, based on the results of histochemical tests and on light microscopy of stained sections, have been advanced to explain the nature of this material. Strong evidence for the involvement of extracellular bacterial polysaccharides in the plugging of vessels has been presented (51, 120, 121). Sutton and Williams (120, 121) suggest that extracellular polysaccharides produced by X. campestris, together with the bacteria themselves, are the primary cause of xylem plugging, but state that pectic substances of the host may also be present. Roth (97), however, concluded that host-formed substances (wound gums) or host degradation products, such as pectins and lignin, constitute the major part of the plugging material.

In the present study the evidence indicates two types of material that may be involved in plugging. These are the fibrillar beaded material found both associated with vessel walls undergoing bacterial degradation (Plate 6) and surrounding bacteria within some invaded vessels (Plate 2, inset), and the reticulate plugging material seen in Plates 7 to 9.

There was no ultrastructural similarity between the extracellular substances observed in Plates 10 and 11 and the plugging materials which occur in the xylem vessels of X. campestris infected cabbage leaves. However, it is likely that concentration by centrifugation, fixation in glutaraldehyde, dehydration in alcohol, and embedding of the treated material in plastic would drastically alter the general form of the material and also the ultrastructure of the individual components. Since the experiment conducted on collodion coated grids, which was designed to reduce artifacts to a minimum, also showed that there was little ultrastructural similarity between the materials observed in the inoculated natural guttation fluid [Plate 12(c)] and either type of vessel plugging material [Plates 12(a) and 12(b)], it was concluded that bacterial extracellular polysaccharides are not major constituents of the plugs. It is evident, however, that in vivo a certain amount of bacterial extracellular material, and the bacteria themselves (Plate 2), play some rôle in vessel plugging in combination with the major plugging materials that arise as a result of bacterial action on the vessel walls.

The fibrillar beaded material observed in Plates 3 and 6 is apparently the result of bacterial enzyme action on primary walls, and is seen only in invaded vessels. Sutton and Williams (120) reported a weakly staining material amongst X. campestris cells within occluded vessels of cabbage. This they interpreted as solubilized vessel wall pectins interspersed within bacterial extracellular polysaccharide. Wainwright and Nelson (122), however, could detect no host wall material other than lignin within bacterial pockets in Pelargonium spp. infected with X. pelargonii. Fibrillar material, bearing some resemblance to that reported here, has been observed at the surfaces of suspension-cultured plant cells and identified as lignofibrils (74). This structural similarity, the apparent insolubility of the material

and the findings of Wainwright and Nelson lead me to suggest that the beaded fibrillar material observed may be some form of lignin.

Further, the close ultrastructural similarity between the material remaining in the lignin-amended guttation fluid after bacterial growth [Plate 12(d) - arrows] and the beaded fibrillar material, observed in invaded xylem vessels of cabbage leaf-veins [Plate 12(a) - arrows], indicates that this plugging material consists largely of non-degradable lignofibrils released during bacterial enzyme action on vessel walls.

Material with a structure somewhat similar to that of the beaded fibrillar material observed in plugged vessels [Plates 2 (inset), 6 and 12(a)], was produced by Huang, Huang and Goodman (47) by mixing lipids isolated from thylakoid membranes of normal tobacco leaf tissue with structural proteins prepared from leaf tissue 6 h after infiltration with water. However the dimensions of the two materials do not correspond.

It is significant that in contrast to the fibrillar beaded material that occurs only in invaded vessels, the occluding plugs of reticulate material are free of bacteria when still entire [Plates 7(a) and 9]. Sutton and Williams (120) possibly observed similar plugs which they described as comprising a reticulate network of bacterial acid mucopolysaccharide that stained deep purple with toluidine blue and thionin. They found that extracellular polysaccharide purified from virulent X. campestris stained similarly to the plugging material. However, the fine structure and localization of the reticulate material in the present study [Plates 7(a), 7(b), 8 and 9] indicates that it is primarily of host origin and that bacterial extracellular polysaccharide is not the major constituent.

The basically similar ultrastructural conformation of the materials present in inoculated pectin- and CMC-amended guttation fluid and the

reticulate-type plugging material is evident when Plates 12(e), 12(f) and 12(b) are compared. This, and the distinct ultrastructural resemblance of the thread-like structures, observed in the inoculated cellulose amended guttation fluid [Plate 12(g) - arrows], to some of the finer threads in the reticulate plugging material [Plate 12(a)], indicate that this type of plug is apparently composed largely of a mixture of partially degraded pectic and cellulosic material of host origin.

Presumably such plugs arise either passively as material of host and/or bacterial origin accumulates, or they may be actively formed by the host in response to the presence of the parasite. In the present study the latter interpretation is supported by the observations that completely plugged bacterium-free vessels are in direct contact with invaded vessels [Plates 7(a) and 9], and that the plugs are generally formed at sites where bacterial action on the primary wall and middle lamella of contiguous vessels is well advanced (Plates 7 to 9). Beckman (4) has suggested that vessel plugs may represent the end result of a host-directed response in which pectinaceous gels released from cell walls react with other host materials and phenolic compounds in the host.

Additional evidence for the host origin of the plugging material is the apparent ability of the bacteria to degrade it partially, particularly at the electron-transparent layer immediately adjacent to the vessel wall (Plate 8). This results in contraction and compaction of the reticulate material [Plates 7(a) and 8] which then appears more dense than that found in neighbouring bacterium-free vessels [Plates 7(a) and 9]. Once the bacteria have caused the initial peripheral damage to the plugs their efficacy as defence mechanisms may be reduced and natural mechanical distortion and disintegration may follow as a result of fluid movement.

The results of the present study indicate that various host materials, bacterial extracellular polysaccharides, and the bacterial cells themselves, are involved in the plugging of vessels in cabbage plants infected with *X. campestris*.

CHAPTER 2

HISTOPATHOLOGY OF TOMATO PLANTS INFECTED WITH PSEUDOMONAS SOLANACEARUM WITH EMPHASIS ON ULTRASTRUCTURE

INTRODUCTION

Among bacterial phytopathogens some are primarily systemic vascular parasites that generally produce wilts in plants, while others occur mainly in parenchymatous tissue and may cause wilting indirectly (10). One of the most important and ubiquitous vascular bacterial plant pathogens is Pseudomonas solanacearum E.F.S., the causal agent of the disease known as southern bacterial wilt or Granville wilt. In South Africa this disease is known as bacterial wilt of tomato . The incitant is particularly destructive in the warmer regions of the world (57) and is unusual among phytopathogenic bacteria in its extremely wide host range (110).

The true vascular pathogens are thought to cause wilting by interfering with the water transport mechanisms of their hosts (10, 59, 111). Several theories have been advanced to explain the mechanism of wilting in plants invaded by P. solanacearum. Firstly, the pathogen produces a systemic toxin that disrupts the osmotic system of tobacco leaves and thereby causes the plant to wilt (54). However, the inability of culture filtrates of the organism to cause wilting of tomato or tobacco cuttings, led Van der Meer in 1929, according to Husain and Kelman (51), to doubt the validity of the toxin theory, and to suggest that gums and tyloses observed in the vessels of infected plants, together with masses of bacterial cells, were the primary causes of wilting. On the other hand the toxin theory was later supported by Kunz (67) who isolated, from broth cultures of P. solanacearum, both a bacterial polypeptide complex, that mechanically

occluded vessels of tomato plants and was thought to be converted to a toxigenic substance by host enzyme action, and a plasma toxin that caused wilting by affecting the semipermeability of the plasma membrane. Another theory on the mechanism of wilting envisioned the partial or complete occlusion of xylem elements of infected tobacco and tomato plants by masses of bacterial cells rather than by gums and tyloses, or the production of toxins (35).

Husain and Kelman (51), after conducting a comprehensive series of experiments with three P. solanacearum strains of differing virulence, concluded that the extracellular slime, produced in greatest amount by the highly pathogenic strain and not at all by the nonpathogenic strain, was the substance that caused wilting by mechanically blocking the xylem vessels of tomato cuttings. Similar conclusions had previously been reached concerning the heteropolysaccharide exudate from Xanthomonas phaseoli (71). This substance caused a non-specific, reversible wilt of bean, tomato and sunflower cuttings by mechanical blocking of water movement rather than by a specific chemical poisoning.

Husain and Kelman (51) excluded the possibility of plasma toxins as the cause of wilting in P. solanacearum-infected plants and also did not ascribe the primary cause of wilting to the mechanical plugging of vessels by masses of bacterial cells alone. They admitted, however, that their conclusion, that the slime material observed in stained preparations of bacterial exudates from diseased plants was the wilt inducing factor in the xylem fluid, was based on indirect evidence. Nevertheless, they claim that most of the criteria for a vivotoxin, as defined by Dimond and Waggoner (20), are satisfied by the wilt inducing slime. These proposals are supported by work which showed that wilting in P. solanacearum-infected banana plants was due to reduced water transport in the invaded conducting tissue, caused by plugging of the vessels with bacterial slime and cells (5).

Smith (107) observed bacteria in the intercellular spaces and dissolution of middle lamellae in xylem parenchyma surrounding extensively disorganized vascular bundles, and suggested that rupture of the vessels was caused by the development of dense masses of bacteria. Considerable degradation of pectic material in the middle lamellae of phloem parenchyma and pith, and occasional disruption of the cortical tissue, have also been reported in P. solanacearum-infected plants and in plants treated with culture filtrates of virulent strains of this organism (49, 50, 51). Cellulose breakdown, indicative of cellulolytic activity in this bacterium, was also observed in parts of the diseased plants where lysigenous cavities had formed (52). The main rôle ascribed to the pectic and cellulolytic enzymes of P. solanacearum is the degradation of host tissues to facilitate spread (60) and rapid lateral and longitudinal movement of the pathogen (52).

The pectinolytic enzymes that P. solanacearum produces include pectin methyl esterase (PME) and endo-polygalacturonase (PG) (40, 49, 52, 65) but not pectin transeliminase [Kelman, unpublished data, cited by Buddenhagen and Kelman (10)]. In addition to pectic enzymes the pathogen produces cellulase (Cx) (49, 50, 52, 60, 65) and lipolytic and proteolytic enzymes (38). The organism appears, therefore, to be well equipped to degrade plant tissues. Although not the primary agents involved in wilting these enzymes cause disorganisation of the vascular tissue (49). This tissue disruption may indirectly impede water movement, thereby increasing the severity of wilting (52).

Buddenhagen and Kelman (10), in a review article written over a decade ago, stated that most references to P. solanacearum referred mainly to occurrence and control. The reviewers suggested that since the host-parasite relations in water-conducting tissue are unique the following sequence of events in pathogenesis caused by P. solanacearum

could profitably be investigated: (i) the initial introduction into a few xylem vessels of a relatively small number of bacterial cells, (ii) localized multiplication of the bacteria in the vessels and longitudinal spread of the pathogen without initial involvement of xylem parenchyma or phloem cells, (iii) the onset of systemic invasion involving a large number of vessel elements, with resulting impairment of water relations and wilting, (iv) breakdown of vessel walls and adjacent parenchyma cells with resulting lysigenous cavity formation and invasion of phloem, pith and cortical tissue.

Apart from work on various chemical aspects of the critical initial stages of infection (15, 87, 88, 99, 100, 102), little research appears to have been done in recent years on the host-parasite relations of this important vascular pathogen. Sequeira (101) stated that despite the frequent involvement of hormones in plant disease, experiments on this aspect of plant pathology seldom take into account the morphological and physiological changes occurring in the host.

In the past few years the host-parasite relations in a number of plant diseases of known bacterial origin have been studied in the electron microscope (18, 23, 48, 73, 103). These studies, however, were mainly concerned with non-vascular diseases. Ultrastructural studies have revealed that many of the plant diseases, which until recently were thought to be caused by viruses or other disease agents such as mycoplasmas, are in fact caused by bacteria or bacterium-like organisms (2, 26, 28, 43, 62, 76, 78, 79, 84, 89, 90, 126, 127). Some of these studies showed the bacteria or bacterium-like pathogens to occur mainly in the xylem vessels of the infected plants (2, 43, 62, 76, 79, 89, 127).

Various aspects of bacterium-induced hypersensitive responses in plants have also been studied in the electron microscope (29, 30, 31, 32, 44, 46, 47).

Except for a few earlier studies at the light-microscope level (7, 51, 57, 107) little work has been done on histopathological aspects of bacterial wilt disease of tomato. Apart from the preliminary work of Buddenhagen and Takata (11), on the ultrastructure of banana roots infected with P. solanacearum, the present author was unable to find any reference to electron microscopic studies on host-parasite relationships of the classical bacterial vascular pathogens.

The present study reports the results of a combined light microscope and ultrastructural examination of the histopathology of tomato plants infected with Pseudomonas solanacearum. Emphasis is placed on the spread of the pathogen in the xylem vessels and the progressive destruction of the conducting tissue of the host. The mechanism of wilt-induction is also discussed.

MATERIALS AND METHODS

Tomato (Lycopersicon esculentum Mill. "Homestead") seeds were germinated on moist filter-paper, the seedlings transferred to sterilized soil in pots and grown in the glasshouse for 4 - 5 weeks until approximately 15 cm in height. The plantlets were then carefully removed from the soil, washed in sterile water, and selected for uniformity in size and amount of root growth. The chosen plantlets were transferred to each of 20 specially constructed 250 ml Erlenmeyer flasks containing a sterile modified Hoagland and Arnon (41) nutrient solution in which the $MnCl_2.4H_2O$ and $H_2MoO_4.H_2O$ were replaced by molar equivalent amounts of $MnSO_4.H_2O$ and $Na_2MoO_4.2H_2O$ respectively, and the iron tartrate by NaFe-EDTA (44,5 µM).

All flasks were painted black with two narrow, diametrically opposed observation slits running vertically the full height of the flasks. These slits were covered with removable black plastic tape to exclude light from the plant roots. Each flask was fitted with a

fine sterile airstone through which a small, finely dispersed jet of sterile air was led from a common air-line. The air flow was carefully regulated so that each flask received equal aeration. Sterile non-absorbent cotton-wool was wrapped around the stems of the plants and inserted into the necks of the flasks so that the roots were suspended approximately midway in the flasks. The cotton-wool was then covered with aluminium foil. A mark just below the neck of each flask indicated the level at which the nutrient solution was to be maintained.

Twenty such flasks were arranged in two equal rows in a plant growth unit maintained at 30±4 °C by means of undersurface heating cables, and the plantlets grown under continuous supplementary light (2 500 to 2 900 lx). Plantlets in one row were subsequently used as test plants while those in the second row served as controls. The plantlets were allowed to remain undisturbed for a week to become fully adapted to their new environment and to ensure that any root damage, suffered during their removal from the pots, had healed.

After this period the plants were transferred to a beaker containing sterile distilled water and, using sterile scissors, the immersed main root of each cut off immediately behind the root-cap. The flasks to contain test plantlets were uniformly inoculated with a bacterial suspension in nutrient solution from a 24 h virulent culture of locally isolated, fully characterized, P. solanacearum grown on tetrazolium medium (58). Estimations by the plate count method showed that the inoculated flasks contained initially 10^4 to 10^5 viable cells/ml nutrient solution. Every 24 h the tape was removed from the observation slits and the level of nutrient solution brought up to the mark in a sterile manner. The amount of solution added to each flask daily was recorded up to the time of death of the test plants (Table 1 and Fig. 1). The experiment was repeated using the same procedure

except that corresponding test and control plants were removed from the flasks at regular intervals after inoculation and treated as described below.

Twelve hours after inoculation the main root and the stem of the first test and corresponding control plant were cut transversely, from the cut root tip upward, into approximately 5mm pieces. The cutting was done under 6% Na cacodylate-buffered glutaraldehyde in a Petri dish on which rested a transparent cm ruler. These pieces were transferred to fresh 6% glutaraldehyde, cut into 3 approximately equal portions, and labelled to indicate their original positions in the plant. The material was prepared for electron microscopy as described in Chapter 1. All sections were cut with a diamond knife on a Reichert OMU3 ultramicrotome.

After trimming each specimen block to remove most of the cortical tissue, thick sections displaying a green interference colour were cut and stained for 2 min in a 1:1 mixture of 1% azure II in distilled water and 1% methylene blue in a 1% aqueous solution of sodium borate mixed immediately prior to staining (78). The prepared slides were heated to approximately 60 ^{o}C to improve penetration of the stain, rinsed in tap water and allowed to dry. Viewing longitudinal sections in a light microscope indicated when the vascular tissue was reached and also facilitated the search for bacteria within infected conducting tissue. When light microscopy revealed the presence of bacteria ultrathin serial sections were cut, collected, and stained for electron microscopy as described in Chapter 1. When sufficient thin sections had been obtained, thick sections were again cut until some interesting new structural feature was observed, whereupon thin sectioning was resumed.

Twenty-four hours after inoculation the main root and the stem of the second test and corresponding control plant were cut longitudinally

in the same manner as described above. The distribution of bacterial cells and the extent of tissue degradation was compared with that of the first test plant. Further samples were taken at 36 h and 48 h after inoculation and thereafter at 24 h intervals. Similar sampling procedure was continued and sections of representative specimens compared until 192 h after inoculation, when the tissue had reached an advanced stage of degradation.

Since a preliminary investigation of transverse sections of the first 5 mm piece above the cut root tip, 12 h after inoculation, had shown the bacteria initially confined to small-diameter cells adjacent to and surrounding the large vessels, attempts were made to identify these cells. After removal of the cortex from healthy tomato roots at an equivalent stage of development, the tissue of the vascular cylinder was gently macerated in a mixture of $KClO_3$ and conc. HNO_3, rinsed thoroughly in water, teased out in a drop of toluidine blue, and examined microscopically.

To investigate the nature of the extracellular polysaccharide of P. solanacearum cells were introduced into drops of nutrient broth + ½% glucose on collodion-coated grids. The grids were incubated, prepared for electron microscopy and examined as described in Chapter 1.

RESULTS

The water relations of healthy and P. solanacearum-inoculated tomato plants, over a period of 8 days, are shown in Table 1 and Fig. 1. During the initial 72 h period fluid uptake in the inoculated plants was 15-20% higher than in corresponding control plants. Thereafter, however, the inoculated plants started to wilt and fluid uptake by the diseased plants became erratic, but nevertheless showed a general decrease over the following 120 h. During this time the healthy plants continued to use increasing amounts of the nutrient

solution.

Light Microscopy

Although in all cases the root-tip was removed just prior to inoculation the bacteria, after 12 h, have invaded and multiplied only in the small-diameter cells adjacent to and surrounding the large vessels of the, as yet, not fully mature root tissue [Plates 13(a) and 13(b)]. Light-microscopic examination of macerated healthy tissue failed to identify unequivocally these cells which are either tracheids, tracheid fibres, or possibly xylem parenchyma cells with unusually thick walls. Examination of tissue from a position 3-4 cm above the cut tip of the root, 12 h after inoculation, showed that relatively few of these cells contained bacteria [Plates 13(a) and 13(b)]. After 24 h additional cells of the same type had become invaded and filled with bacteria [Plate 13(c)], while all the large xylem vessels and the majority of the smaller vessels remained free of the organism [Plates 13(a) and 13(b)].

Since the progressive stages of disease development are well illustrated in the tissue 3-4 cm from the cut root tip all subsequent comparative light- and electron microscopic observations, unless otherwise stated, were made on tissue from a similar position in the root.

Approximately 24 h after inoculation the invaded cells are stimulated to form tyloses [Plate 13(c)]. Tyloses protrude through many of the pits in the wall of the invaded cell and bulge into the lumen of the adjacent xylem vessel [Plates 14(c) and 14(d)]. The tyloses develop rapidly and 72 h after inoculation partially block the lumina of the vessels [Plates 14(a), 14(c) and 14(d)]. Tyloses were not observed in corresponding sections of healthy plant tissue [Plate 14(b)].

TABLE 1. Fluid uptake in healthy and Pseudomonas solanacearum infected tomato plants

DAY	PLANT CONDITION	VOL NUTRIENT SOLUTION (MLS) TAKEN UP IN 24 HOURS										MEAN VOL TAKEN UP IN 24 HOURS (MLS)
		FLASK NUMBER										
		1	2	3	4	5	6	7	8	9	10	
1	HEALTHY	10,0	12,0	10,0	10,0	8,5	12,0	14,5	9,5	10,5	14,0	11,10
	DISEASED	12,0	10,5	13,0	12,5	14,0	10,0	11,0	13,5	14,5	13,0	12,40
2	HEALTHY	13,0	13,0	12,0	13,0	10,5	14,0	17,0	12,0	13,5	17,0	13,50
	DISEASED	15,5	13,5	15,5	15,0	17,0	16,5	19,0	18,0	18,0	17,0	16,50
3	HEALTHY	14,5	14,5	13,5	16,0	14,5	19,0	19,5	15,0	16,5	20,0	16,30
	DISEASED	17,0	14,5	19,0	19,5	22,0	20,5	23,0	23,5	20,5	18,5	19,80
4	HEALTHY	17,0	16,0	15,0	18,0	15,0	20,5	20,0	16,0	18,0	21,5	17,70
	DISEASED	13,5	11,0	13,5	13,5	14,0	13,0	15,0	13,5	15,0	14,0	13,60
5	HEALTHY	17,5	16,5	15,5	19,0	16,0	21,5	20,5	17,0	18,5	22,0	18,40
	DISEASED	7,0	5,5	6,5	7,5	7,5	6,0	9,0	6,0	8,5	8,5	7,20
6	HEALTHY	19,5	17,0	16,0	20,5	17,0	22,0	21,5	18,5	20,0	25,0	19,70
	DISEASED	6,0	2,0	3,5	7,0	6,0	3,0	8,0	2,5	7,0	7,0	5,20
7	HEALTHY	20,0	18,0	17,0	21,5	19,0	24,0	23,0	19,5	21,0	28,0	21,10
	DISEASED	2,0	0,0	1,0	3,0	1,5	0,0	4,0	0,0	2,5	3,5	1,75
8	HEALTHY	21,0	19,5	19,0	23,0	20,0	25,0	24,5	21,0	22,0	30,0	22,50
	DISEASED	0,1	0,0	0,0	0,3	0,0	0,0	0,5	0,0	0,0	0,5	0,14

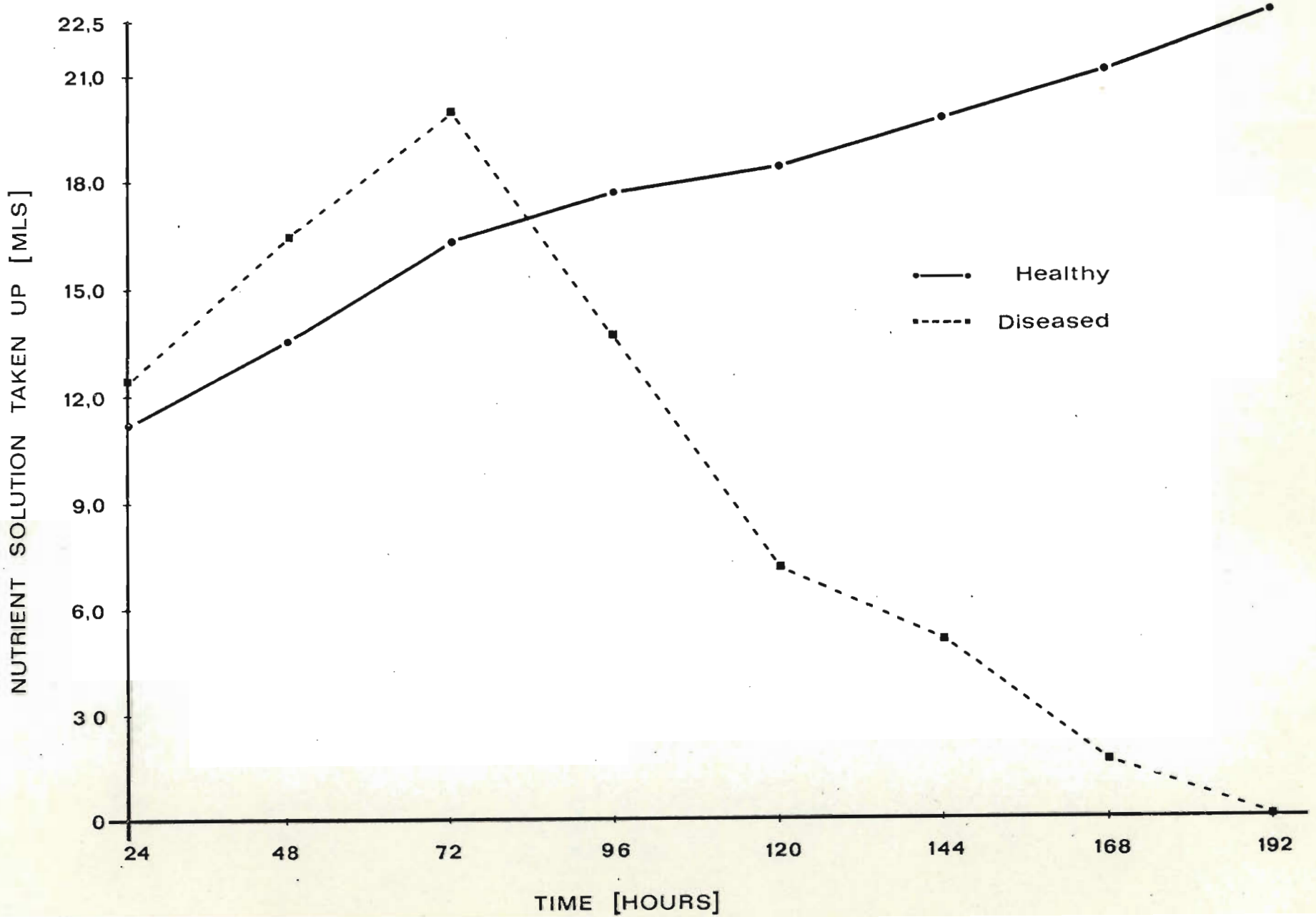
22,5
21,0
18,0
15,0
12,0
9,0
6,0
3 0
0
NUTRIENT SOLUTION TAKEN UP [MLS]
24
48
72
96
120
144
168
192
TIME [HOURS]
Healthy
Diseased

From the invaded cells the bacteria pass through a narrow, slightly elongated neck [Plate 14(d)] and enter the lumen of the tylosis, which gradually becomes filled with large numbers of bacterial cells [Plates 14(a), 14(c) and 14(d)]. However, not all invaded tyloses contain equal numbers of bacteria and some are apparently bacterium-free [Plates 14(a), 14(c), 14(d) and 15(a)]. The necks of the tyloses in Plates 14(d) and 15(b) are in different planes and may even arise from different cells, which could explain the uneven distribution of bacteria within them.

As the tyloses continue to increase in size they wedge between the bars of secondary thickening and assume the conformation of the opposite wall of the vessel thus partially or completely occluding the vessel [Plate 15(a)].

Often tyloses form in vessels adjacent to those that are occluded by these structures [Plate 15(a)]. The walls of the tyloses appear to be plastic, at least initially, as their shapes are governed by their position relative to each other and by structural features of the vessels in which they form [Plates 14(a), 14(c), 14(d), 15(a) and 15(b)]. An unidentified substance appears to be deposited in [Plate 15(c)], and around [Plate 14(d)], the tyloses necks. This substance is observed in the pit cavities before the tyloses form [Plate 15(d)].

Bacteria are observed in moderate numbers in the large xylem vessels 96 h after inoculation [Plate 16(a)]. The number of bacteria in the vessels of equivalent tissue 120 h after inoculation is shown in Plate 16(b). Tissue collapse occurs after 168 h and results in the formation of large lysigenous cavities after 192 h [Plate 16(c)].

Longitudinal spread of the pathogen in the host tissue shows two distinct phases. During the intial stage of disease development migration is relatively slow; no bacteria being observed at a distance greater than 3,5 cm from the cut root tip 48 h after inoculation.

After 72 h, small numbers of bacterial cells are observed in tissue up to 7,0 cm from the cut end of the root. Thereafter, however, the rate of spread increased dramatically, the bacteria moving to just below the apical region of the stem during the next 24 h period; an average distance of approximately 22 cm from the inoculated cut root tip.

Electron Microscopy

Apart from supplying additional information on ultrastructural aspects of the host-parasite relationship at the cellular level, electron microscopy in most instances verified the observations made during the light microscope study. Twelve hours after inoculation some of the cells, possibly tracheids or tracheid fibres or xylem parenchyma cells, adjacent to large xylem vessels, were seen to contain fairly large numbers of bacteria interspersed with a fine granular substance [Plate 17(a)]. This material accumulates particularly in regions between the bars of secondary thickening [Plates 17(a) and 17(b)] which, in these cells, are unilaterally placed [Plate 17(a)]. At this early stage of infection no damage is caused to the walls of these cells [Plates 17(b) and 17(c)]. Many of the bacteria contain large electron-transparent areas; possibly granules of some storage product such as poly-β - hydroxybutyric acid or volutin [Plates 17(a) and 17(b)].

Within the invaded host cells the bacteria show considerable variation in shape [Plates 18(a) and 18(b)] and appearance [Plates 18(c) and 18(d)]. In some instances the bacteria are in close contact with the host cell wall and appear to become orientated toward the spaces between the bars of secondary thickening [Plate 18(a)]. A layer of electron-dense material is deposited on the inner wall surface of these host cells.

However, in other host cells most of the bacteria are contained by an apparently 'membrane'-bounded bag-like structure, which effectively prevents them from coming into direct contact with the plant cell wall [Plate 18(b)]. In such cells the primary wall remains unaffected [Plate 18(b)] and resembles that of the vessels in healthy plants [Plates 24(d) and 24(e)], but some electron-dense substance, possibly remains of cytoplasm, accumulates in the adjacent cell [Plate 18(b)]. Bacterial cells that contain large cytoplasmic inclusions generally have relatively smooth walls and indistinct nuclear regions [Plate 18(c)], whereas those which lack these inclusions usually have a deeply scalloped cell wall, densely ribosomal cytoplasm, and a distinct nuclear region [Plate 18(d)]. In the latter type cells the nuclear region is often distinct even when the cell is apparently not dividing [Plate 22(d)].

As tyloses appear to form rapidly it was not possible to observe the progressive stages in their development. It seems the plasmalemma of certain host cells enters a pit cavity and ruptures the primary wall or pit membrane, which is pushed to one side of the opening thus formed between adjacent bars of secondary thickening [Plates 20(a) and 20(c)]. The tylosis enlarges rapidly and balloons into an adjacent vessel and the somewhat elongated neck fills the pit through which it passes [Plates 20(a) and 20(c)]. Apparently an extension of the host cell plasmalemma is continuous with the outer layer of the tylosis wall [Plates 19(b), 19(d), 20(a) and 20(c)]. Bacteria migrate into the tyloses from the invaded cell [Plate 20(a)] as described in the section on light microscopy. A layer of material, continuous with a similar apposition layer on the plasmalemma in the cell, is deposited on the inner surface of the bounding membrane of the tylosis [Plate 19(b), 20(a) and 20(c)]. The inset in Plate 20(a), which illustrates the walls of two adjoining tyloses, shows the

detailed fine structure of the wall. The inner deposition layer seems to be composed partly, at least, of bacterial extracellular material as the slime, sloughing off bacterial cells within a tylosis, is very similar to the deposited material [Plate 20(b)]. The uneven distribution of bacteria in the different tyloses is very marked [Plate 20(a)].

In some instances the neck of the tylosis becomes filled with a mass of debris and, possibly, bacterial extracellular material [Plate 20(c)]. Some of the non-invaded cells of infected plants [Plate 19(d)] also produce tyloses which bulge into adjacent non-invaded xylem vessels.

Structures, filled with a coarse granular material, are also sometimes observed protruding between bars of secondary thickening into vessels adjacent to invaded cells [Plates 19(a) and 19(c)].

During the first 48 h of disease development no bacteria are observed within the large xylem vessels [Plate 20(a)]. Although the actual process of disruption was not observed, collapse of tyloses, with resultant release of bacteria into the xylem vessels, must have occurred between 48 h and 72 h after inoculation, since many disrupted tyloses, together with bacteria and reticulate material, are observed in the lumina of the large vessels 72 h after inoculation [Plate 21(a)]. Occasionally bacteria are trapped between the collapsed tyloses walls and the wall of the vessel [Plate 21(c)]. After 96 - 120 h many tyloses, formed by non-invaded cells, are also observed in various stages of disruption within bacterium-free xylem vessels [Plates 21(b) and 21(d)]. The disrupted tyloses assume unusual shapes [Plates 21(a), 21(b) and 21(c)] and appear to proliferate giving rise to secondary structures [Plate 21(d)].

After 72 h small numbers of bacteria were observed for the first time in the vessels of the root in which they had spread 3 cm above

the region of tylosis collapse [Plate 22(a)], an average distance of approximately 2 cm below the crown in the experimental plants. During the next 24 h period the number of bacteria in the vessels of the root 3-4 cm from the site of inoculation steadily increased [Plates 22(b) and 22(c)] and bacteria were observed for the first time in the stem vessels 21-22 cm above the inoculation site [Plate 22(d)]. In some root vessels the primary wall shows signs of degradation at positions between the bars of secondary thickening [Plate 22(c)].

While the number of bacteria in the vessels is still relatively small the majority are concentrated in regions between the bars of secondary thickening [Plates 22(c) and 22(d)]. The bacteria are often embedded in a finely granular, apparently viscid, material which, in some vessels, is clearly delimited from the more fluid regions by a delicate 'membranous' interface [Plate 22(b)]. In other vessels the interface is less well defined [Plate 22(d)], while in some instances both types of interface occur in the same vessel [Plate 22(c)]. Much of the material accumulated in these areas, particularly against the vessel wall, appears to consist largely of disrupted bacterial cells and fine granular material, possibly bacterial extracellular products [Plate 22(d)].

As the number of bacteria in the vessels increases large amounts of fine granular reticulate material accumulate [Plates 23(a) and 23(b)]. In some vessels, 120 h after inoculation, the bacteria are in clear areas surrounded by this material [Plate 23(a)], whereas in others the bacteria and reticulate material are interspersed [Plate 23(b)]. In the majority of vessels degeneration of wall material is negligible at this stage of pathogenesis [Plate 23(a)]. Occasionally the bacteria seem to occur in 'pockets' which, although not bounded by any visible barrier, are distinctly separated from each other by regions containing

material apparently composed of degenerating bacterial cells and bacterial extracellular products [Plate 23(c)]. A membrane-bounded structure with coarse granular contents distinct from the bacterial materials, was occasionally observed in a clear space bounded by primary wall, bars of secondary thickening and bacterial mass [Plate 23(c)]. After 144 h bacterial numbers reach such large proportions that the cells become compressed into irregular shapes [Plates 23(c) and 23(d)]. Even when massed together in this way the bacteria remain restricted to certain areas and do not enter adjacent debris-filled regions, despite the absence of any visible delimiting structure [Plate 23(d)]. In many invaded vessels of both the root [Plates 23(d), 24(c) and 25(a)] and the stem [Plate 24(b)] a relatively thick layer of electron-dense material is deposited on the primary wall and often completely fills the spaces between the primary wall and the bases of the bars of secondary thickening. A similar layer is not observed in the vessels of healthy tomato plants in which the primary wall usually has a finely dispersed granular appearance at positions between the bars of secondary thickening [Plates 24(d) and 24(e)] possibly as a result of host enzyme action.

Longitudinal spread of the bacterium is rapid in the stem and large numbers of bacterial cells are found in the vessels 18 cm above the site of tylosis collapse, 144 h after inoculation [Plate 24(a)]. A fine granular material accumulates in the vessel, particularly against the wall, and adjacent cells are filled with fibrillar and granular material, possibly degenerating cytoplasm [Plate 24(a)]. However, at no stage during pathogenesis do the bacterial cells and noncellular materials become compressed into such dense masses in the stem vessels, as in the vessels of the root. In some regions the bacteria, embedded in a finely granular material, are closely appressed to the vessel wall, especially in the spaces between the bars of

secondary thickening [Plate 24(b)], whereas in others a 'membrane'-like structure, stretched over the thickenings, prevents them from coming into direct contact with the primary wall [Plate 24(c)]. In both cases, however, a thick layer of electron-dense material accumulates on the primary wall in regions between the bars of secondary thickening. The fine granular material, which first became noticeable 120 h after inoculation [Plates 23(a) and 23(b)], increases in amount during the next 24 h [Plate 25(a)] until many xylem vessels are completely filled after 168 h [Plates 25(b) and 25(c)]. In the majority of xylem vessels bacterial cells and cell debris are embedded in this material [Plate 25(b)]. A material with an identical structure is produced by P. solanacearum growing in a liquid laboratory medium [Plate 25(b), inset]. Some degradation of spiral thickenings, with concomitant release of fibrillar material, is observed after 168 h [Plate 25(c)].

In addition to the fine granular material various other plugging substances occur in the vessels and cells of diseased plants, for example, a reticulate-type substance [Plate 25(d)] different from that described previously [Plates 23(a) and 23(b)] and an electron-dense, very coarse granular material [Plate 26(b), upper vessel]. Many vessels and cells contain mixtures of different plugging substances; some are occluded with masses of bacterial cells and fine granular material [Plates 26(a) and 26(b), lower cell], or very dense finely granular material free of bacteria surrounded by a reticulate-network in which bacteria are embedded [Plate 26(c)]. In addition some vessels in infected plants are partially filled with a mixture of small vesicular inclusions and a fine granular substance [Plate 26(d)].

Approximately 192 h after inoculation, when the remaining test plants are completely wilted, a very dense darkly staining material, which appears to be of vessel wall origin, accumulates in many vessels.

This material occurs where bacterial action has resulted in collapse of vessel walls [Plate 27(a) and 27(b)] and also in the large lysigenous cavities which form when the bacteria have degraded the vessel walls [Plate 27(c)].

DISCUSSION

The reason for the observed increase in water uptake by the infected plants during the initial 72 h period after inoculation was not determined as this falls outside the scope of this study. However, this phenomenon might reflect one of the many host responses which, according to Kelman (59), occur during the critical early stages of pathogenesis in plants infected with P. solanacearum.

The subsequent marked decrease in water uptake and the first signs of wilting began approximately at the time when tyloses, after having reached maximum size and often occluding the vessels, collapse, disrupt, and release bacteria into the xylem vessels. Although in the present study no transpiration determinations were made, it is known from work done on banana plants infected with P. solanacearum (5) that vascular occlusion, rather than toxin-induced increased transpiration, is the primary cause of wilt. Wilting of P. solanacearum-infected tomato plants or cuttings has also been attributed mainly to interference with water transport in the stem rather than to reduced uptake by the roots or excessive loss by the leaves (35, 51).

Initial bacterial invasion of, and multiplication in, the small-diameter cells adjacent to large vessels [Plates 13, 14(a), 14(c), 14(d), 15, 18(a) and 20(a)] is surprising since this pathogen is regarded as essentially a vascular parasite, confined initially to the xylem vessels (10, 51, 52, 57, 59, 87, 88). Smith (107), however, stated that although mainly a pathogen of the vascular bundles, this organism is less strictly confined to the bundles than other bacterial

PLATE 13. Light micrographs of longitudinal sections of root tissue 3-4 cm above site of inoculation; (a) & (b) 12 h after inoculation, (c) after 24 h. (a) Bacteria (B) in a few cells (C) adjacent to large bacterium-free vessel, XV. (x 270.) (b) Detail of serial section of boxed area in (a) showing distribution of bacteria (B) in, and structure of invaded cells, C. Note relatively thick cell walls (arrows). (x 680.) (c) Bacteria in additional small-diameter cells, C. Note bacteria in pit cavities (arrows) adjacent to bacterium-free vessel (XV), tyloses (T) and degeneration of cell contents in maturing tracheids, TR. (x 650.)

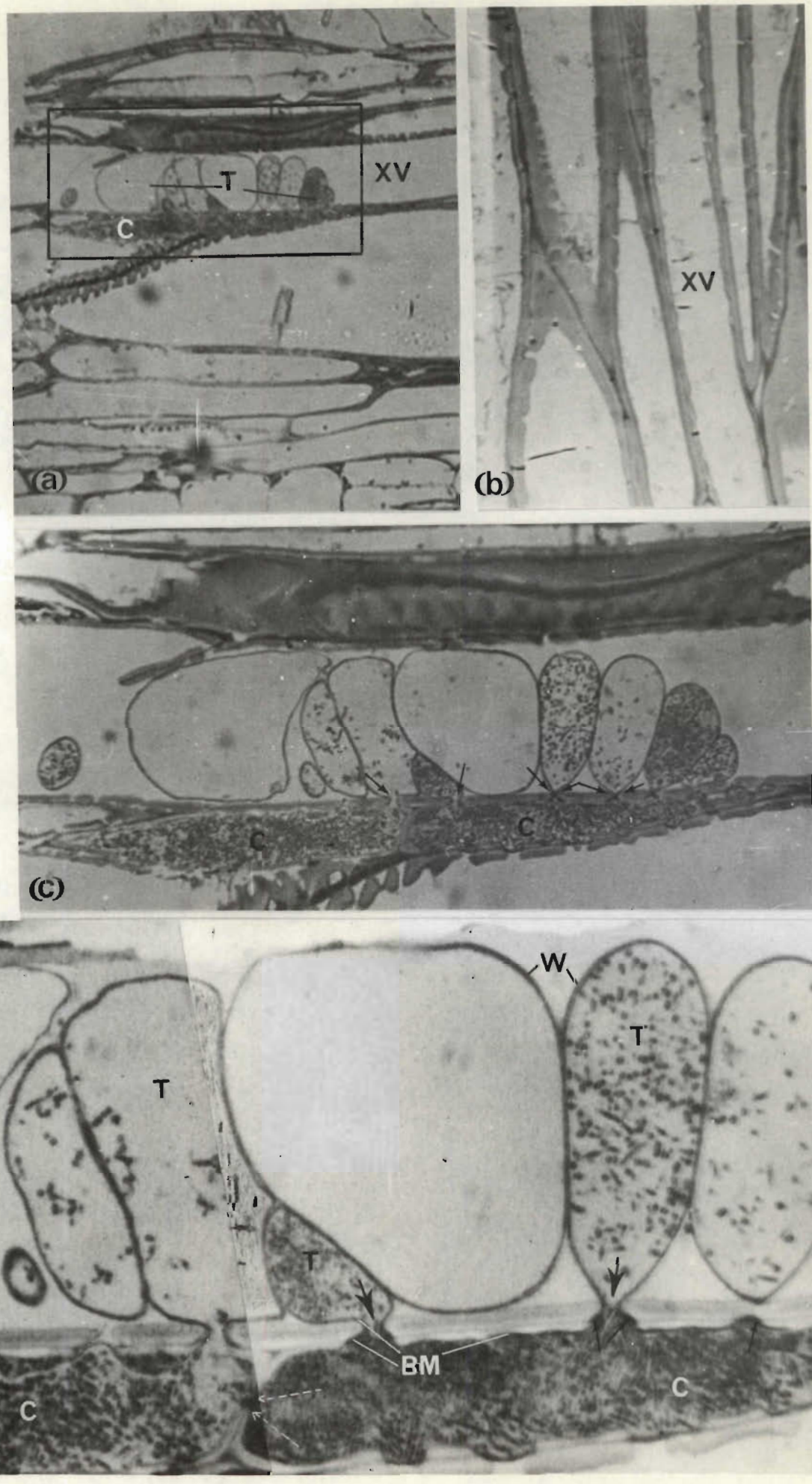

PLATE 14. (a)-(d) Light micrographs of longitudinal sections of root 3–4 cm above inoculation site 72 h after inoculation. (a) Many tyloses (T) protrude into lumen of adjacent bacterium-free vessel (XV) from invaded cell, C. (x 270.) (b) Corresponding healthy tissue with no tyloses (x 450.). (c) Detail of boxed area in (a) showing tylosis necks passing through pits (arrows) and uneven distribution of bacteria among tyloses, some of which are apparently bacterium-free. Masses of bacteria fill the lumen of tylosis-forming cells, C. (x 700.) (d) Further detail of tyloses. Note: relatively thick walls (W); passage of bacteria through tylosis necks (arrows) that penetrate pits in different planes; continuity of bounding membrane (BM) of invaded cell (C) and tyloses. T: passage of bacteria through open end walls (broken arrows) between

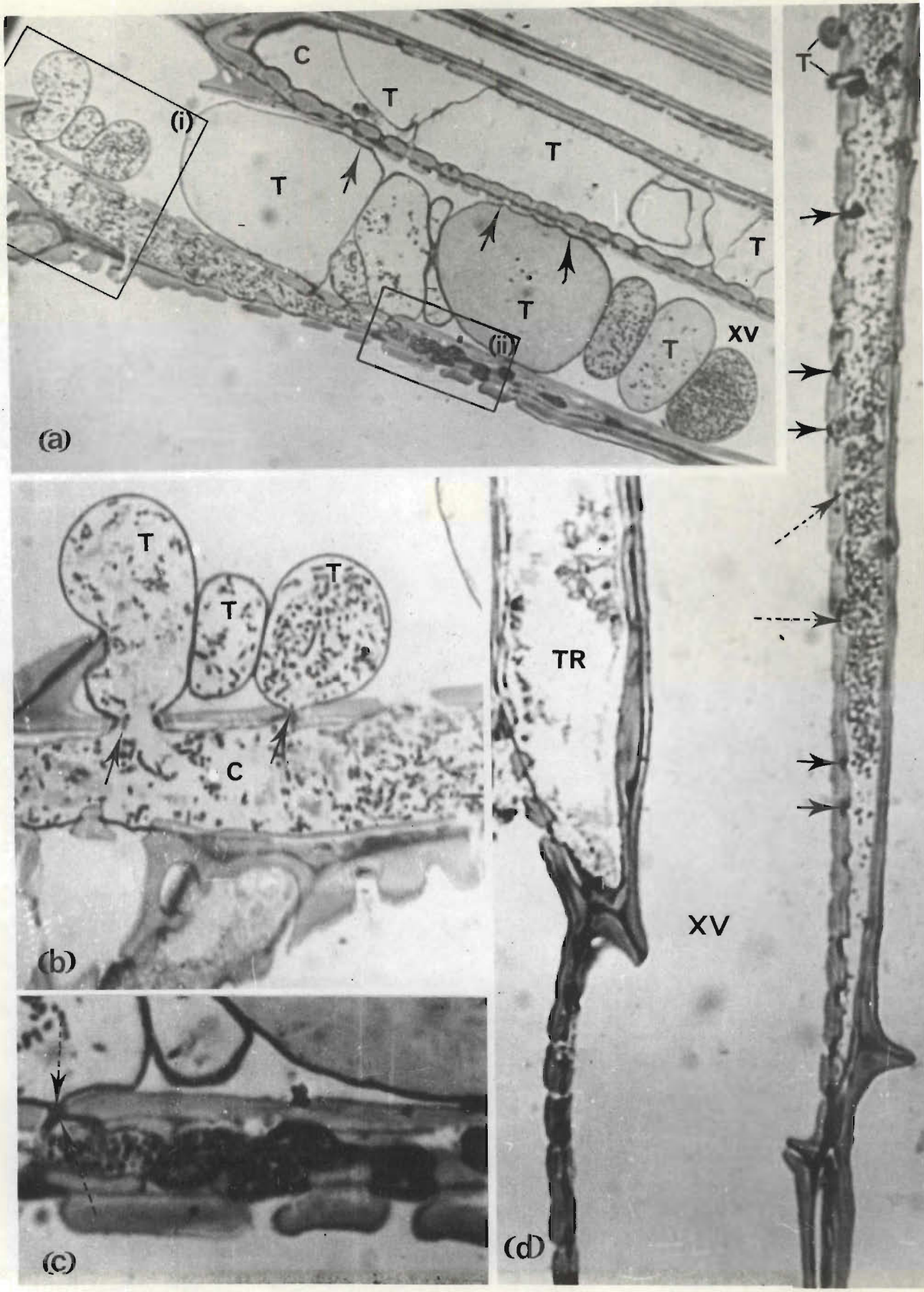

PLATE 15. (a)-(d) Light micrographs of longitudinal sections of root 3-4 cm above site of inoculation 72 h after inoculation. (a) Tyloses (T) bridging lumen of xylem vessel (XV) and wedging against opposite wall (arrows). Adjacent cell (C) contains a number of bacterium-free tyloses, T Note uneven distribution of bacteria among tyloses. (x 710.) (b) Detail of serial section of boxed area (i) in (a) illustrating apparent plasticity of tylosis walls, uneven distribution of bacteria in invaded cell (C) and among tyloses (T), and passage of bacteria into tyloses (arrows) which penetrate pits in different planes. (x 1 700.) (c) Detail of boxed area (ii) in (a) showing apparent deposit of densely staining material in tylosis neck (broken arrows). (x 2 380.) (d) Enlargement of part of Plate 13(c) showing tyloses (T) protruding into vessel (XV) and apparent deposition of electron-dense material in pit cavities (arrows) before tylosis development. Note bacteria in pit cavities (broken arrows) and degenerating cytoplasm of tracheid, TR. (x 1 020.)

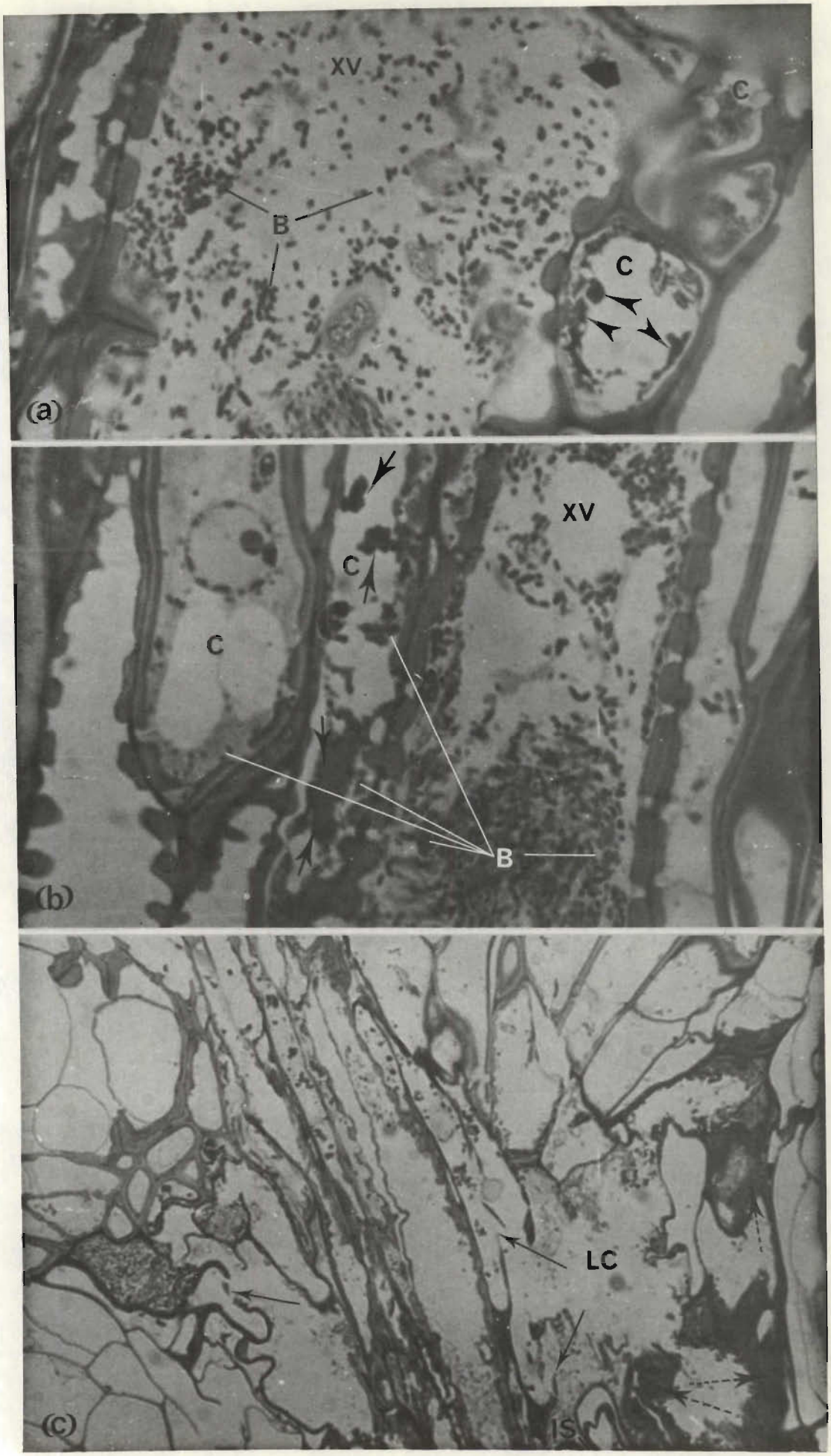

PLATE 16. (a)-(c) Light micrographs of longitudinal sections of root 3-4 cm above inoculation site. (a) Moderate numbers of bacteria (B) in large vessel (XV) 96 h after inoculation. Contents of adjacent cells (C) collapse and darkly staining material accumulates (arrows). (x 1 650.) (b) Equivalent tissue 120 h after inoculation showing bacteria (B) in invaded xylem vessel (XV) and adjacent cells, C. Note accumulated darkly-staining material (arrows) in adjacent cell. (x 1 650.) (c) Bacteria in a developing lysigenous cavity (LC) 192 h after inoculation. Note disrupted cell walls (arrows) and accumulation of degradation material (broken arrows). (x 180.)

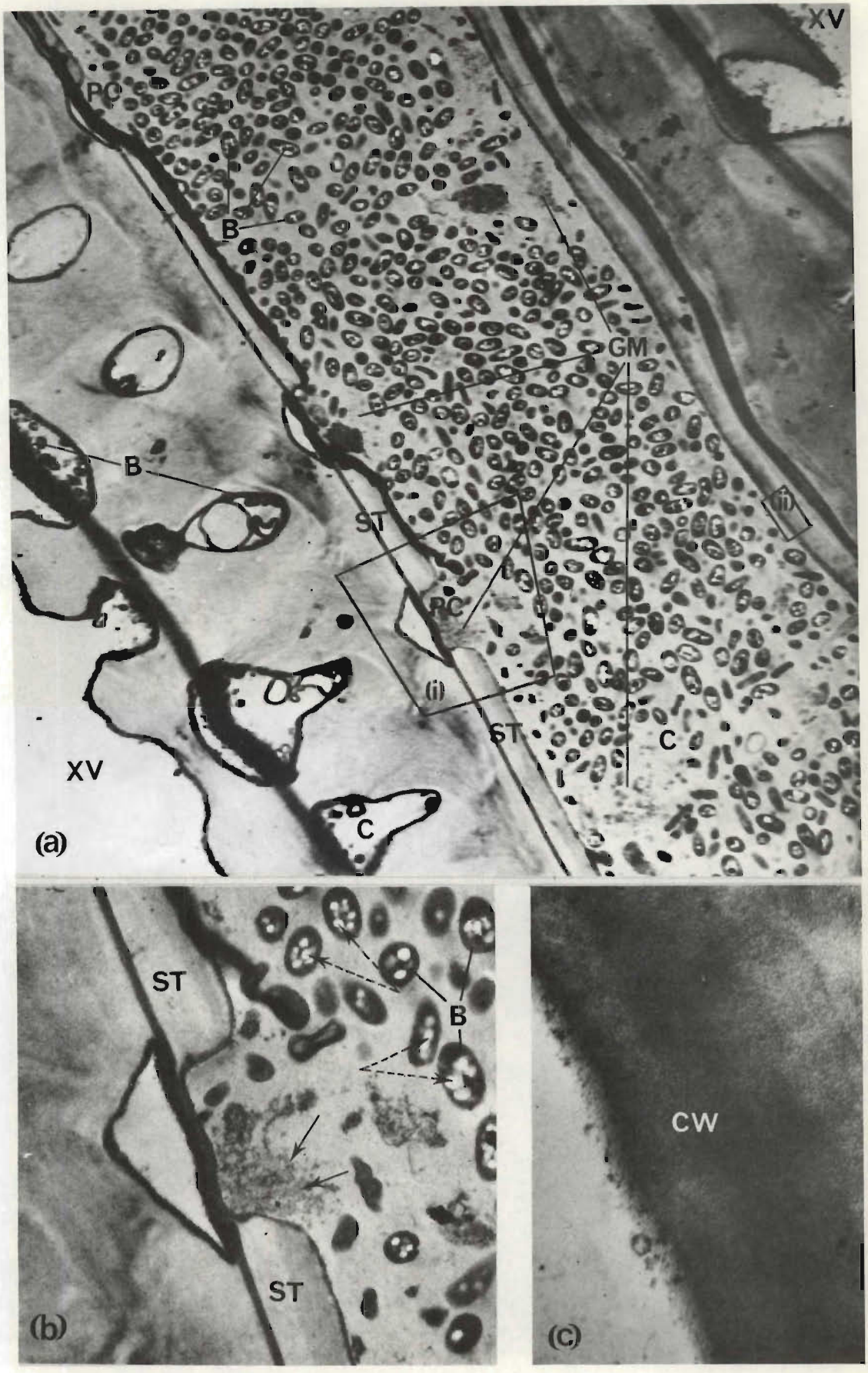

PLATE 17. (a)–(c) Electron micrographs of root-tissue 3–4 cm above inoculation site 12 h after inoculation. (a) Bacteria (B), in thick walled cells (C) between xylem vessels (XV), interspersed with fine granular material (GM) that accumulates in pit cavities (PC) between bars of secondary thickening, ST. (x 5 400.) (b) Detail of boxed area (i) in (a) showing finely granular, reticulate structure of accumulated material (arrows); large electron-transparent inclusion bodies (broken arrows) within bacteria (B); and non-degraded appearance of secondary thickenings, ST. (x 14 200.) (c) Detail of boxed area (ii) in (a) showing absence of cell wall (CW) degradation. (x 53 200.)

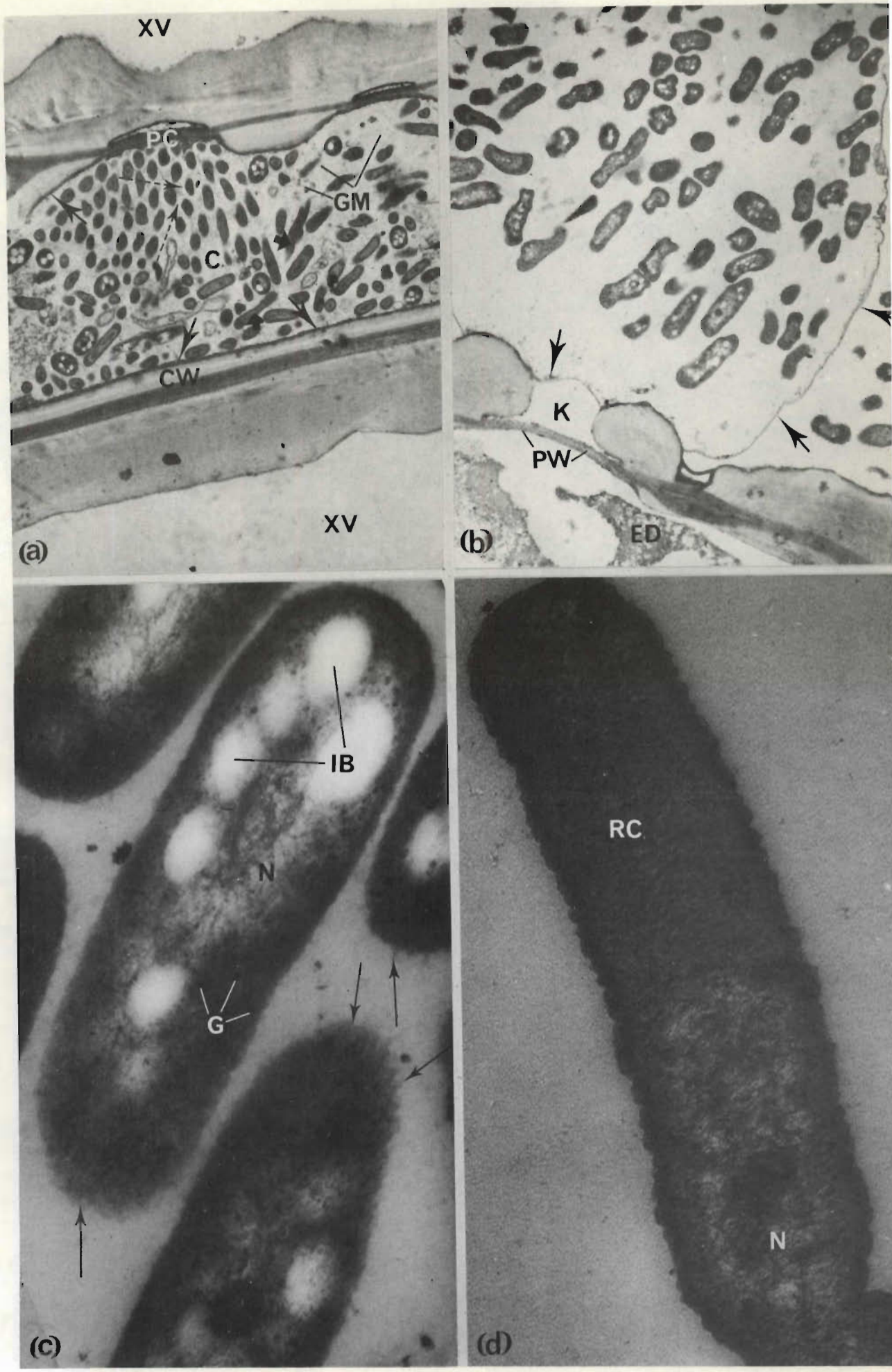

PLATE 18. (a) and (b) Electron micrographs of root tissue 3–4 cm above cut root tip 24 h after inoculation. (a) Bacteria interspersed with fine granular material (GM) within thick-walled, unilaterally pitted cell (C) between vessels, XV. Note marked pleomorphism of bacteria, some of which are filamentous (thick arrows) and layer of electron-dense material (arrows) deposited on cell wall, CW. Bacteria, surrounded by electron-transparent capsule (broken arrows), orientated toward spaces between bars of secondary thickening, PC. (x 8 350.) (b) Pleomorphic bacteria within an apparently membrane-bounded bag-like structure (arrows). Note clear area (K) between bacterial mass and unaffected primary wall (PW) and accumulation of electron-dense material (ED) in adjacent cell. (x 11 200.) (c) Smooth-walled form of bacterium showing large cytoplasmic inclusion bodies (IB), electron-dense granules (G), indistinct nuclear region (N), and reticulate extra-

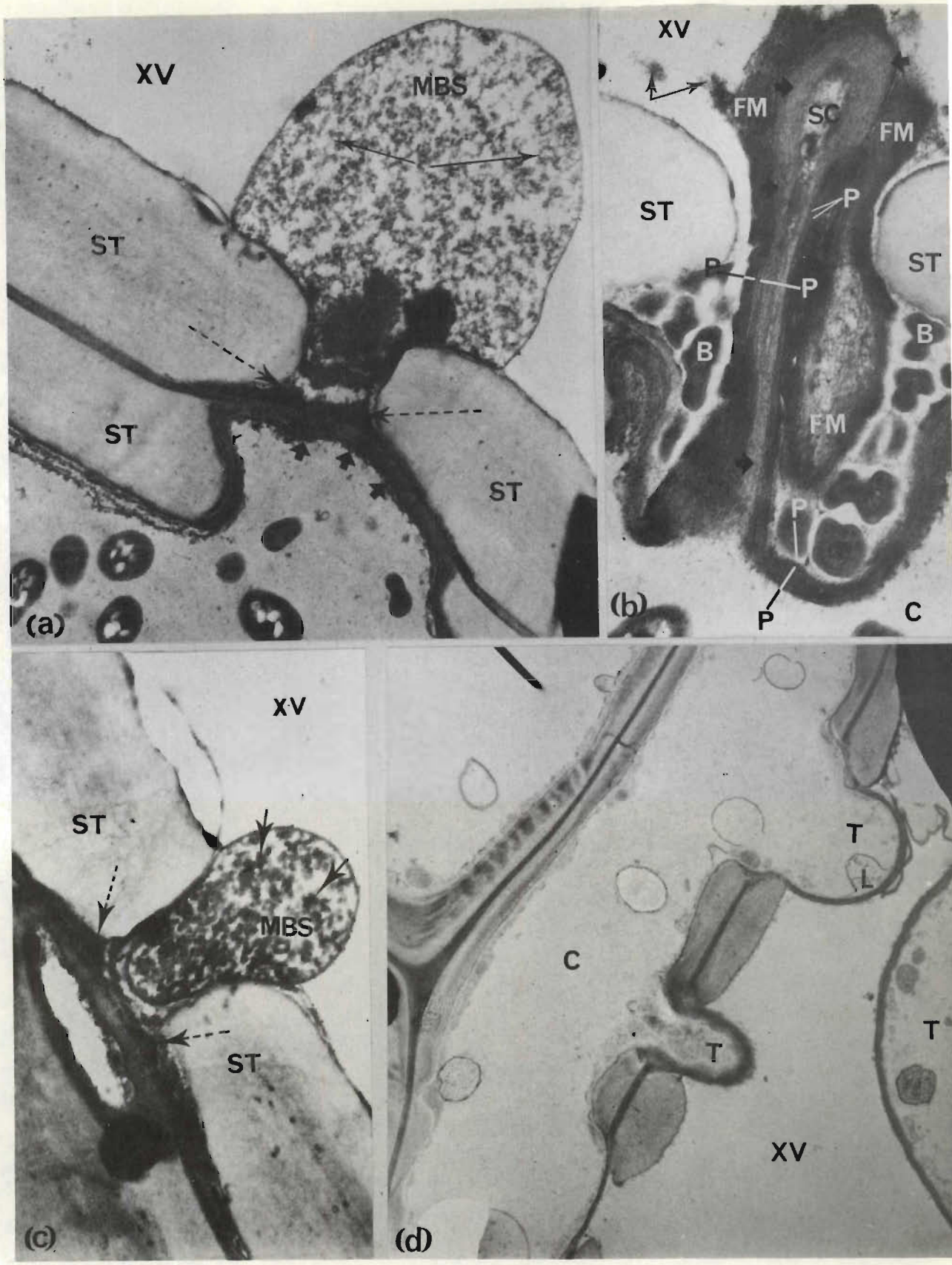

PLATE 19. (a)-(d) Root tissue 3-4 cm above cut root tip 24 h after inoculation. (a) Membrane bounded structure (MBS) filled with coarse granular material (arrows) protruding into lumen of non-invaded vessel, XV. Note electron-dense material in pit cavity (thick arrows) and at base of protruding structure (broken arrows). (x 20 500.) (b) Tangential section of tylosis showing parallel layers of plasmalemma (P) apparently continuous with plasmalemma of cell of origin, C. Note thick layer of material apposited on inside surface of plasmalemma (thick arrows) and around small sac-like cavity, SC. Note fibrillar material (FM) accumulated on outer surface of plasmalemma partially released (fine arrows) into vessel (XV) and bacteria compressed between cell membrane and bars of secondary thickening, ST. (x 27 500.) (c) Semi-tangential section of membrane-bounded structure (MBS), filled with coarse granualr material (arrows), protruding between bars of secondary thickening (ST) into adjacent bacterium-free xylem vessel, XV. Electron-dense material (broken arrows) accumulates below base of structure. (x 21 700.) (d) Developing tyloses (T) protruding from non-invaded cell (C) into lumen of adjacent bacterium-free xylem vessel, XV. Note lomasome (L) attached to wall of tylosis. (x 8 400.)

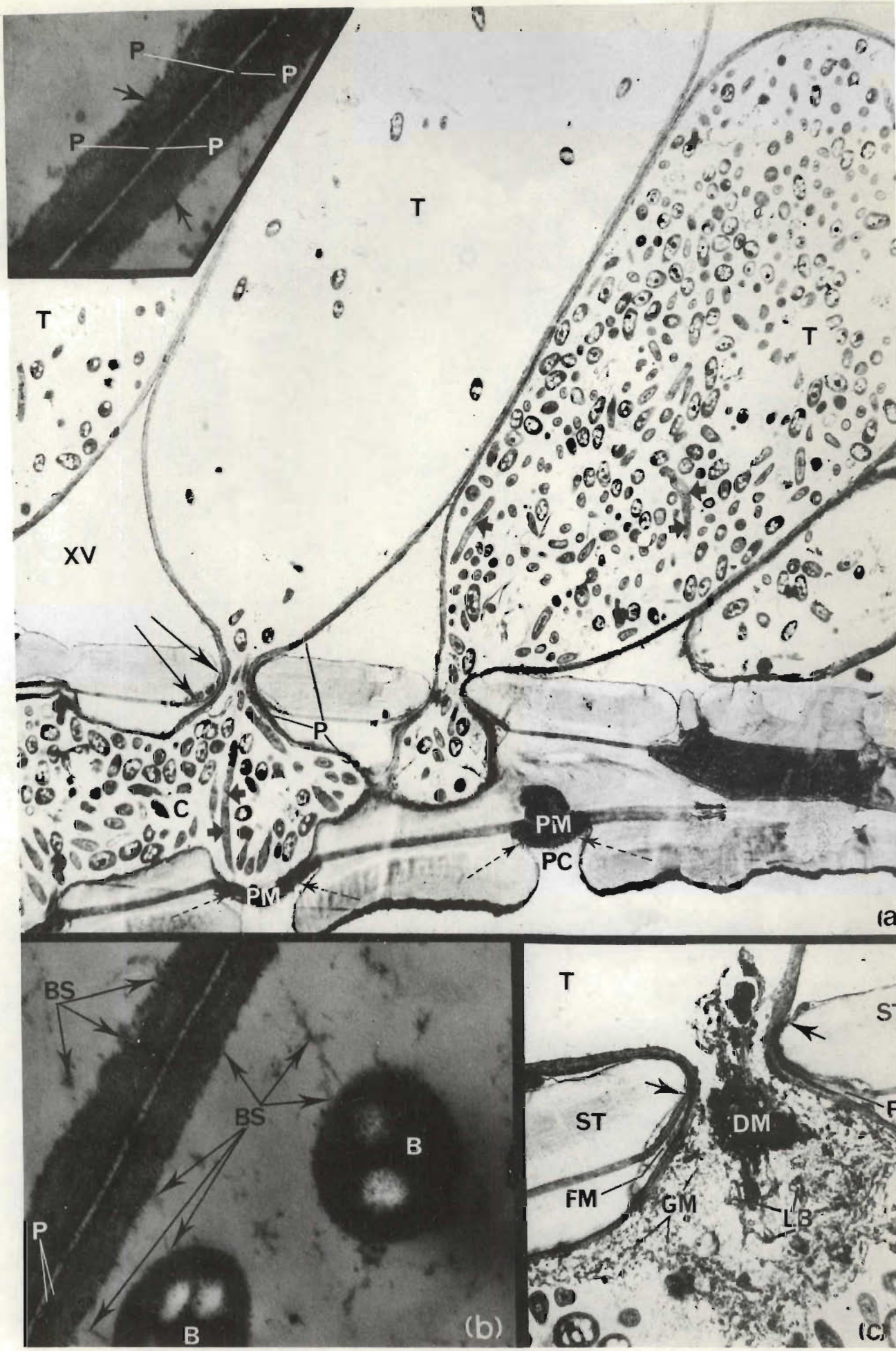

PLATE 20. (a)-(c) Root tissue 3-4 cm above site of inoculation after 48 h. (a) Mature tyloses (T) with narrow, elongated necks filling pit cavities between invaded cell (C) and adjacent bacterium-free xylem vessel, XV. Note rupture of primary wall (arrows), passage of bacteria into tyloses, and uneven distribution of markedly pleomorphic bacteria, some of which are filamentous (thick arrows), among tyloses. Plasmalemma of invaded cell and tyloses is continuous. Electron-dense material (broken arrows) accumulates on inner surface of plasmalemma (P), pit-membrane (PM) and in pit-cavity, PC. (x 6 750.) Inset. Detailed structure of walls of two adjacent tyloses showing outer triple-track plasmalemma (P) and inner electron-dense amorphous layer (arrows). (x 65 600.) (b) Detailed wall structure of two adjacent tyloses showing plasmalemma (P) on outside. Note similarity between material comprising inner amorphous layer and material (BS) sloughing from bacterial cells, B. (x 65 600.) (c) Fine granular material (GM), bacterial debris (LB) and dense mass of electron-opaque material (DM) accumulated

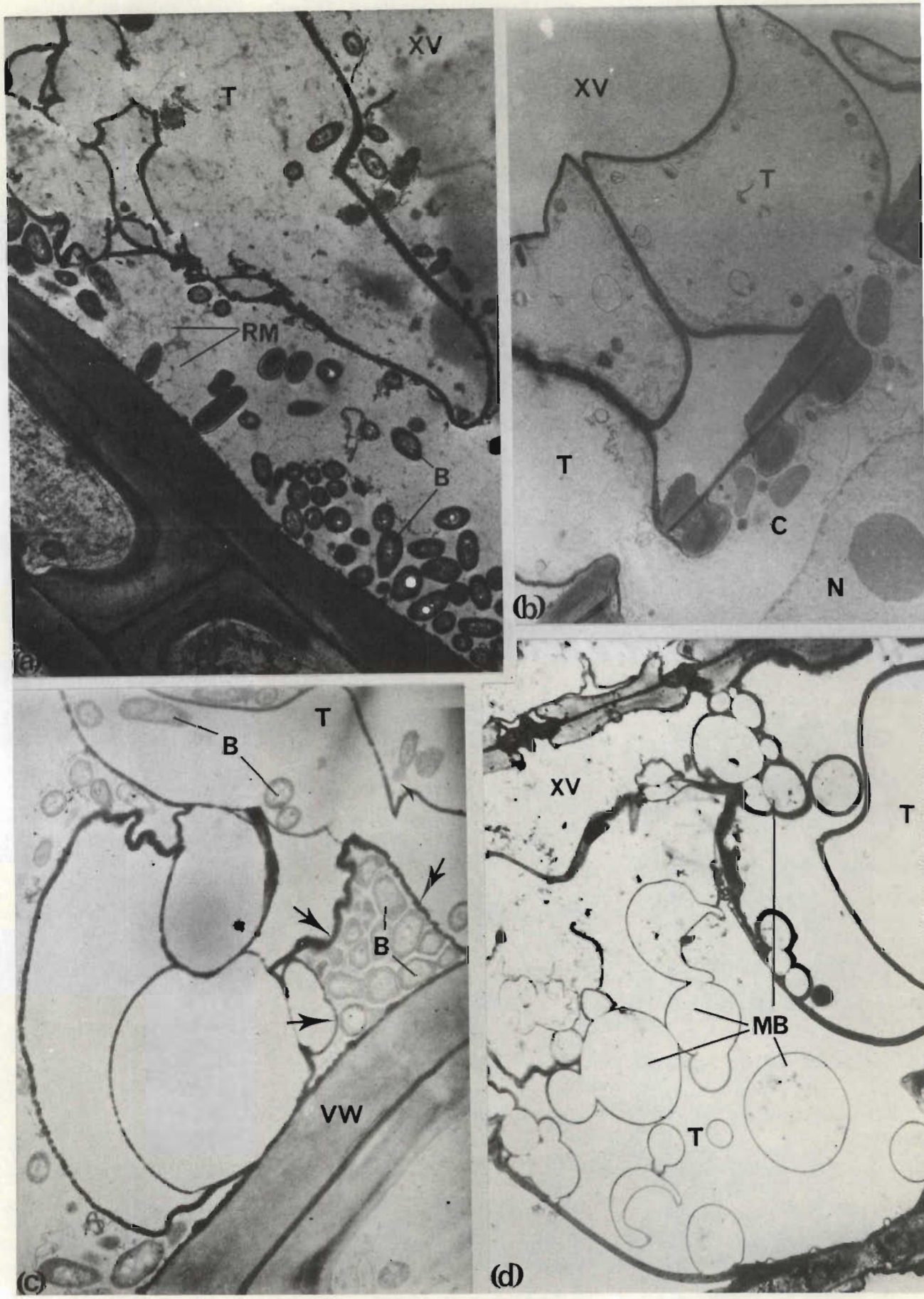

PLATE 21. Root tissue 3-4 cm above inoculation site; (a) & (c) after 72 h; (b) after 96 h; (d) after 120 h. (a) Disrupted tylosis (T) with released bacteria (B) and reticulate material (RM) within lumen of large xylem vessel, XV. Note bacteria still within collapsed tylosis. (x 9 350.) (b) Early stage in collapse of non-invaded tyloses (T) in bacterium-free vessel (XV) of inoculated plant. Note tylosis-forming cell (C) is free of bacteria and still has a nucleus, N. (x 5 850.) (c) Bacteria (B) trapped either within lumen of collapsed tylosis (T) or between walls of collapsed tyloses and the vessel wall, VW. (x 14 850.) (d) Late stage in collapse of non-invaded tyloses (T) in bacterium-free vessel, XV. Numerous secondary proliferations (MB) occur within and outside the lumen of the collapsed tylosis. (x 4 450.)

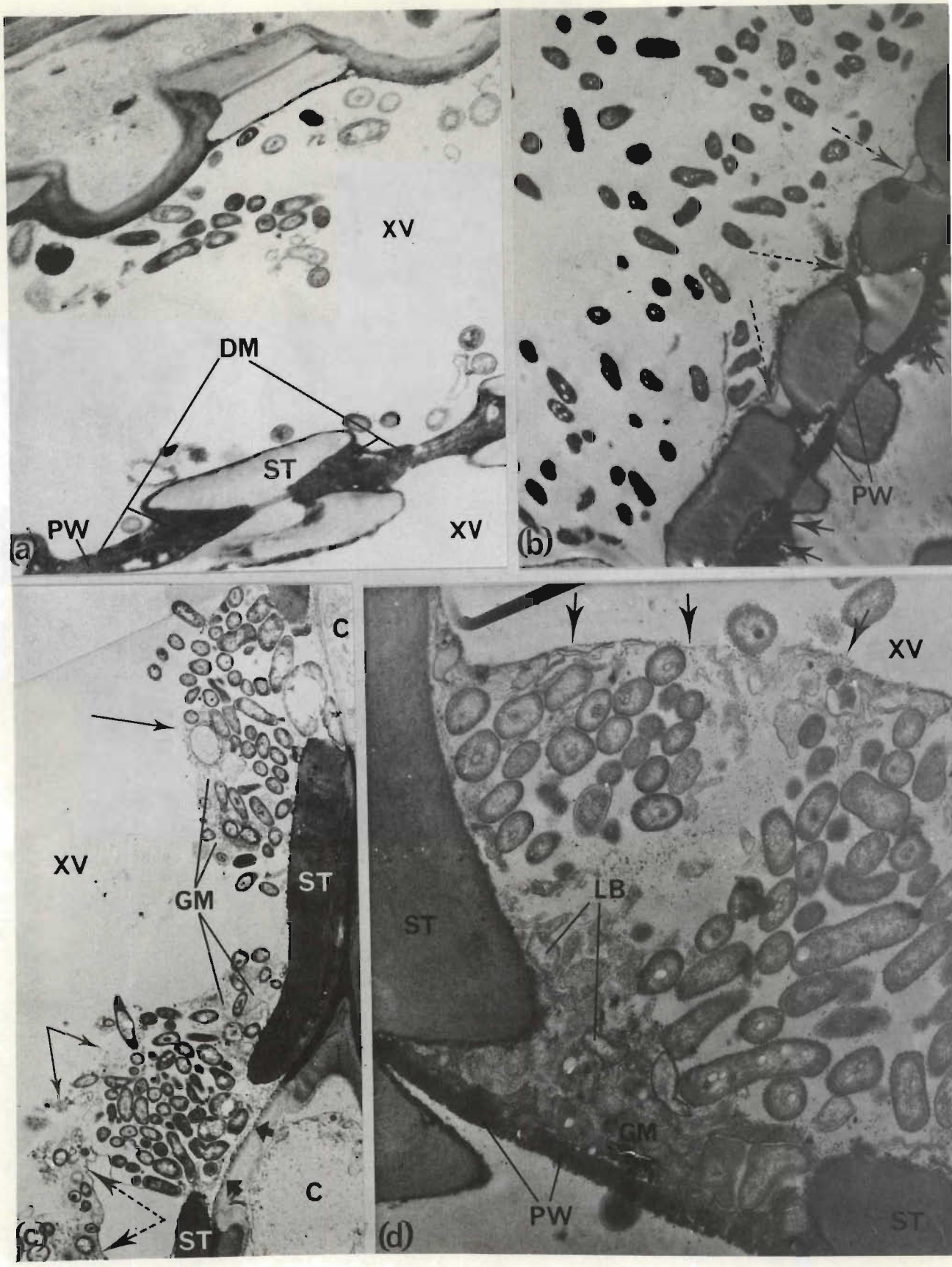

PLATE 22. (a) Small number of bacteria in xylem vessel (XV) of root 3 cm above site of tylosis collapse, 72 h after inoculation. Bacteria concentrated mainly at or near vessel walls. Note thick layer of electron-dense material (DM) overlying primary wall (PW) in pit areas and filling space between primary wall and base of spiral thickening, ST. (x 10 900.) (b) Increased number of bacteria in root vessel 3–4 cm above site of inoculation after 96 h. Note accumulated material on primary wall (PW) in interspiral region (arrows) and restriction of bacteria from pit cavities by 'membranous' interface (broken arrows). (x 9 150.) (c) Aggregation of bacteria in regions between bars of secondary thickening (ST) of invaded xylem vessel (XV) adjacent to bacterium-free root cells 3–4 cm above inoculation site after 96 h. Bacteria embedded in fine granular material (GM) surrounded either by distinct 'membrane'-like interface (broken arrows) or by less well defined interface (arrows). Note degradation of primary wall material in regions between bars of secondary thickening (thick arrows) (x 6 350.) (d) Stem tissue 18 cm above site of tylosis collapse, 96 h after inoculation, showing xylem vessel (XV) with bacteria aggregated in lens-shaped mass between bars of secondary thickening, ST. Bacteria embedded in a matrix composed largely of disrupted bacterial cells (LB) and fine granular material (GM) concentrated particularly against primary wall, PW. Note ill-defined interface between bacterial mass and clear region of xylem vessel (arrows). (x 18 300.)

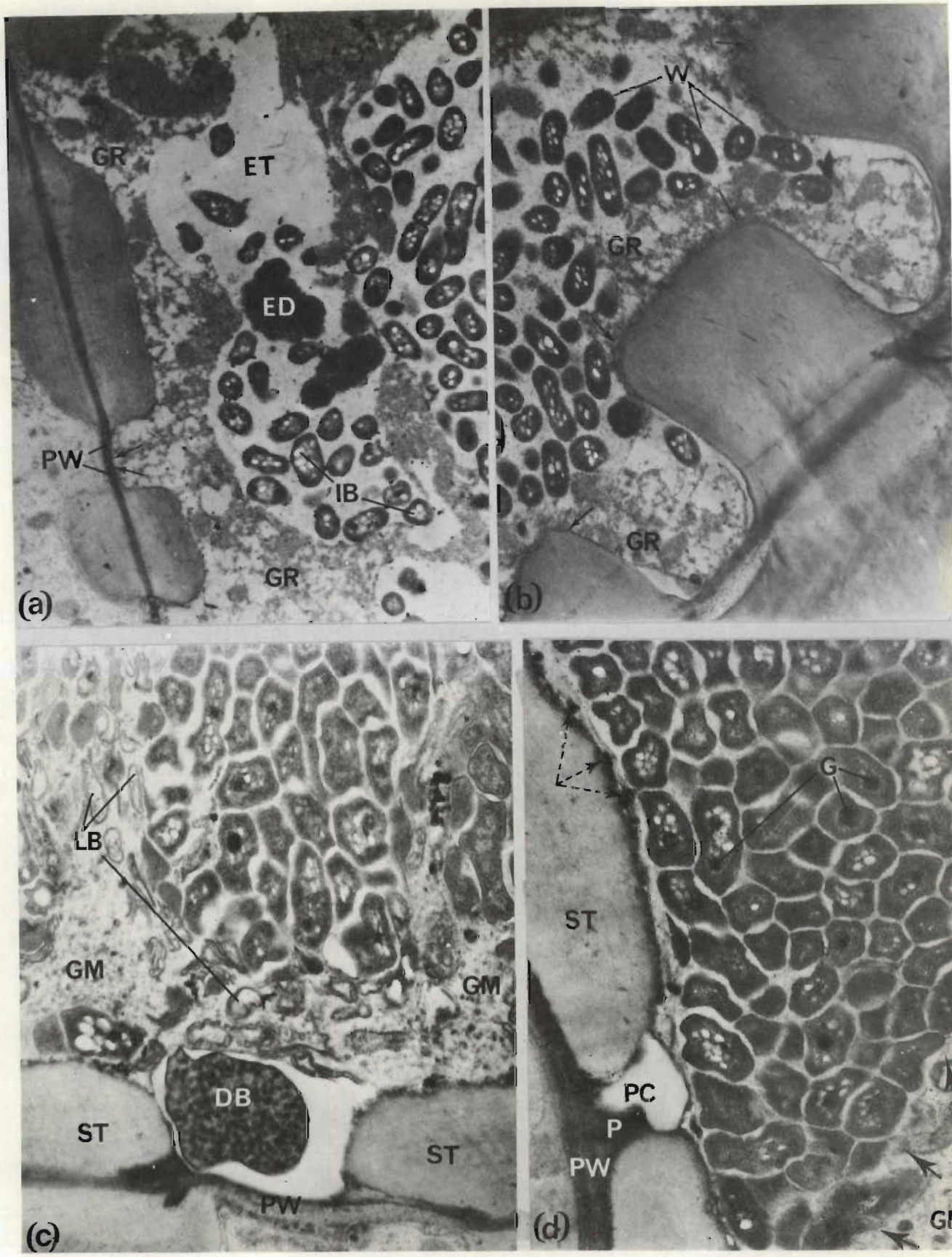

PLATE 23. Root tissue 3-4 cm above site of inoculation; (a) & (b) after 120 h, (c) & (d) after 144 h. (a) Bacteria with large inclusion bodies (IB) in relatively clear areas (ET) surrounded by loose network of fine granular reticulate material, GR. Note large aggregates of electron-dense material (ED) within clear areas, negligible vessel wall degradation, and electron-dense nature of primary wall (PW) particularly in pit region (arrows). (x 10 800.) (b) Bacteria, with scalloped cell walls (W) and large inclusions, interspersed with fine granular reticulate material (GR) that accumulates particularly adjacent to vessel wall (arrows). (x 13 900.) (c) Vessel with bacteria compressed in 'pockets' between dense masses of detritus comprising degenerated bacterial cells (LB) and fine granular extracellular material, GM. Note electron dense body (DB) filled with coarse granules in clear space bounded by bars of secondary thickening (ST), primary wall (PW) and bacterial mass. (x 18 500.) (d) Bacteria, compressed into irregular shapes, possibly prevented from entering adjacent debris-filled areas (arrows) by density of fine granular material, GM. Note absence of any visible delimiting structure. Large granules (G) occur in some bacteria and in fibrillar material (broken arrows) in close proximity to bar of secondary thickening, ST. Dense mass of material (P) is deposited on primary wall (PW) and in pit cavity (PC), in regions between bars of secondary thickening. (x 24 400.)

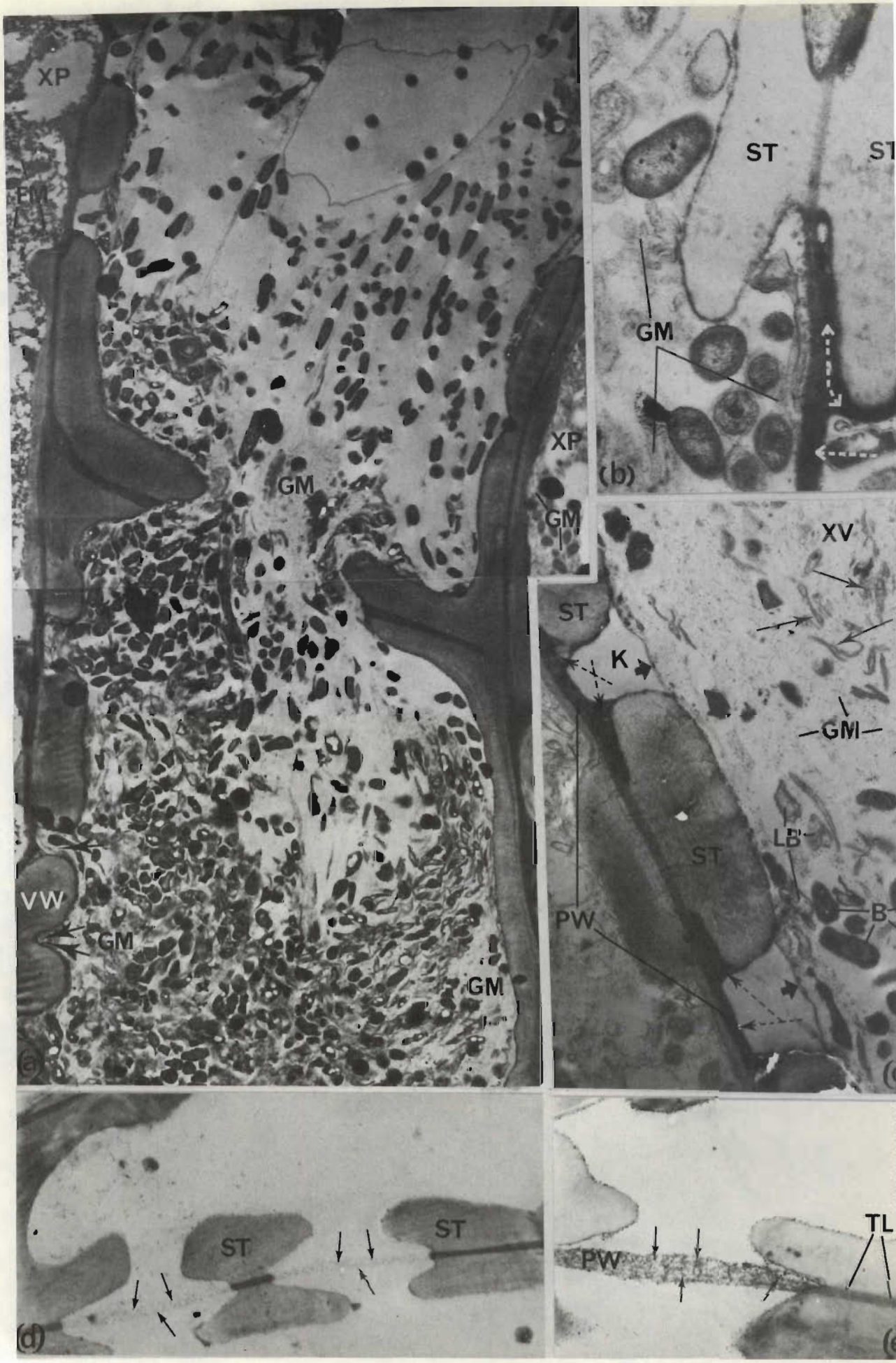

PLATE 24. (a) Bacterial passage through open end wall between vessel members in stem 18 cm above site of tylosis collapse, 144 h after inoculation. Note uneven distribution of bacteria and accumulation (arrows) of fine granular material, GM. Vessel wall shows no degradation and large masses of fibrillar (FM) and granular (GM) material accumulate in contiguous cells, XP. (x 5 820.) (b) Bacteria embedded in matrix of finely granular material (GM) in stem vessel 12 cm above site of tylosis collapse, 144 h after inoculation. Note thick layer of electron-dense material (broken arrows) deposited on primary wall between spiral thickenings, ST. (x 23 500.) (c) Viable (B) and lysed (LB) bacteria and detritus (arrows) embedded in dense finely granular material (GM) within root vessel 3 cm above site of tylosis collapse, 144 h after inoculation. Thick layer of electron-dense material (broken arrows) deposited on primary wall (PW) is separated from substances in vessel (XV) by membrane-like structure (thick arrows), resulting in clear space (K) between bars of secondary thickening, ST. (x 14 200.) (d) Vessel in healthy root tissue 3-4 cm above cut root tip after 144 h. Note hydrolysis of primary wall material (arrows) between bars of secondary thickening, ST. (x 5 450.) (e) Detail of vessel wall in healthy root tissue showing finely dispersed electron-dense granules (arrows)

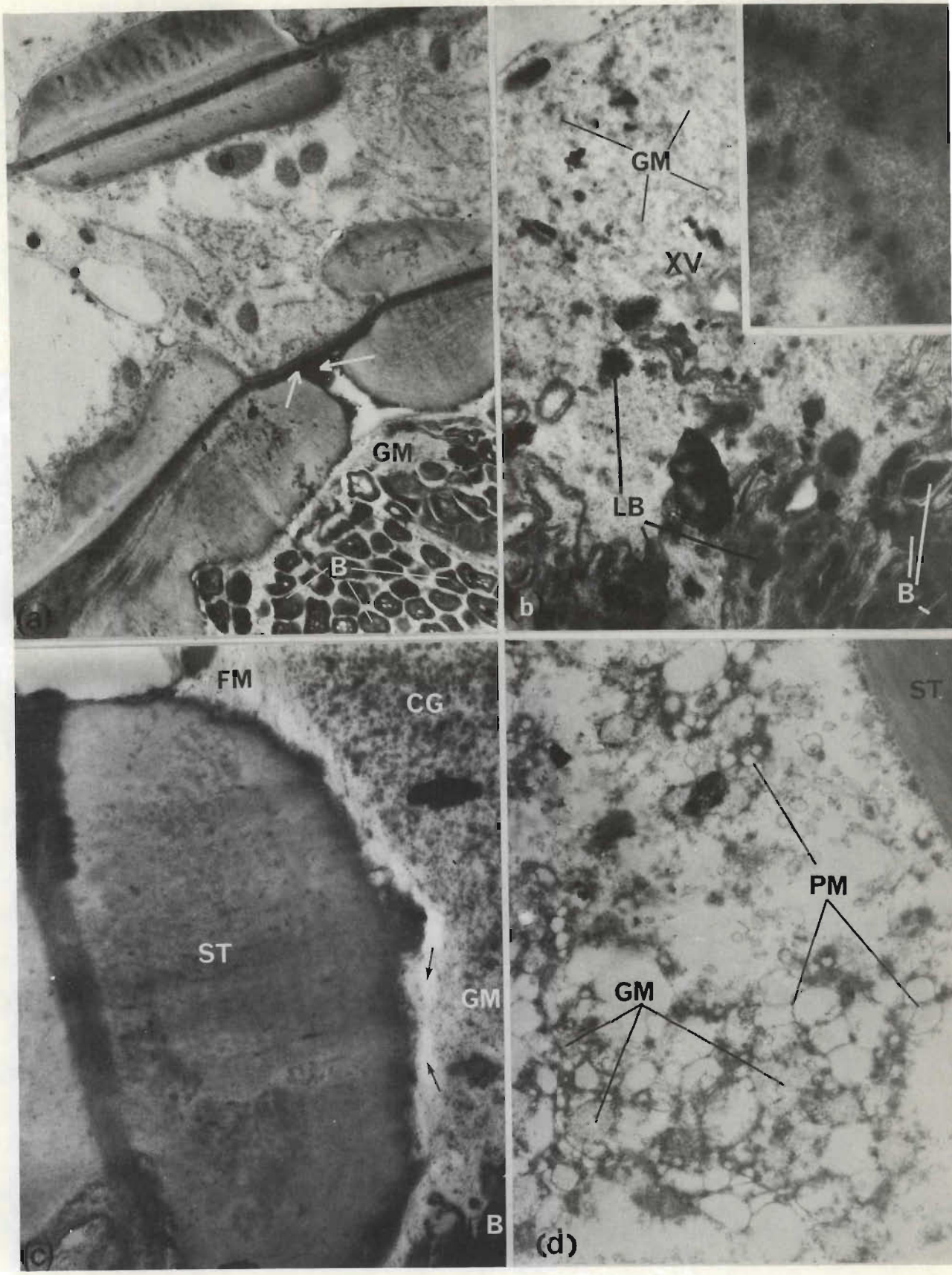

PLATE 25. Infected root tissue 3-4 cm above site of tylosis collapse; (a) after 144 h, (b)-(d) after 168 h. (a) Vessel containing compact mass of pleomorphic bacterial cells (B) embedded in dense matrix of granular material, GM. Note deposition of very dense electron-opaque material (arrows) on primary wall in interspiral regions. (x 12 600.) (b) Accumulation of bacterial cells (B), bacterial debris (LB) and fine granular material (GM) entirely filling lumen of xylem vessel, XV. (x 27 300.) Inset. Extracellular material produced by P. solanacearum in nutrient broth + 1/2 % glucose. Note close similarity of this material to the fine granular material (GM) in xylem vessel of infected plant - Plate 25 (b). (x 27 300.) (c) Xylem vessel completely occluded with mixture of coarse granular material (CG), fine granular material (GM), and fibrillar material (FM) arising from apparent degradation of surface layers of spiral thickening, ST. An electron-transparent area (arrows) lies immediately adjacent to spiral thickening. (x 25 100.) (d) Mixture of reticulate material (PM) and fine granular material (GM) completely occluding vessel. (x 27 300)

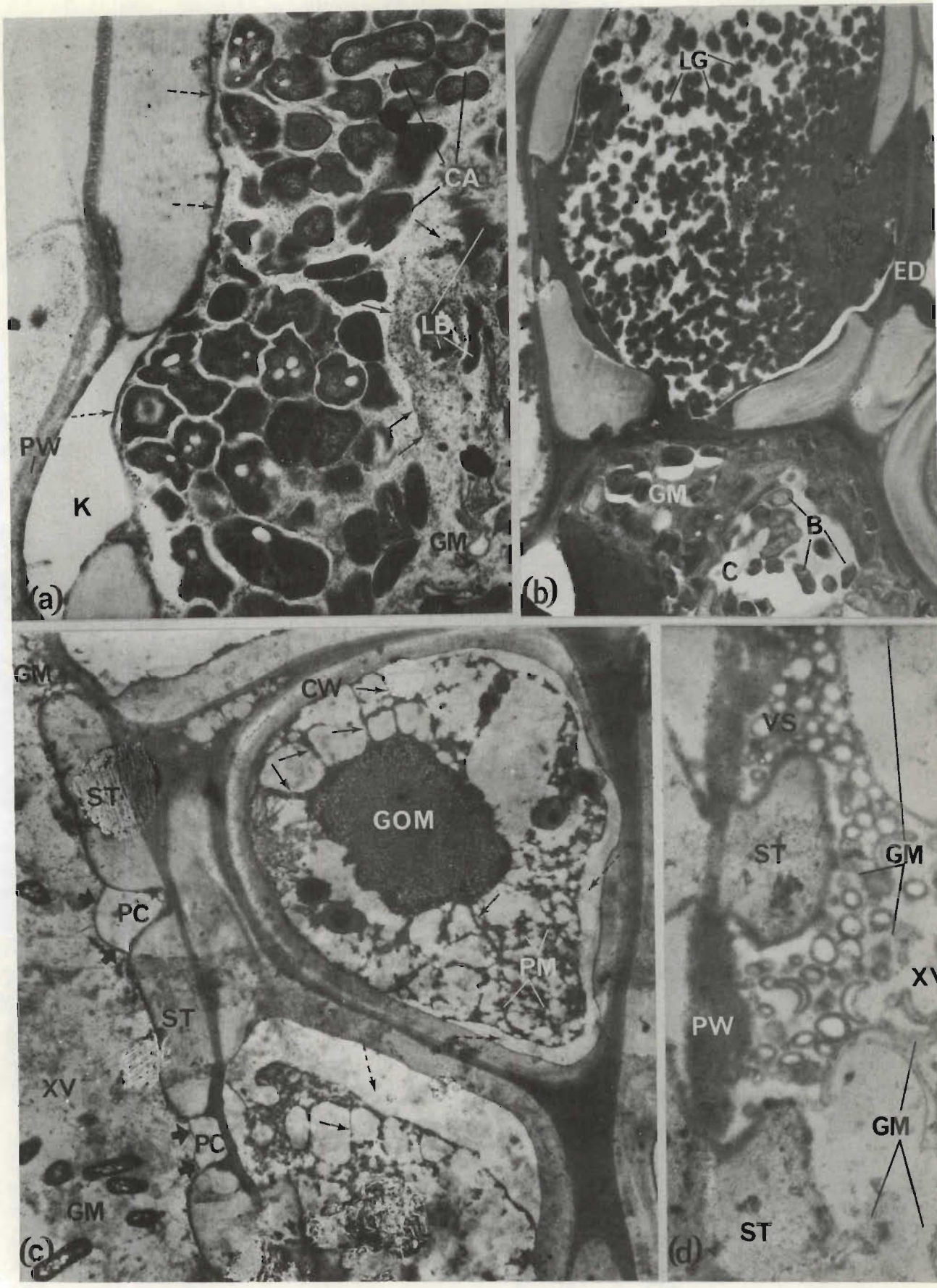

PLATE 26. (a)-(d) Infected root tissue 3-4 cm above site of inoculation after 168 h. (a) Bacteria in vessel surrounded by matrix of various substances. Granular material (arrows) and disrupted bacteria (LB) fill the bacterium-free area. Many bacteria, surrounded by electron-transparent material (CA) possibly of a capsular nature, show extreme pleomorphism. Note layer of electron-dense material stretched between, and deposited on, inner surface of bars of secondary thickening (broken arrows), clear area (K) in pit cavity and apparent lack of primary wall (PW) degradation. (x 22 150.) (b) Transverse section showing vessel almost plugged with large granules, LG. Note electron-dense material (ED) deposited on primary wall of adjacent cell. Lower cell (C) partially filled with bacteria (B) embedded of matrix of fine granular material, GM. (x 9 000.) (c) Vessel (XV) completely filled with fine granular material (GM) separated from primary wall by 'membrane'-like structure (thick arrows) overlying relatively clear areas in pit cavities (PC) between apparently unaffected bars of secondary thickening, ST. Adjacent cells contain central dense mass of fine granular material (GOM) connected to cell wall (CW) by strands (arrows). In some places a clear area separates reticulate material (PM) from the cell wall (broken arrows). (x 9 300.) (d) Vessel (XV) filled with fine granular (GM), and vesicular (VS) material. Note swelling and shredding of primary wall (PW) between spiral thickening, ST. (x 19 300.)

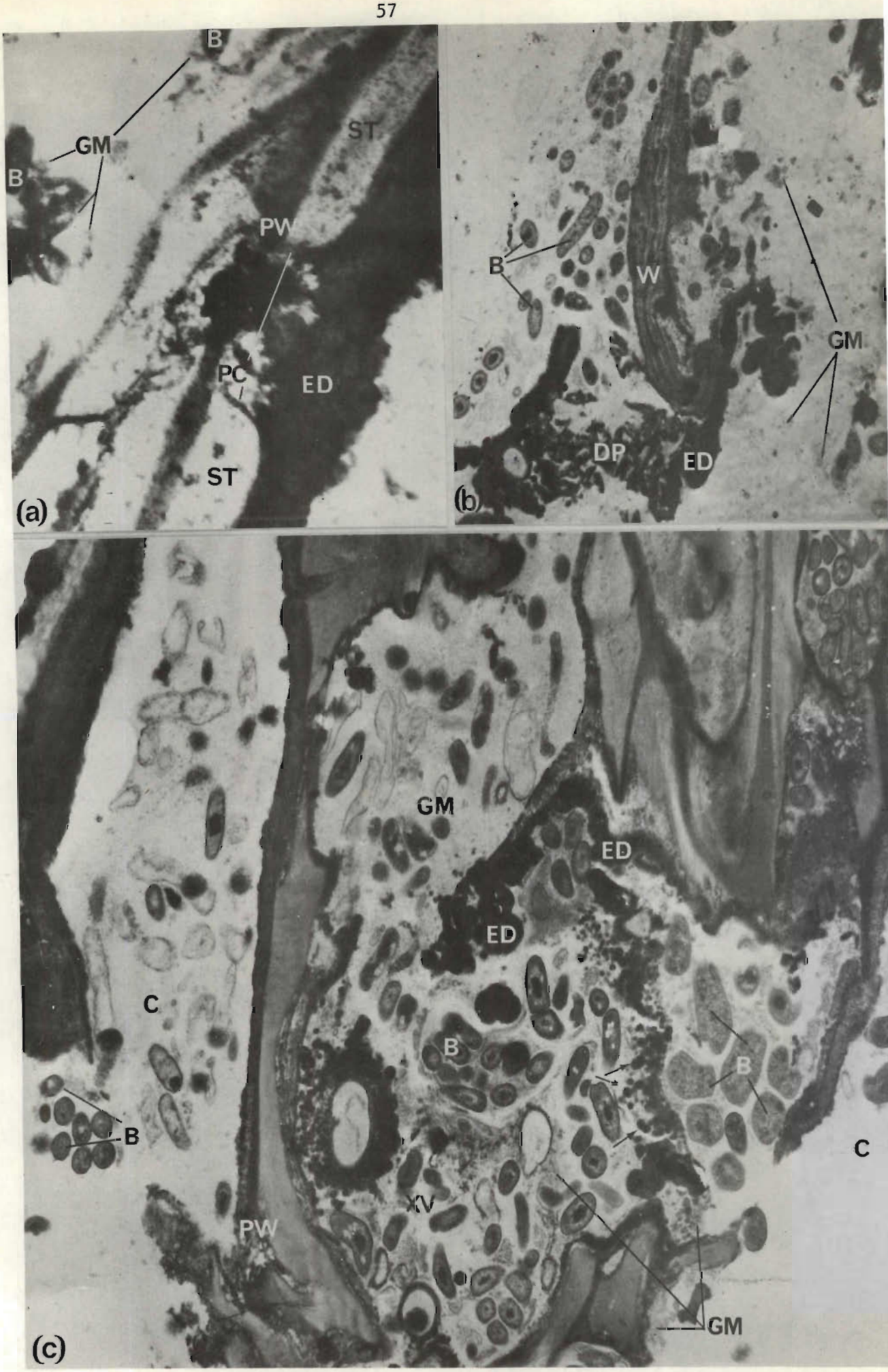

PLATE 27. (a)-(c) Infected root tissue 3-4 cm above site of inoculation after 192 h. (a) Advanced stage of tissue degradation showing dissolution of primary wall material (PW) and accumulation of large amounts of very darkly-staining material (ED) against bars of secondary thickening (ST) and in pit cavity, PC. Bacteria (B), which appear to be degenerating, are associated with fine granular material, GM. (27 300.) (b) Disruption of tissue during final stages of pathogenesis. Note: large amounts of electron-dense material (ED) accumulated in regions of wall collapse; bacteria (B) and tissue breakdown products (DP) associated with collapsing walls (W) and presence of fine granular material (GM) in disrupted vessel. (x 8 250). (c) Large lysigenous cavity resulting from wall breakdown in vessel (XV) and adjacent cells, C. Note dissolution of primary wall (PW) and accumulation of bacteria (B), fine granular material (GM), large electron-dense granules (arrows) and electron-dense amorphous material (ED) in disrupted, degenerating tissue. (x 13 500.)

vascular pathogens such as Bacillus tracheiphilus (Erwinia tracheiphila) and Bacterium campestre (Xanthomonas campestris). Disease development is thought to be influenced by the conditions under which the host is grown (107). It is possible that the method and site of inoculation may also influence the course of the disease.

Most of the reported work on histopathological aspects of bacterial wilt of tomato has been based on examination of stem tissue and occasionally petiole and leaf tissue of needle-prick, stem-inoculated plants, usually only after onset of wilting (51,107). The early stages of tomato infection with P. solanacearum, especially through the root system, do not appear to have been examined in detail. In the present study bacteria were first observed in vessels of the root in sections cut 6-7 cm from the inoculation site approximately 72 h after inoculation [Plates 21(a), 21(c), and 22(a)]. Thereafter bacterial numbers increased rapidly in the vessels of the root [Plates 22(b) and 22(c)] and bacteria were observed in the large stem vessels, 96 h after inoculation [Plate 22(d)], approximately 16 cm above the inoculation site. At this stage of pathogenesis the plants had already started to wilt. It is conceivable that needle-prick inoculation of the stem would introduce the bacterium directly into the vessels in which movement of the bacterium appears to be more rapid than in the vessels of the root; the bacteria spreading approximately 7 and 3 cm vertically in the stem and root vessels respectively, in 24 h. However, at no time, or in any region of the stem, did the bacteria become as numberous in the vessels of the stem as in the vessels of the root.

The method of inoculation used in this study also permits free access of bacteria to the vessels; however, it is possible that, while plants are transferred to growth flasks, after cutting the main root under water, the water columns in vessels of this root are broken. This would prevent these vessels from serving as suitable avenues of

bacterial entry to the plant. Alternatively, the observation, that during the initial 24h period after inoculation only few of the cells adjacent to large vessels contained bacteria [Plates 13, 14(a), 14(c), 14(d) and 15] may indicate that at any particular stage of development of the host plant only certain cells are physiologically predisposed for invasion.

The apparent lack of damage to walls of invaded root cells during initial stages of pathogenesis [Plate 17] possibly reflects a low level of cellulolytic and pectinolytic enzyme activity while bacterial numbers are still relatively small. P. solanacearum is not regarded as being highly cellulolytic (60) especially when compared to other organisms such as the fungi Trichoderma viride and Myrothecium verrucaria (59). However, after bacterial numbers increase considerably degradation of primary wall material in the vessel is apparent [Plate 25(a)]. This enzyme activity verifies the results of previous in vitro (40, 49, 52, 65), and in vivo (50), experiments with P. solanacearum.

The observed concentration of bacteria at, and their orientation toward, the bordered pits between vessels and adjacent cells [Plates 18(a) and 22(c)] or between contiguous vessels [Plate 22(d)] indicates that the bacteria are either attracted to these areas by substances diffusing into the vessel from the adjacent living cells, or that they are simply drawn to these areas along an osmotic pressure gradient. A similar situation has been reported in a light-microscopic study on carnations infected with the bacterial vascular pathogen P. caryophylli (82). Compartmentilization of bacterial masses [Plates 18(b), 22(b) and 22(c)] has likewise been reported by these authors, but in parenchyma cells and not in vessels, as observed in the present study. The origin, nature, and function of such compartments could not be explained.

The pleomorphism exhibited by the bacterium within host tissue [Plates 17(a), 18(a), 18(b), 20(a), 22(c), 23(c) and 23(d)] has been reported also in banana roots infected by P. solanacearum (11). However, the thicker cell walls of bacteria entrapped in either globular or fibrillar material described by these authors, was not observed in tomato plants. Elongated bacteria, possibly similar to the filamentous 'minicell' -bearing forms of Erwinia amylovora (45), were occasionally observed in cells and tyloses [Plates 18(a) and 20(a)] of P. solanacearum-infected tomato plants. The scalloped appearance of the wall of some bacteria [Plate 18 (d)] is similar to that of P. phaseolicola in bean tissue (103) and to that of the bacterium causing Pierce's disease of grapes (79, 89). A well-defined nuclear region and densely ribosomal cytoplasm, similar to that of P. phaseolicola in susceptible beans (103), was observed in some bacterial cells [Plate 18(d)].

The presence of large inclusion bodies of reserve food materials within many of the bacterial cells [Plates 17(b) and 18(c)] indicates that the bacteria are metabolically active in the host tissue, even when they are compressed due to pressure of numbers [Plates 23(c) and 23(d)].

Formation of tyloses both by invaded cells [Plates 13(c), 14(a), 14(c), 14(d), 15(a), 15(b), 15(c), 15(d), 19(a), 19(b), 20(a) and 20(c)] and by non-invaded cells [Plates 19(d) and 21(b)] of infected plants and their absence in healthy plants, suggests that, although infection stimulates the host cells to produce these structures, the physical presence of bacteria is not necessary. It seems that infection with P. solanacearum incites the host plant to produce higher levels of indole acetic acid (IAA) and other growth substances (88) which, when present in abnormal amounts, may stimulate tylosis formation (10, 102). Higher levels of IAA in P. solanacearum-infected plants are well

documented (88, 99, 100), and it is thought that the host synthesizes most of this compound during the critical initial stages of pathogenesis, while synthesis of IAA by the pathogen becomes important only at advanced stages of the host-parasite relationship (100).

Apparently bacteria enter a preformed tylosis at any stage of its development since many large tyloses are seemingly bacterium-free [Plates 14(c), 14(d), 15(a), 15(b) and 20(a)]. The origin of tyloses is possibly related to the increased IAA levels in P. solanacearum-infected plants (100). Tyloses may play an important rôle in preventing spread of bacteria by occlusion of vessels, although in the tomato plants used in this investigation affected vessels remained occluded by intact tyloses for 48 - 72 h only. Such structural defence may be augmented by the partial blocking effect of the tyloses after collapse [Plate 21(d)]. On the other hand sudden release of large numbers of bacteria from disrupted tyloses may cause rapid and successful colonization of the xylem vessels to occur.

As the layer of amorphous material on the inner surface of the tylosis wall resembles the material sloughing from the surface of the bacterial cells within tyloses [Plate 20(b)] it seems likely that this layer is composed partly, at least, of bacterial extracellular slime. Since tyloses balloon into the vessels in the absence of bacteria it is obvious that the pressure in vessels is lower than that within the tyloses. Thus any materials of low weight, either formed within the tyloses or entering them from the cell of origin, would accumulate against the wall. As the collapse of tyloses and onset of wilting in the host are almost contemporaneous it seems certain that accumulated non-cellular materials of both host and bacterial origin, together with bacterial cells, are released into the vessels and constitute a major cause of the wilt symptom. The contribution to this effect by tyloses in the vessels is probably a minor or

The factors governing tylosis collapse are unknown but may include

degradative action by bacterial extracellular enzymes. However, additional factors must be involved since non-invaded tyloses also collapse [Plates 21(b) and 21(d)], albeit later than those that are invaded. Thus collapse and disruption of bacterium-containing tyloses, after secondary proliferation [Plate 21(c)], may result from degradation of their walls by the combined action of both bacterial and host enzymes, in addition to the increasing pressure exerted by the multiplying bacterial cells, their extracellular materials and the accumulating host degradation products.

The apparent plasticity of intact tyloses and the structural similarity of the secondary proliferations in disrupted non-invaded tyloses [Plate 21(d)] to lipid-depleted thylakoid membranes isolated from tobacco (47), would seem to confirm the presence of membrane material in the tylosis wall.

Whether or not the same pattern of host invasion, as described above, occurs in natural root infections in the field is not known. Once in the xylem vessels the vertical rate of spread of the pathogen is comparable to that of other vascular bacterial pathogens (13, 19, 125).

Notable features of this investigation are the large amounts and wide variety of non-cellular material found in the vessels and adjoining cells of diseased plants [Plates 22(d), 24(a), 24(b), 24(c), 25(a), 25(b), 25(c), 25(d), 26(a), 26(b), 26(c), 26(d), 27(a), 27(b) and 27(c)]. These materials begin to form immediately after the bacteria enter the cells and continue to increase rapidly in amount until many of the vessels are completely filled [Plates 25(b), 25(c), 25(d), 26(b) and 26(c)]. This tends to support the theory (51, 52) that wilting in P. solanacearum-infected plants is due primarily to restricted water passage through the tissues, caused by plugging of the vessels with the extracellular slime produced by the organisms.

However, at the electron microscope level vessel plugging is seen to be more complex than suggested by these authors since, as indicated above, many structurally different materials occur in occluded vessels.

The release of fibrillar material from degenerating vessel walls [Plate 25(c)] and tylosis walls [Plate 19(b)], indicates that plant degradation products also contribute to the plugging of vessels. As only limited amounts of this material are observed it appears that in P. solanacearum-infected plants, vessel wall breakdown products, although contributing, do not form an important component of the vessel plugging material. This supports the theory that pectic or cellulolytic enzymes are not the primary agents involved in the wilting mechanism of P. solanacearum (49). The various other materials, with either reticulate [Plates 25(d) and 26(c)], coarsely granular [Plate 26(b)], or globular [Plate 26(d)] structure, that occur in occluded vessels were not identified.

Husain and Kelman (51, 52) are of the opinion that the extracellular slime produced by P. solanacearum is the principal factor involved in wilting of infected tomato plants. These authors claimed that, contrary to the findings of Grieve (35), plugging of vessels by masses of bacterial cells is not the primary cause of wilting. To substantiate their claim they put forward the argument that histological observations on the stems and petioles of completely wilted plants did not indicate that all, or a majority of the vessels, were entirely blocked by masses of bacterial cells (51). They did concede, however, that masses of bacterial cells surrounded by slime may contribute to wilting.

Since the fine granular material observed in invaded vessels [Plates 23(c), 24(b), 24(c) and 26(a)] is produced by P. solanacearum on artificial media also [Plate 25(b), inset], it appears to be the extracellular slime described by Husain and Kelman (51). As this is

the most commonly occurring substance in infected plants it is probably the major contributing factor to vessel plugging, and therefore to wilting of the host, as suggested by Husain and Kelman (51).

In the present study also only few vessels in the stem tissue of wilted, diseased plants were seen to be entirely occluded with masses of bacterial cells. However, in the roots of wilted plants the majority of vessels are so filled with bacteria that the bacterial cells are compressed into almost unrecognizable shapes [Plates 23(c) and 23(d)]. Failure of the bacteria to move into adjacent slime-filled areas relatively free of bacterial cells [Plates 23(c), 23(d), 25(a) and 26(a)] seems to indicate that the slime material is so viscid that it resists compression by the massed bacteria and is impenetrable to them. It appears likely that such densely packed masses of bacterial cells would restrict passage of water through the roots and thus be an important cause of wilting. Many of the bacteria within these compressed masses were disrupted [Plates 23(c) and 25(b)] indicating that bacterial detritus may also contribute to the occlusion of vessels.

An interesting and possibly significant ultrastructural observation is that a thick layer of very dense electron-opaque material accumulates on the primary wall between the spiral thickenings and often fills the pit-cavities between abutting invaded vessels [Plate 24(b)], adjoining invaded and non-invaded vessels [Plate 22(a)], and contiguous invaded vessels and adjacent non-invaded cells [Plates 23(d), 24(c) and 25(a)]. Such a layer does not occur in the pit region of healthy plants in which the primary wall is composed of a loose network of fibrillar and finely granular material [Plates 24(d) and 24(e)]. It is conceivable that this dense layer may prevent entry of water and nutrients into the cells from adjacent invaded vessels, thereby eventually causing their death. If many such cells are killed it would lead to wilting and ultimate death of the host plant. This material possibly corresponds

to the dense material observed in P. solanacearum-infected banana plants and identified by Buddenhagen and Takata (11) as melanin. In banana roots, however, the material was observed in parenchyma cells adjacent to the vessels (11), whereas in the present study the electron micrographs showed the material occurred on the vessel side of the abutting walls.

During advanced stages of tissue collapse large amounts of dense electron-opaque material, possibly melanin, accumulate on the vessel walls [Plate 27(a)] and also in the lysigenous cavities formed [Plates 27(b) and 27(c)]. During cavity formation the cell walls are destroyed [Plate 27(c)], but apparently not by the pressure exerted by masses of bacteria, as suggested by Smith (107), since cell numbers were not always large [Plates 27(b) and 27(c)]. Observations in the present study indicate that vessel wall destruction [Plate 27(c)] and collapse of surrounding cells are more likely the result of bacterial enzyme activity.

It would appear that wilting in tomato plants infected with P. solanacearum is due to a combination of several factors. These include: the presence of large amounts of apparently extremely viscous bacterial slime which often completely fills the vessels, thereby effectively reducing or completely prohibiting water movement in the plant; the presence of densely compressed masses of bacterial cells in the majority of vessels in the roots; the plugging of vessels with a wide variety of unidentified materials; the blocking action of both intact and collapsed tyloses in the vessels of the roots; deposition of a dense material on the primary pit membranes between invaded vessels and adjacent non-invaded cells, in some cases filling the pit cavity, may effectively prevent movement of water and nutrients from vessels into cells, resulting in death of the cells; the presence of host breakdown products resulting from the degradative action of bacterial pectinolytic

and cellulolytic enzymes on vessel and cell walls, particularly during the later stages of pathogenesis.

CHAPTER 3

ULTRASTRUCTURAL HISTOPATHOLOGY OF TOMATO PLANTS INFECTED WITH *CORYNEBACTERIUM MICHIGANENSE*

INTRODUCTION

Bacterial canker or the Grand Rapids disease of tomato, incited by *Corynebacterium michiganense* (Smith) Jensen and first reported by Smith (104) in 1910, is an important bacterial vascular disease in South Africa. Some authors consider the organism to be strictly a wound parasite (1, 36), while others state that wounding is not necessary for infection (3, 9). Undamaged leaf and stem stomata (106) and uninjured foliar (66, 69), petiole, stem and fruit trichomes (69) are reported as suitable sites of bacterial entry into the host plant. According to Layne (69) injury to these structures, however, increases the severity and overall incidence of disease. The roots of infected plants may be either free of bacteria (9, 106) or completely invaded, especially in the pith region (9). Generally, however, the roots show little evidence of infection even if this has occurred through the root system from the soil (9). Ark (1) obtained negative results with root inoculations while Strider (115) failed to produce uniform infections by inoculating roots and suggested that in plants, growing under field conditions, roots are not a common or favoured site for infection.

Originally *C. michiganense* was thought to be primarily a phloem invader (8, 106). However, Bryan (9) subsequently reported the bacterium initially to be present in the inner vessels of the wood and only at later stages of pathogenesis in the phloem, pith and cortex of the upper plant parts where cavities are ultimately formed. The pith is often completely disrupted, particularly at the bases of petioles, which are especially susceptible (9). Some researchers, however, retained the belief that phloem invasion was the primary

feature of early pathogenesis (61, 80, 123). Dowson (21) reported the bacterium in both the phloem and xylem during early stages of disease development, but stated that, in older wood of wilting shoots, the bacteria were mainly in the spiral vessels. Layne and Rainforth (70) reported the bacterium to be associated with vascular bundles, but did not elaborate further. On the other hand Cass Smith and Goss (12) specifically claimed that it is the xylem that is primarily invaded.

In the most comprehensive study to date on the pathological histology of tomato plants infected with C. michiganense, Pine, Grogan and Hewitt (91) paid special attention to the tissue invaded during early stages of disease development and to longitudinal spread of the bacterium in the upper stem portions of petiole-inoculated plants. During the first 24 h after inoculation the bacterium invaded the xylem elements only; no movement outward from these vessels was seen even though some were almost filled with masses of bacteria. After five days the bacterium was observed in pockets adjacent to invaded xylem vessels. Some of these pockets, resulting from lateral spread of the bacteria, extended inward to the internal phloem and pith. Rothwell (98) also reported breakdown of pith adjacent to invaded conducting vessels.

According to Pine, Grogan and Hewitt (91) lateral movement of the bacterium outward into the cortex was slow and followed a similar pattern to the inward movement into the pith. At no time did these authors observe any extended longitudinal movement of the bacterium in sieve tubes or in other phloem cells. The rapid multiplication of bacterial cells lodged in small clumps between the spiral thickenings, soon resulted in the lumina of many xylem vessels becoming completely filled with large numbers of the organism. Lateral spread, which was most rapid between contiguous vessels of the same bundle, was initiated

at the sites of bacterial aggregation where the primary cell wall was apparently weakened. Bacteria were observed in the intercellular spaces in areas adjacent to sites where initial accumulation between spiral thickenings had occurred. This was ascribed to dissolution of the pectic substances in the primary wall at these points, but the exact mechanism by which breakdown of the wall developed was not determined. These authors studied only the histopathology of diseased plants and spread of the pathogen through the plant tissue, and did not investigate the mechanism responsible for wilting associated with the disease.

Vessel plugging by various polymeric substances is the most commonly accepted explanation of the wilt-inducing mechanism in plant diseases (4, 6, 20, 42). Bacterial phytopathogens in which vascular occlusion has been implicated in wilting include Erwinia tracheiphila and Phytomonas (Xanthomonas) stewarti (37), Xanthomonas phaseoli (71) and Pseudomonas solanacearum (10, 51). Hodson, Peterson and Riker (42) propose that wilting is possibly correlated with the molecular weight of the polymer involved, and that these substances mechanically plug vessels.

According to Lelliott (72) the plant pathogenic corynebacteria may be grouped into two categories, one containing organisms that cause vascular wilts the other containing those species that produce fasciations or hypertrophies. Corynebacterium michiganense belongs to the former category and forms a single group with the closely related C. insidiosum and C. sepedonicum.

Two theories have been proposed concerning the wilt mechanism in phytopathogenic Corynebacterium species, namely, the mechanical plugging theory and the toxic action theory (114). Lelliott (72) states that although some circumstantial evidence indicates that certain coryne-bacteria may produce wilt inducing toxins, the wilts caused by these

species are probably the result of mechanical plugging of the vessels and enzymatic disruption of the water conducting tissue.

Work on C. sepedonicum in tomato and C. insidiosum in lucerne (109), C. flaccumfaciens in beans (128) and C. michiganense in tomato [Patino-Mendez, cited by Rai and Strobel (94)], led the researchers to suggest that vessel plugging was the major cause of wilting observed in their experimental plants. Ries (96) is of the opinion that the mechanism of wilt caused by C. insidiosum in lucerne may be vessel plugging, in addition to some other unspecified mechanism. It has been suggested that a bacterial secretion, which is either mechanically active or feebly toxic, might be responsible for the symptoms produced in tomato by C. sepedonicum (86).

Other authors consider toxins to be more important and express the opinion that the polysaccharides (glycopeptides) produced by C. michiganense (92, 93, 94), C. sepedonicum (39, 92, 116, 117, 118, 119) and C. insidiosum (92, 117) are phytotoxins that cause wilting by damaging various host cell membranes, causing a water imbalance in the host, rather than by mechanically plugging the vessels of infected plants. These phytotoxic polysaccharides are all nonspecific, antigenic, and serologically related (92). According to Rai and Strobel (94) electron microscopy of the vascular tissue of wilted C. michiganense-toxin-treated tomato plants shows no indication of occlusions in the vessels or in any of the other cells in this region. Unfortunately these authors presented no electron micrographs. Strobel and Hess (118) published electron micrographs of C. sepedonicum-infected tomato stem tissue. However, their study was concerned mainly with membrane damage to chloroplasts and mitochondria, disruption of plasmalemmae and cell walls in non-conducting tissue and no reference was made to vessel occlusion.

Strobel (117), discussing C. sepedonicum and C. insidiosum, concluded that, although there is good evidence for a toxic effect on cellular membranes, the possibility still exists that vascular plugging occurs in infected plants and that bacteria, bacterial slime and various host polymers could all be involved in plug formation.

The present electron microscopic study investigates both the spread of C. michiganense in the tissues of young infected tomato plants and progressive tissue breakdown during pathogenesis.

MATERIALS AND METHODS

Twenty tomato (Lycopersicon esculentum Mill."Homestead") plantlets were grown from healthy seed until approximately 15 cm tall and then transferred to flasks containing modified Hoagland and Arnon (41) nutrient solution as described in Chapter 2. In this experiment, however, plant inoculations were made, after a one week adaptation period, by severing with a sterile scalpel, 0,5 cm from the base, a petiole located approximately midway between the crown and stem apex and applying, with a sterile pipette, a drop of Corynebacterium michiganense suspension, 10^5 bacteria/ml distilled water, to the cut surface of the petiole stump. The ten control plantlets were similarly treated except that a drop of sterile distilled water was applied instead of the bacterial suspension.

A similar procedure to that described in Chapter 2 was used to follow both the spread of the organism in the host tissues and the progressive stages of tissue damage. In this case a single test and a corresponding control plant were removed every 24 h, over a period of 240 h, and cut transversely, into 5 mm pieces, from the apex of the stem to the tip of the root. These tissue portions were fixed, dehydrated and plastic-embedded in sequence as described in Chapter 1.

Longitudinal and transverse sections were cut on a Reichert OMU3 ultramicrotome and stained for electron microscopy as described in Chapter 1.

RESULTS

In the sections examined 24 h after inoculation the bacterium is found in small numbers restricted to a few vessels of the stem, 2 cm below attachment of the inoculated petiole, mainly in close association with the vessel wall [Plate 28(a)]. Forty-eight hours after inoculation spread of the organism had progressed to approximately 3,5 cm below the base of the inoculated petiole, the bacterium passing through the open end walls of the vessel elements [Plate 28(b)]. At this time the number of bacteria in the xylem vessels, 2 cm below the attachment of the inoculated petiole, had increased significantly compared to the numbers seen 24 h previously [Plate 28(c)]. The bacteria partially fill the lumen of the vessel and enter between the spiral thickenings, causing the primary wall to bulge slightly into the adjacent non-invaded vessel [Plate 28(c)]. During the next 24 h period bacterial movement through the vessels in the stem progresses to a point 5 cm below the inoculated petiole and bacterial numbers, between this point and the petiole stump, increase as shown in Plate 28(d). A relatively bacterium-free region separates those bacterial cells that lodge between the spiral thickenings of the vessel walls and those that aggregate in a central position in the lumen of the vessel [Plate 28(d)].

Ninety-six hours after inoculation bacteria are observed for the first time in vessels of the stem at positions up to 2,5 cm above the inoculated petiole, while downward movement has progressed to 8,5 cm below the site of inoculation. At this time the vessels, 2,5 cm below the site of inoculation, are filled with masses of bacteria and some

fibrillar material [Plate 29(a)]. The numbers of bacteria in the interspiral regions increase, and may cause the partially degraded primary walls to bulge into the contiguous non-invaded vessel [Plate 29(a)] and rarely into the adjacent bacterium-free parenchyma cells [Plate 29(b)].

The reaction of the primary walls to the presence of bacteria varies considerably during the early stages of pathogenesis [Plates 28(c), 29(a), 29(b) and 29(c)] and bulging of the walls, where it occurs, is usually more pronounced between contiguous invaded and non-invaded vessels that it is between invaded vessels and adjacent non-invaded parenchyma cells [Plates 28(c) and 29(a)]. In this respect the bulging seen in Plate 29(b) is rare. In the xylem parenchyma cells adjoining invaded vessels the cytoplasm rapidly degenerates [Plates 29(a) and 29(b)].

Swelling and shredding of the primary wall of invaded vessels, first observed in sections cut 96 h after inoculation [Plate 29(c)], are common features of this disease and are seen repeatedly as pathogenesis progresses. Between contiguous vessels, either or both invaded, the adjoining primary walls swell and shred [Plates 31(a), 32(d), 33(b), 33(d), 34(b) and 34(c)]. In cases where an invaded or non-invaded parenchyma cell adjoins an invaded vessel it is only the primary wall of the vessel that undergoes these changes, the wall of the parenchyma cell remaining, initially at least, apparently unaffected [Plates 29(c), 30(a), 30(c), 30(d), 37(a), 37(b), 37(c) and 37(c) - inset]. During this process of swelling and shredding large amounts of fibrillar material may be released and in many cases the bacteria occur in cleared areas within the penetrated and separated swollen network of fibrillar material [Plates 29(c), 30(a), 30(c), 31(a), 32(d), 33(d) and 34(b)]. In some instances the swollen wall is not penetrated by the bacteria [Plate 32(a)].

Although portions of the 5 mm lengths of tissue, cut from the entire length of the plant, continued to be examined, it was found that the progressive stages of pathogenesis, observed in the tissue 2-3 cm below the site of inoculation, were representative of changes in other parts of the plant and therefore all subsequent electron micrographs are, unless otherwise stated, of tissue from this position in the host.

Continued breakdown of vessel primary wall structure, between 96 - 120 h after inoculation, results in the spiral thickenings, often still attached to portions of the degenerated primary wall, coming adrift, thereby facilitating bacterial entry into the space which develops between the degenerating primary wall and the wall of an adjacent parenchyma cell [Plate 30(a)]. This space continues to enlarge during the next 24 h [Plate 30(b)], due to bacterial activity on the vessel primary wall material [Plate 30(c)]. The bacterium appears able also to separate the bases of spiral thickenings from their attachment to the primary wall [Plate 30(d)]. At this stage of pathogenesis, 144 h after inoculation, the bacteria were observed in sections cut from the stem 12 cm below and 7 cm above the inoculated petiole.

As mentioned above swelling and shredding of walls are common features and in some cases the primary walls between contiguous vessels were seen to be considerably swollen 144 h after inoculation [compare Plates 31(a) and 31(a) - inset]. Similar phenomena are seen where a vessel and parenchyma cell abut [compare Plates 32(a) and 32(b)]. Occasionally tyloses are observed bulging into [Plate 31(a)] and, in some cases, completely bridging the lumen of the vessel, being wedged between the spiral thickenings [Plate 31(b)]. At this time after inoculation small numbers of bacteria were seen in a few degenerating xylem parenchyma cells adjacent to invaded vessels [Plate 31(c)].

Some bacteria in close contact with vessel primary walls, at positions between spiral thickenings, are surrounded by a relatively wide electron-transparent zone, possibly indicating the presence of capsular material [Plates 31(d) and 31(e)]. An electron-dense layer of fine granular material, in which the bacteria are occasionally partly embedded, accumulates against the primary wall [Plate 31(e)].

Certain regions of the primary walls of vessels are sometimes entirely destroyed without becoming swollen and penetrated by the bacteria [Plates 32(c) and 33(b)]. Alternatively the contiguous primary walls may rupture, without being penetrated or markedly degraded, enabling the bacteria to move freely between the adjacent vessels [Plate 33(a)]. It is at about this time, 144 h after inoculation, that the test plants first show signs of wilting.

In addition to the primary wall material the bars of secondary thickening are apparently degraded during advanced stages of pathogenesis as indicated in sections cut 168 h after inoculation [Plate 34(a)]. The spiral thickenings may remain attached to the residual primary wall material which, at this stage of disease development, forms convolutions into which the bacteria pass [Plate 34(b)]. Swelling and shredding of contiguous vessel primary walls occurs also in apparently non-invaded vessels in which even the bases of the bars of secondary thickening may be affected [Plate 34(c)].

At this time the bacteria are in the vessels at the crown and stem apex, 14 cm below and 15 cm above the site of inoculation respectively, and spread laterally from vessel to vessel in the vascular bundles. The bacterial cells are not evenly distributed in or among the vessels [Plate 35(a)]. In addition to vessels with spiral thickening vessels with scalariform secondary walls are also invaded [Plate 35(b)]. In the outermost vessels of a xylem bundle bacteria aggregate in the spaces between bars of secondary thickening causing the primary wall

to form protruberances that bulge into the lumen of the adjacent non-invaded parenchyma cell some of which are seen to be ruptured with released bacteria in the adjacent parenchyma cell [Plate 35(c)]. A coarse, granular, electron-dense material accumulates within the surrounding degenerated parenchyma cells [Plates 35(c) and 35(d)].

At this stage of pathogenesis, 168 h after inoculation, the test plants are severely wilted and the primary walls between many contiguous vessels and parenchyma cells have disappeared completely, enabling the bacteria to pass freely between coils of the detached spirals that remain intact among the masses of bacterial cells [Plates 36(a), 36(b) and 36(c)]. In scalariform vessels the bacteria occasionally aggregate in distinctly demarcated areas against the bars of secondary thickening [Plate 36(d)].

The bacterium appears to multiply rapidly in xylem parenchyma cells when these lie between vessels [Plates 37(a) and 37(c)], however, the primary wall of the parenchyma cell remains relatively unaffected [Plates 37(b), 37(c) and 37(c) - inset]. Even under these circumstances it is primarily the outer layers of the xylem vessel wall that are degraded, the wall of the parenchyma cell and the inner layers of the vessel wall initially remaining virtually unaffected [Plates 37(a) and 37(b)].

As pathogenesis progresses the bacteria spread laterally to the outermost vessels of a bundle as previously mentioned. In some cases, however, instead of bulging into the adjacent parenchyma cell the primary wall of the vessel disappears entirely in some regions, enabling the bacteria to move out of the vessel. The wall of the adjacent parenchyma cell becomes indented, allowing the bacteria to move into the resulting large space [Plate 38(a)]. Continued wall destruction and cell collapse leads to extensive tissue degeneration and the formation of large bacterium-filled cavities, the collapsed

cells apparently becoming compressed into a dense layer on the periphery of the cavity [Plate 38(b)]. Large amounts of electron-dense amorphous material, similar to that seen in invaded xylem parenchyma cells [Plate 31(c)], accumulate in the disrupted tissue filled with bacteria [Plate 38(c)]. From the cavities, which in some instances attain large proportions, the bacteria move between the host parenchyma cells, apparently by dissolving the cementing substances, and, by continued multiplication, cause the host cells to separate [Plate 38(d)]. The isolated cells are plasmolysed and the cytoplasmic contents degenerate [Plate 38(d)].

At this stage of pathogenesis, 168 h after inoculation, the phloem tissues, especially the sieve elements, are still free from bacteria but show extensive cytoplasmic disorganization [Plate 39(a)]. The bacteria spread through the ground tissue and enter the phloem region approximately 192 h after inoculation [Plate 39(b)]. Multiplication of the bacteria between the phloem parenchyma cells causes the latter to separate and collapse, resulting in the formation of large bacterium-filled spaces adjacent to the sieve elements [Plates 39(b) and 39(c)]. Progressive degeneration of the nucleus and cytoplasmic contents of companion cells is shown in Plates 39(b) and 39(c).

After 216 h the bacteria are seen in the phloem elements, of which they fill the lumina, and occasionally between invaded elements where the middle lamella is undergoing dissolution [Plate 40(a)]. During the next 24 h the phloem cells collapse and many small vesicular structures form in the resulting cavities between the collapsed bacterium-containing cells [Plates 40(b) and 40(c)]. After this the tissue became unsuitable for electron microscopic observation as the test plants were completely collapsed.

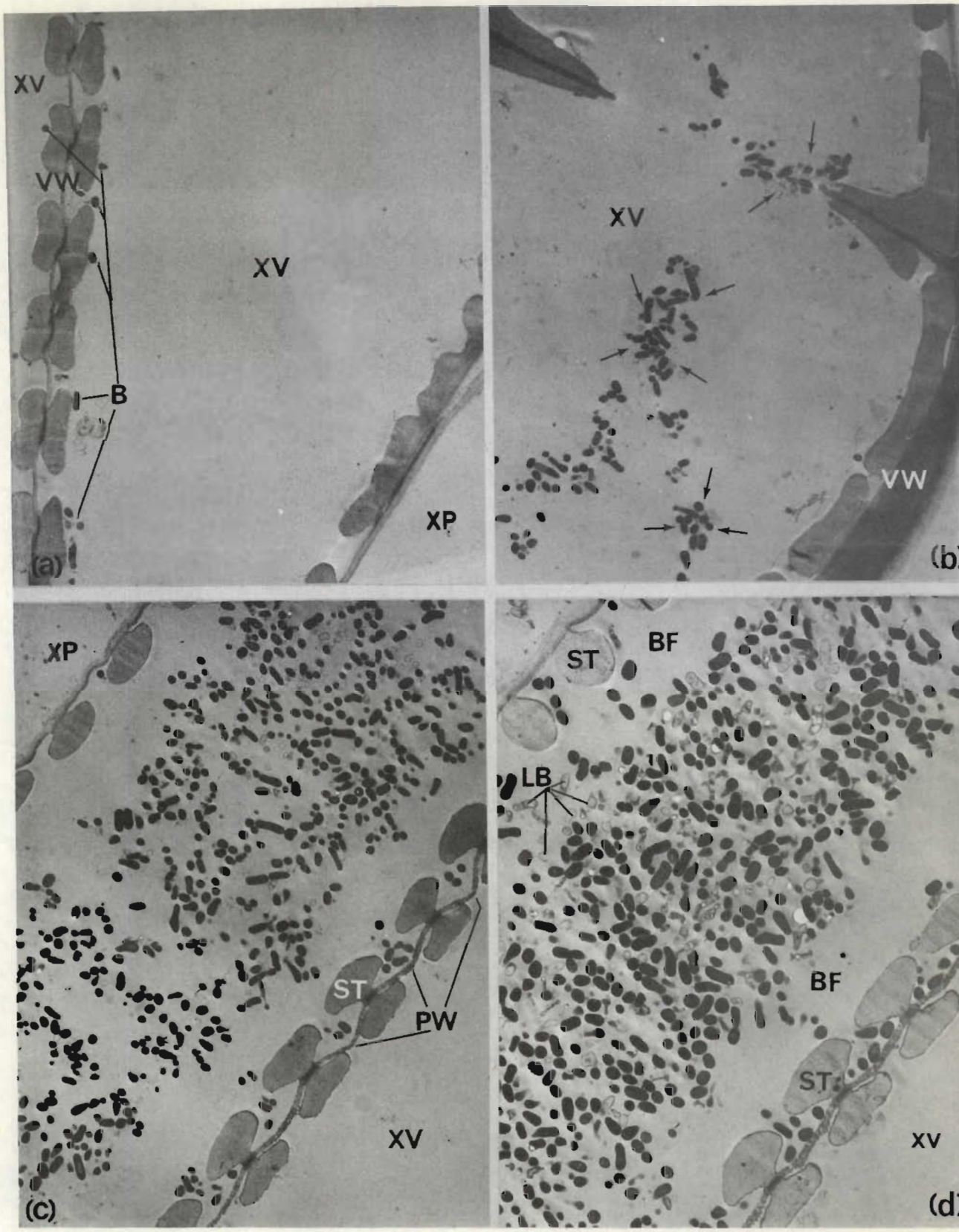

PLATE 28. (a) Few bacteria (B) in close contact with walls (VW) of smaller vessels (XV) in stem 2,5 cm below inoculation site after 24 h. (x 4 200.) (b) Bacteria in vessel 3,5 cm from inoculation site after 48 h. Note increased number of organisms, passage of bacteria through open end-walls of vessel element (XV) and clumping of the bacteria (arrows). No damage to vessel walls (XV) is apparent. (x 4 200.) (c) Stem vessel 2,5 cm below inoculation site after 48 h. Note increased number of bacteria in lumen of vessel compared to 24 h previously [Plate 28(a)]. Bacteria aggregate between spiral thickenings (ST) and primary wall (PW) bulges slightly into adjacent non-invaded vessel, XV; no bulging occurs between invaded vessel and adjacent xylem parenchyma cell, XP. (x 4 200.) (d) Stem tissue 2,5 cm below inoculation site after 72 h. Bacteria, many of which appear to have lysed (LB), have further increased in number. Note relatively bacterium-free region (BF) between bacteria aggregated in central lumen of vessel and those between the spiral thickenings, ST. (x 5 900.)

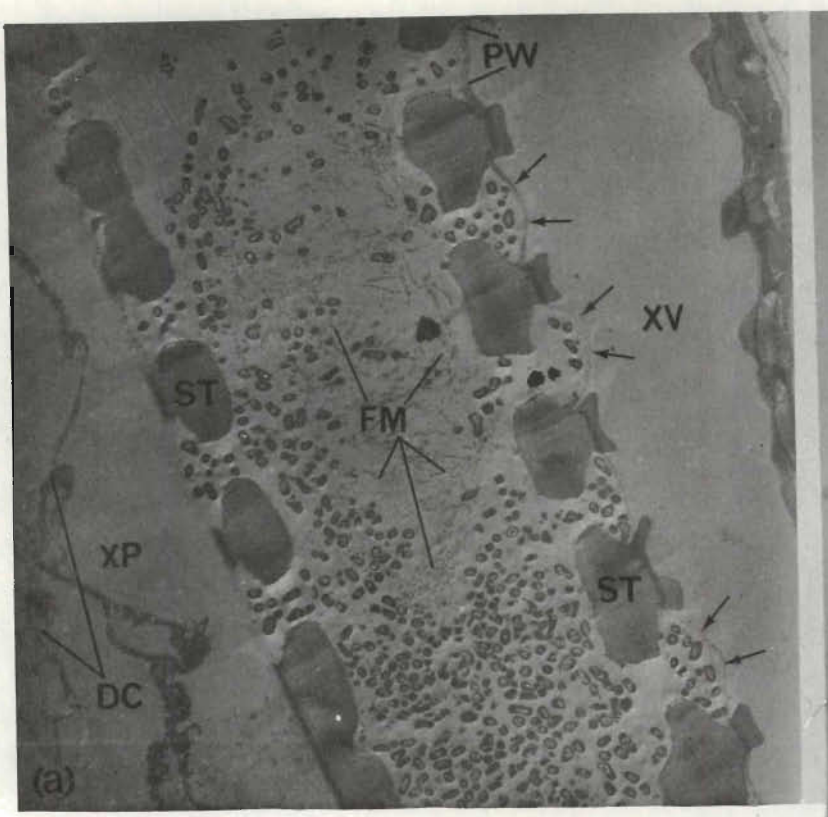

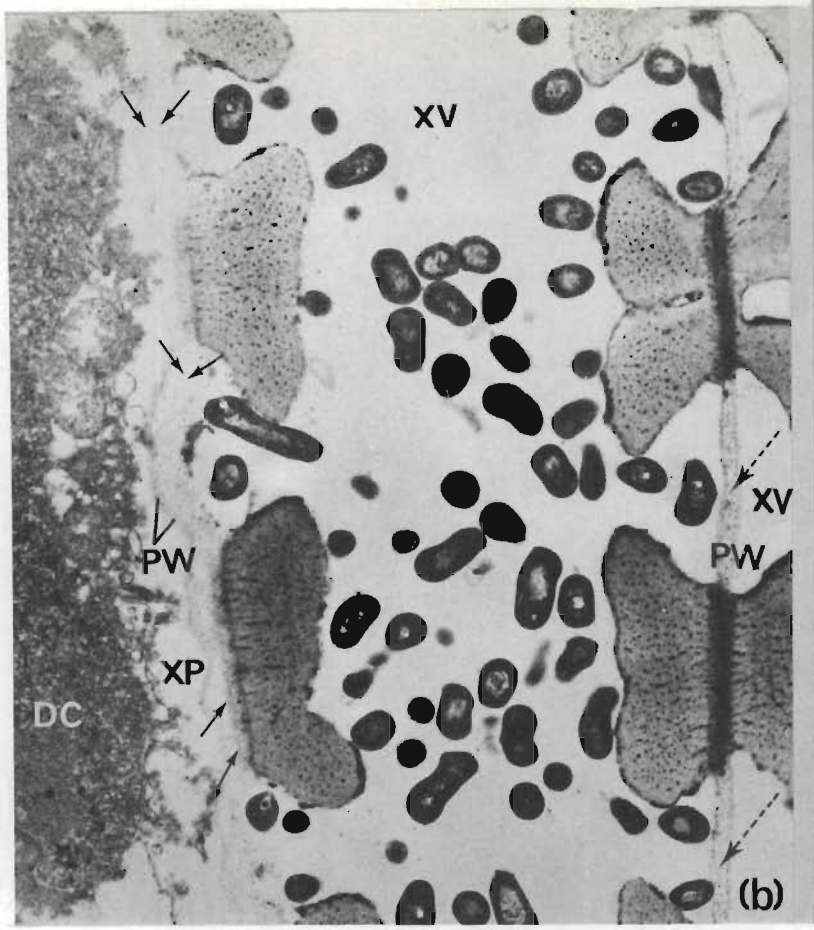

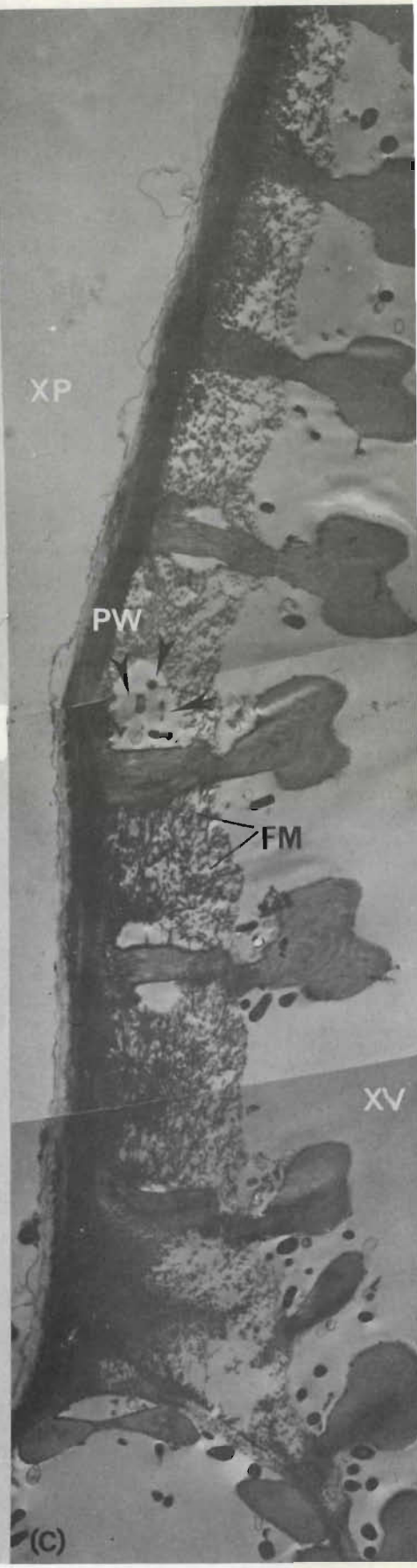

PLATE 29. (a)-(c) Stem tissue 2,5 cm below inoculation site after 96 h. (a) Lumen of vessel filled with masses of bacteria and some fibrillar material, FM. Bacterial action on primary wall (PW) between spiral thickenings (ST) causes weakened wall to bulge (arrows) into adjacent non-invaded vessel, XV. Note only slight bulging into adjacent non-invaded xylem parenchyma cell (XP) in which cytoplasm (DC) is degenerating. (x 3 900.) (b) Primary walls between invaded vessel (XV) and non-invaded xylem parenchyma cell (XP) swell and bulge, causing separation of the walls in region of middle lamella (arrows). Note accumulation of dense masses of granular material (GM) in lumen of parenchyma cell and relatively unaffected primary walls (PW) between the invaded vessel and contiguous non-invaded vessel (broken arrows). (x 15 300.) (c) Shredding of swollen primary wall (PW) of vessel (XV) with concomitant release of masses of fibrillar material, FM. Note bacteria in clear areas (arrows within the released fibrillar material, and unaffected wall of xylem parenchyma cell, XP. (x 5 900.)

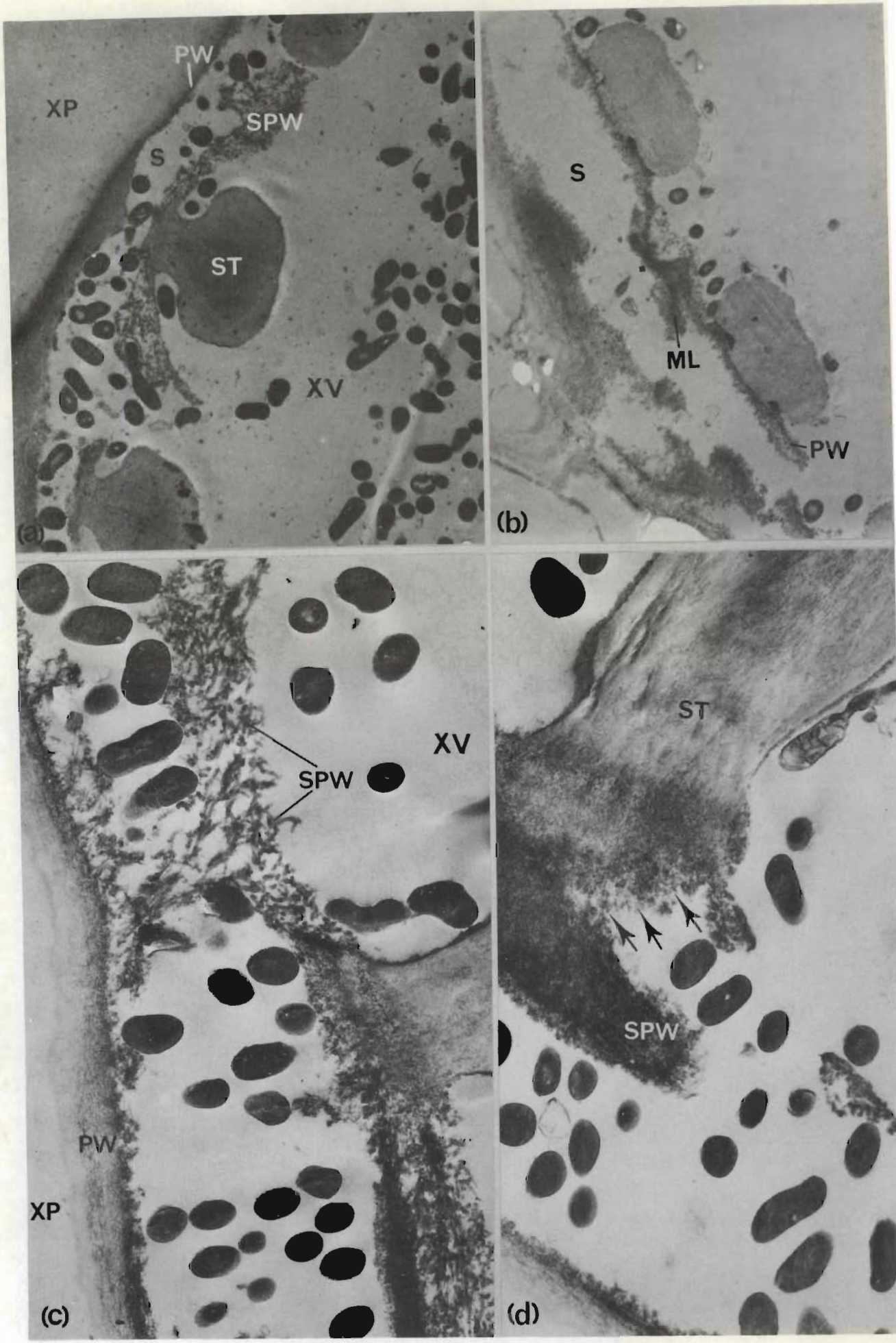

PLATE 30. (a)–(d) Stem tissue 2.5 cm below site of inoculation. (a) Bacteria in space (S) between shredded primary wall (SPW) of vessel (XV) and primary wall of adjacent parenchyma cell (XP) 120 h after inoculation. Remnants of degraded primary wall of vessel still attached to secondary thickenings, ST. (x 10 800.) (b) Vessel primary wall (PW) and middel lamella (ML) breakdown after 144 h. Note continued bacterial enzyme action has caused space (S) to enlarge. (x 14 800.) (c) Almost complete dissolution of shredded primary wall (SPW) of invaded vessel (XV), 144 h after inoculation. Primary wall (PW) of adjacent xylem parenchyma cell (XP) appears unaffected, retaining its layered appearance. (x 23 500.) (d) Partial degradation of base of secondary thickening (ST) at position of attachment (arrows) to primary wall residue, SPW. (x 23 500.)

PLATE 31. (a)-(e) Infected stem tissue 2,5 cm below site of inoculation after 144 h. (a) Swelling and shredding of entire primary wall complex (arrows) between contiguous vessels (XV) to many times thickness of primary wall complex between vessels in healthy tomato, - inset. (x 4 150.) Bacteria penetrate the swollen walls and destroy the shredded material with resultant formation of cavities, BC. Note tyloses (T) bulging into lumen of vessel from adjacent parenchyma cell, XP. (x 4 150.) (b) Tyloses (T) wedged between spiral thickenings (ST) completely bridging lumen of vessel, XV. Note degenerating cell contents in lower tylosis. (x 4 150.) (c) Bacteria (B) and mass of electron-dense material (ED) in degenerating xylem parenchyma cell (XP) adjacent to invaded vessel, XV. Note dissolution of vessel primary wall (PW) in regions between bars of secondary thickening (ST) which appear unaffected. Primary wall (PW) and middle lamella (ML) between contiguous xylem parenchyma cells also relatively unaffected. (x 9 200.) (d) Large amounts of capsular material (CM) surround some bacteria (B) in close proximity to vessel wall (VW) which appears unaffected. (x 28 100.) (e) Layer of fine granular material (GM) accumulated against

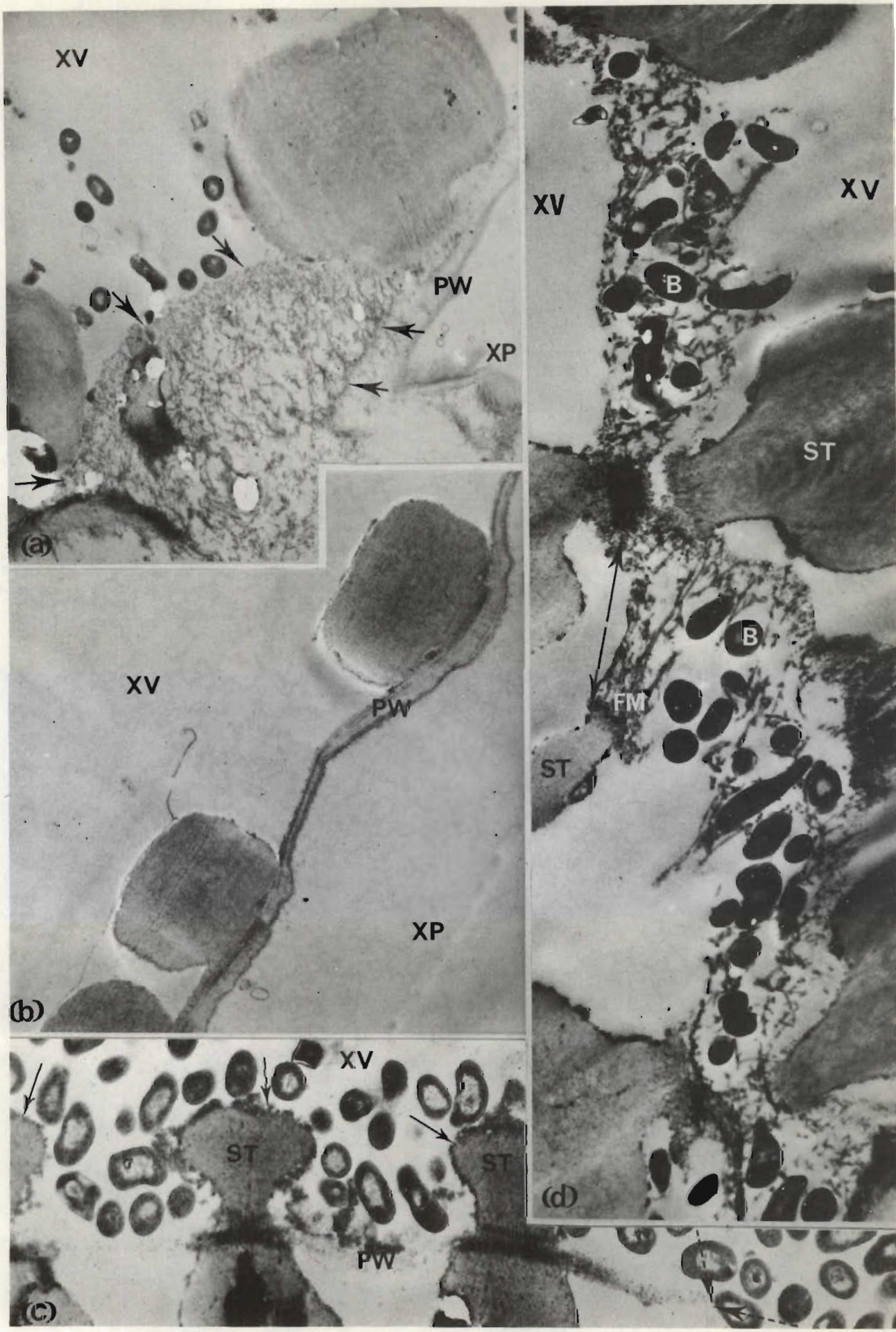

PLATE 32. (a)-(d) Stem tissue 2,5 cm below cut surface of petiole after 144 h. (a), (c) and (d) infected; (b) healthy. (a) Swelling of primary wall material (PW) between invaded xylem vessel (XV) and adjacent non-invaded parenchyma cell, XP. Note shredding of material (arrows) occurs primarily on vessel side of separating wall complex. (x 14 100.) (b) Healthy material showing structure of the primary wall complex (PW) between xylem vessel (XV) and adjacent parenchyma cell, XP. (x 14 000.) (c) Bacteria in vessel (XV) are aggregated in spaces between spiral thickenings (ST) which appear to be shredding (arrows). Primary wall (PW) showing advanced degradation has disappeared in some places (broken arrows). (x 19 300.) (d) Advanced stage of primary wall dissolution with bacteria penetrating the fabric of the shredded walls. Residual fibrillar material (FM) remains attached to spiral thickenings (ST) which may become displaced (arrows). (x 20 800.)

PLATE 33. (a)-(d) Infected stem tissue 2,5 cm below site of inoculation after 144 h. (a) Complete rupture of primary wall complex (arrows) between contiguous vessels, XV. Bacteria aggregate in close proximity to the primary walls in regions between spiral thickenings, ST. A cell (CE), below the plane of the adjacent vessels, is free of bacteria. (x 5 850.) (b) Contiguous vessels (XV) with partially intact middle lamella (arrows) between degraded primary walls, PW. Note large amounts of fine granular material (GM) accumulated in lumen of vessel at left. (x 19 500.) (c) Bacteria multiplying in space (S) formed in the primary wall material (PW) between adjacent vessels, XV. Note that splitting seems to occur in the swollen primary wall material of invaded vessel while the middle lamella (ML) remains partially intact. (x 19 200.) (d) Large bacterium-filled pockets forming within the primary cell wall material of invaded vessel, XV. Note continuity between primary wall at point of attachment (TL) of bars of secondary thickening (ST) and material of inner layer of

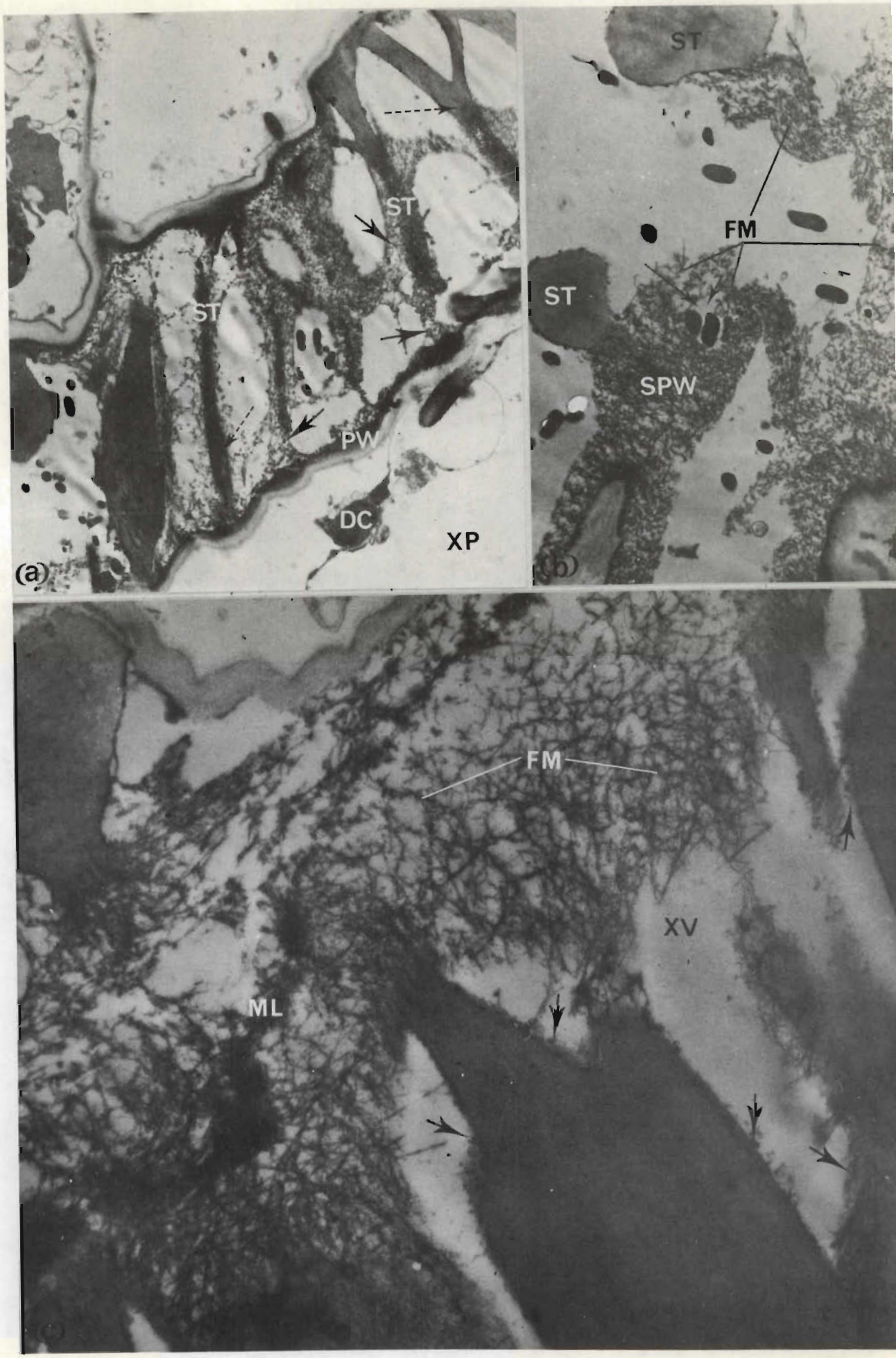

PLATE 34. (a)–(c) Infected stem tissue 2,5 cm below inoculation site after 168 h. (a) Invaded vessel showing shredding and dissolution of the bars of secondary thickening (ST) some of which are almost completely degraded (arrows) while others remain largely intact (broken arrows). Primary walls (PW) also show shredding. Note degenerating cytoplasm (DC) in adjacent parenchyma cells, XP. (x 5 875.) (b) Invaded vessel showing infolding of fibrillar residual primary wall material (FM) which may remain attached to secondary thickenings, ST. Bacteria enter the convoluted region and penetrate the fibrillar material (FM) with resultant formation of clear pockets (arrows). (x 11 000.)

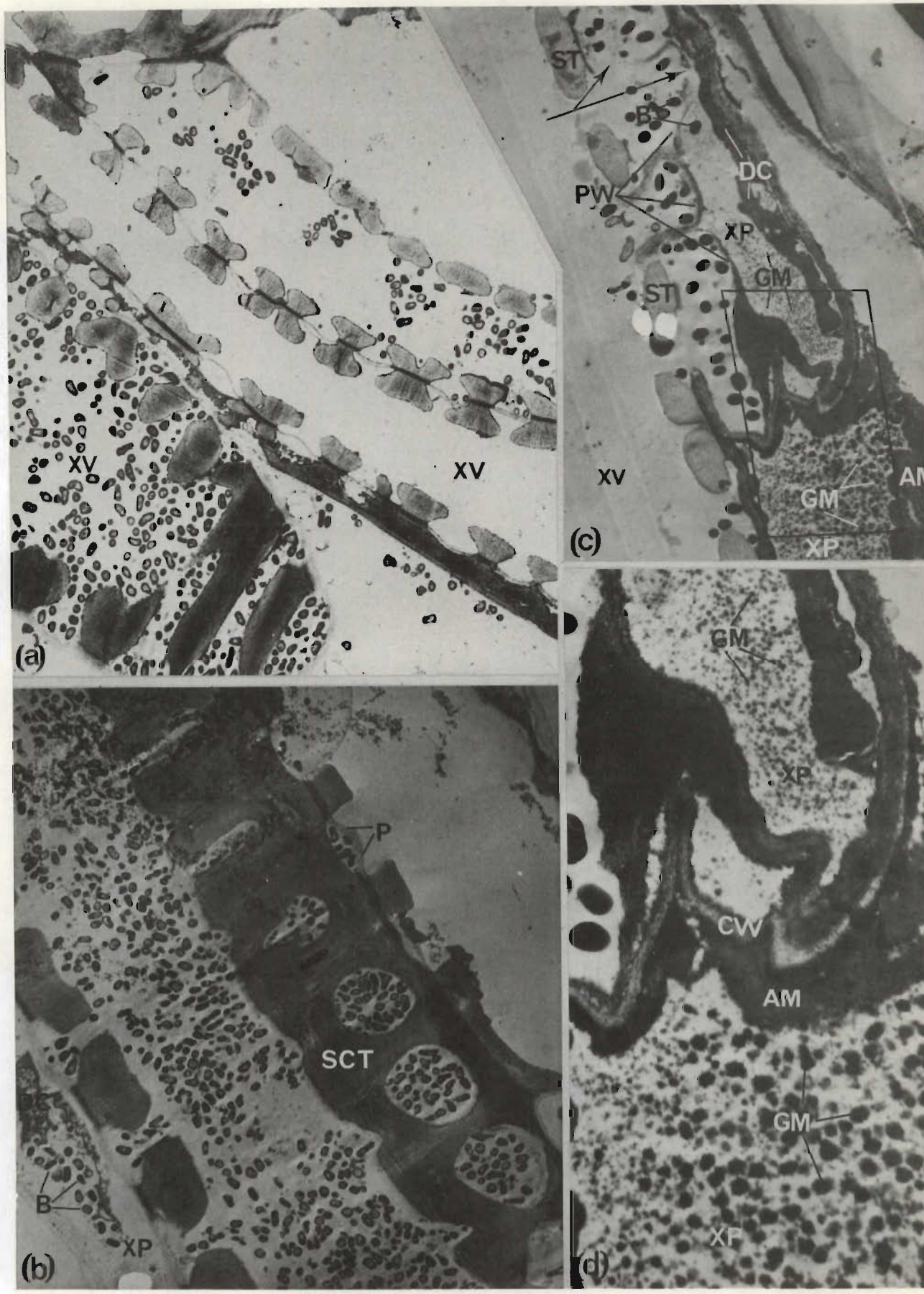

PLATE 35. (a)–(d) Infected stem tissue 2,5 cm below site of inoculation after 168 h. (a) Adjacent vessels (XV) showing uneven distribution of bacteria. (x 4 625.) (b) Invasion of vessel with scalariform secondary thickening, SCT. Note bacterium-filled protruberances (P) bulging into lumina of adjacent non-invaded cell. Parenchyma cell (XP) adjacent to vessel contains degenerating cytoplasm (DC) and bacterial cells, B. (x 4 100.) (c) Bacteria aggregated in interspiral regions in an outer vessel of bundle. Primary wall (PW) forms bacterium-filled protruberances that bulge between spiral thickenings (ST) into lumen of adjacent xylem parenchyma cell (XP) which contains degenerate cytoplasm (DC) and fine granular material, GM. Note ruptured protruberance (arrows) and released bacteria (B) in lumen of parenchyma cell. Adjoining parenchyma cell below is filled with coarse granular material (GM) and electron-dense amorphous material, AM. (x 5 850.) (d) Detail of boxed area indicated in Plate 35 (c), showing structure of granular material (GM) and layer of electron-dense amorphous material (AM) adhering to cell walls, CW. (x 13 850.)

PLATE 36. (a)-(d) Infected stem tissue 2,5 cm below inoculation site after 168 h. (a) Tissue breakdown showing complete absence (arrows) of primary walls between spiral thickenings (ST) of contiguous vessel (XV) and xylem parenchyma cell, XP. Note absence of degradation in scalariform walls. (x 4 150.) (b) Detail of boxed area in Plate 36(a) showing bacteria passing freely between spiral thickenings (ST) in regions where primary wall has disappeared (arrows). Note spirals (ST) and abutting thickened wall (TW) are not degraded. (x 11 200.) (c) Bacteria passing (arrows) between spiral thickenings (ST) of contiguous vessels (XV) and abutting parenchyma cell, XP. Note primary wall of scalariform vessel protruding (thick arrows) into lumen of adjacent parenchyma cell (XP) at top left. (x 5 900.) (d) Bacteria in scalariform vessel aggregated in distinctly demarcated areas against the thickening bars, ST. (x 8 500.)

PLATE 37. (a)-(c) Infected stem tissue 2,5 cm below site of inoculation after 168 h. (a) Swelling and shredding of vessel outer primary wall layers (arrows) between contiguous vessel (XV) and parenchyma cell, XP. Note aggregation of bacteria in both vessel and parenchyma cell. (x 5 875.) (b) Detail of boxed area in Plate 37(a) showing normal layered appearance (arrows) of wall of invaded parenchyma cell, XP. Note swelling and shredding of vessel outer primary wall layers and partial disorganization of inner layer of vessel primary wall (broken arrows). (x 12 350.) (c) Large numbers of bacteria in xylem parenchyma cell (XP) between two vessels, XV. Note primary wall (PW) of invaded vessel is degraded (arrows) whereas that of adjacent invaded parenchyma cell is unaffected (broken arrows). (x 4 200.) Inset. Detail of boxed area showing degradation of vessel primary wall, PW. Note intact middle lamella (ML) and unaffected primary wall of adjacent parenchyma cell, XP. Bases of secondary thickenings also show partial degradation (arrows). (x 14 000.)

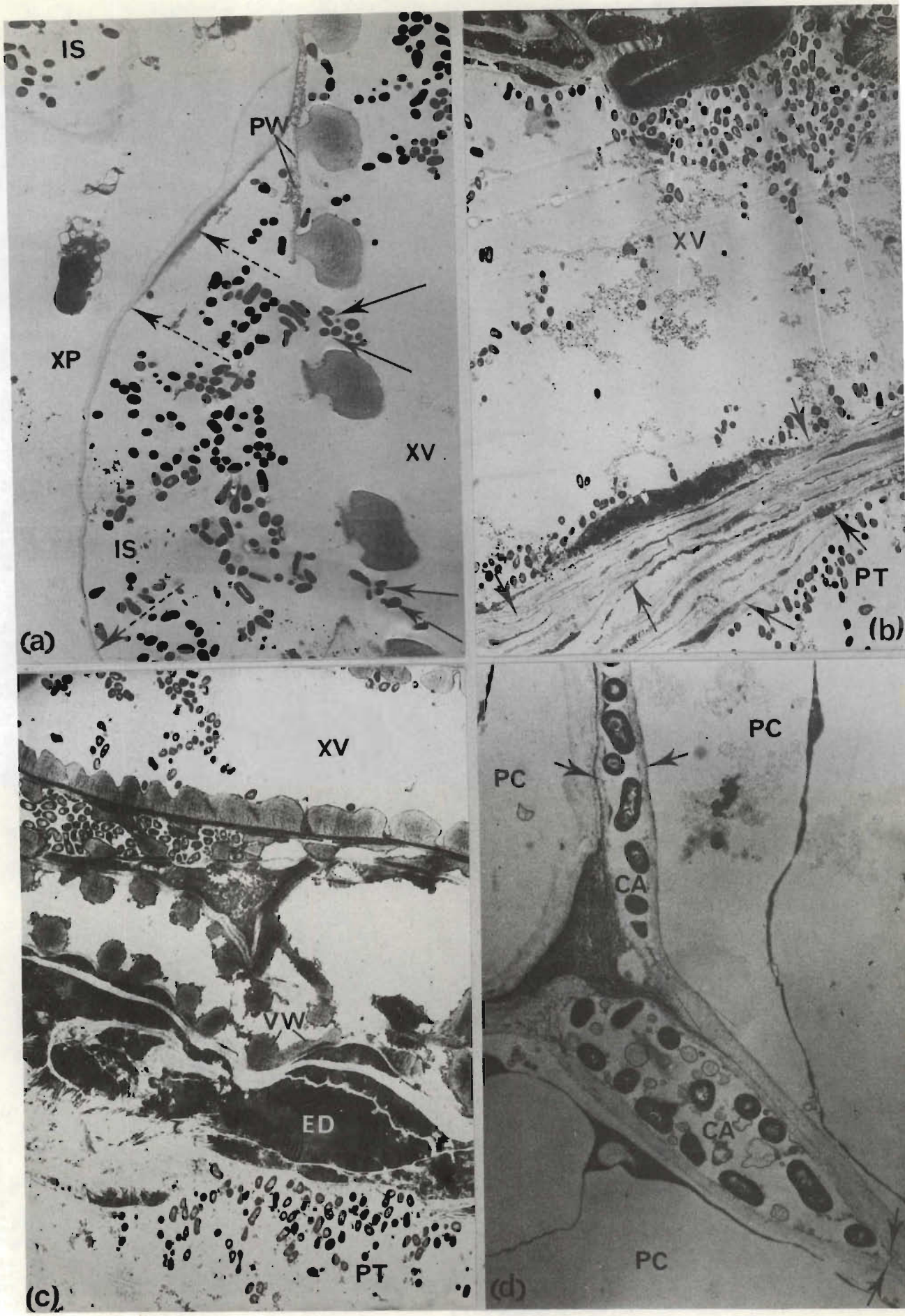

PLATE 38. (a)-(d) Infected stem tissue 2,5 cm below inoculation site after 168 h. (a) Vessel on periphery of bundle showing passage of bacteria into intercellular space (IS) at places (arrows) where degraded primary wall (PW) has disappeared. Note indented wall (broken arrows) of contiguous xylem parenchyma cell (XP) and bacteria in enlarged intercellular space (IS) at top left. (x 4 375.) (b) Tissue disruption showing bacteria in collapsing xylem vessel (XV) on periphery of bundle and in a cavity forming in the disrupted parenchymatous ground tissue, PT. Note remains of compressed parenchyma cells (arrows) between the invaded vessel (XV) and bacterium-containing cavity, PT. (x 4 525.) (c) Bacteria in cavity (PT) within disrupted parenchymatous ground tissue. Note large amount of amorphous electron-dense material (ED) adjacent to collapsing xylem vessel wall, VW. (x 4 600.) (d) Bacteria between cells (PC) of the parenchymatous ground tissue. Note separation of the cells (arrows) with resultant formation of cavities, CA. (x 11 900.)

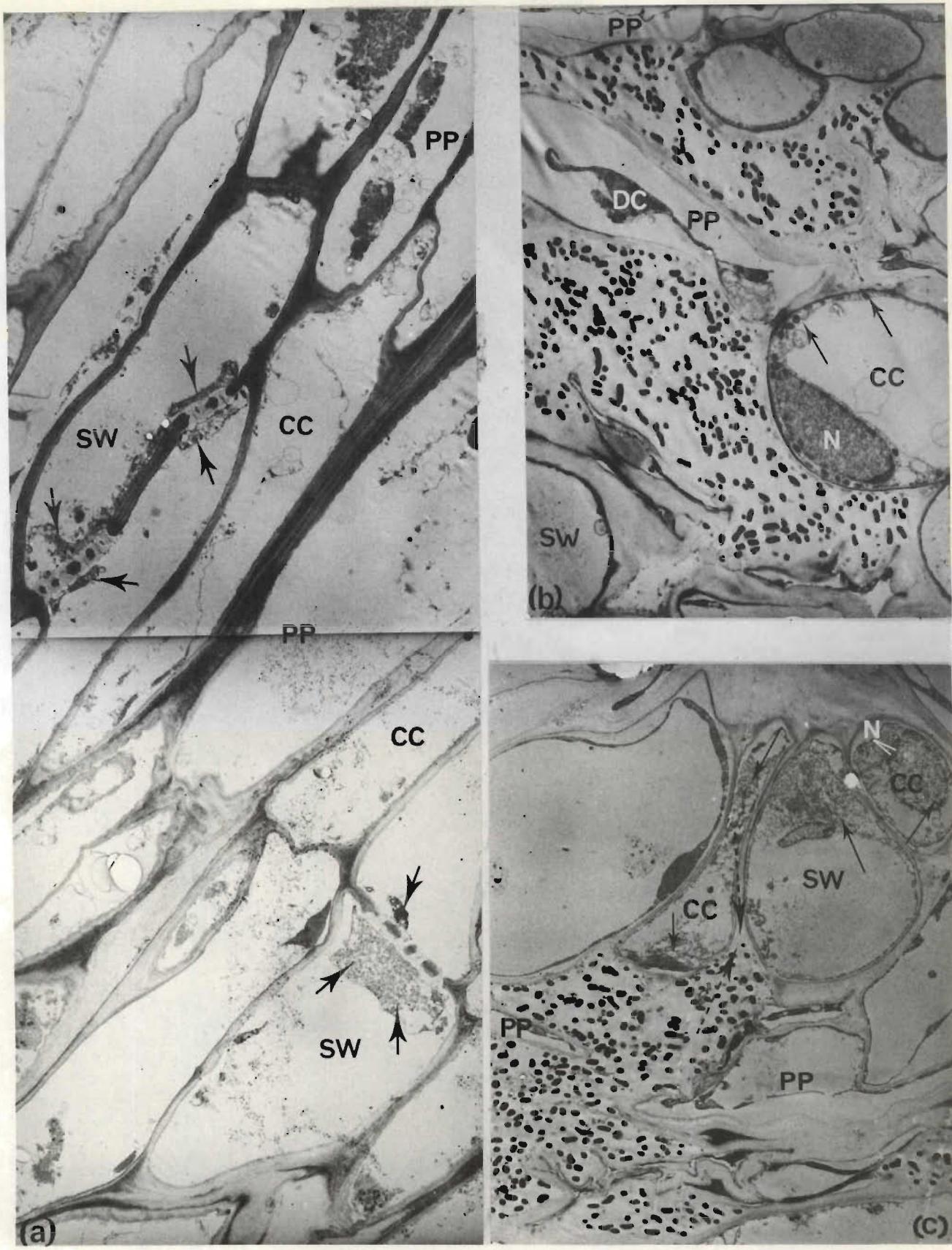

PLATE 39. (a) Montage of phloem tissue in infected stem 2,5 cm below site of inoculation showing sieve tubes (SW) and companion cells (CC) free of bacteria 168 h after inoculation. Cytoplasm of adjacent phloem parenchyma cells (PP) is degenerating. Note accumulation of electron-dense material at sieve plates (arrows). (x 4 200.) (b) Phloem tissue 168 h after inoculation showing peripheral cytoplasm (arrows) and almost normal appearance of nucleus (N) in companion cell, CC. Note fibrillar material, possibly P-protein, in sieve tubes, SW. Phloem parenchyma cells (PP) are collapsed within the bacterium-filled cavity. (x 4 200.) (c) Bacteria in spaces between collapsed phloem parenchyma cells (PP) 192 h after inoculation. Note bacteria entering the intercellular space (broken arrows) between a sieve tube (SW) and companion cell (CC) in which the nucleus (N) and cytoplasm are degenerated. (x 4 200.)

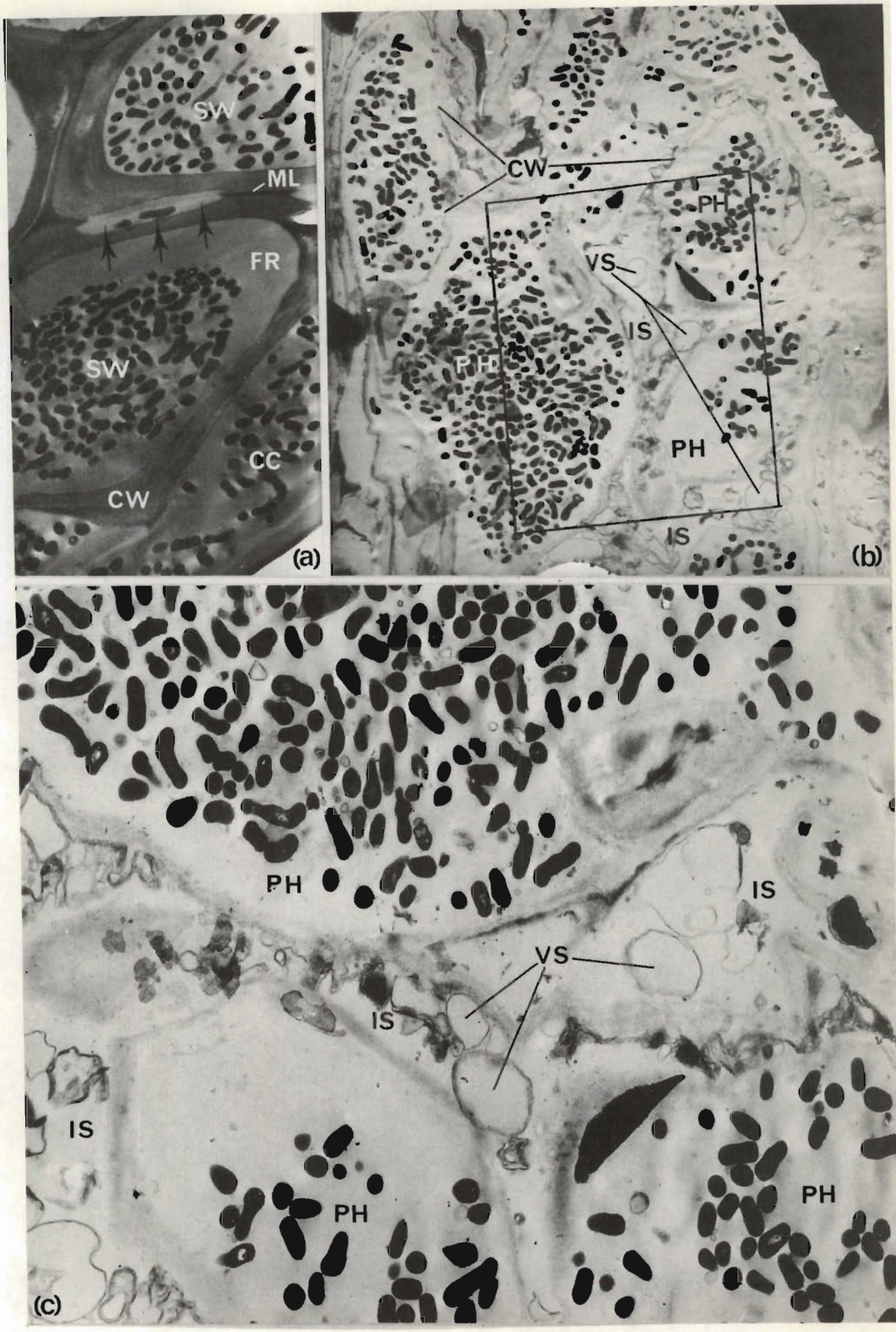

PLATE 40. (a) Bacteria within sieve tubes (SW) and companion cells (CC) in stem tissue 2,5 cm from inoculation site after 216 h. Note dissolution of middle lamella (ML) and bacteria within the resultant cavity (arrows). In some cells bacteria, aggregated in central lumen, are surrounded by bacterium-free zone (FR) adjacent to cell wall, CW. (x 8 300.) (b) Infected stem tissue 2,5 cm below inoculation site after 240 h, showing collapsed bacterium-containing phloem elements (PH). Note large number of vesicular structures (VS) in the spaces (IS) formed between the collapsing cell walls, CW. (x 4 200.) (c) Detail of boxed area in Plate 40(b) showing the vesicular structures (VS) within the spaces (IS) formed between collapsing phloem elements, PH. (x 11 200.)

DISCUSSION

According to Beckman (4) swelling of the walls of infected vessels can be ascribed to an increase in acidity, or the presence of cation complexing organic acids which may serve to weaken and loosen the lattice structure of the polymeric substance in the primary walls and middle lamellae. All the evidence presented in the present study indicates that where an invaded xylem vessel lies adjacent to a non-invaded vessel the contiguous walls and the middle lamella are all subject to bacterial attack /Plates 29(a), 31(a), 32(c), 32(d), 33(a), 33(b), and 33(c)/. Complete degradation of the walls may be preceded by swelling and shredding of their structural components /Plates 31(a) and 32(d)/, or the walls may degenerate without swelling /Plates 32(c), 33(a) and 33(b)/. On the other hand when an invaded vessel lies adjacent to a non-invaded parenchyma cell the vessel wall is degraded but the middle lamella and contiguous parenchyma cell wall remain, initially at least, relatively unaffected /Plates 29(c), 30(a), 30(c) and 30(d)/. This seems to indicate that during the early stages of pathogenesis it is mainly cellulolytic enzymes produced by the bacteria that are involved in tissue degradation. As degradation of primary wall material, and later of middle lamella material occurs in both the presence /Plates 29(b), 29(c), 30(a), 30(b), 30(c), 30(d), 31(a), 32(a), 32(c), 32(d), 33(b), 33(c), 33(d), 34(b), 37(c) and 37(c) - inset/ and in the absence /Plate 34(c)/ of bacteria, it seems that extracellular enzymes produced by the bacteria and transported in the conducting tissue of the host, play an important rôle in pathogenesis. Larson (68) reported possible enzyme action in advance of the bacteria in tomato plants infected with C. sepedonicum.

The subsequent complete dissolution of all layers of the primary

walls of vessels [Plates 30(c), 32(c) and 32(d)] and parenchyma cells [Plates 36(a), 36(b) and 36(c)], together with the ability of the bacterium to degrade the area of attachment of secondary thickening and primary wall [Plate 30(d)] and also possibly the secondary thickening itself [Plate 34(a)], indicate that C. michiganense produces all the enzymes necessary to degrade plant cell wall substances. Passage of C. michiganense between contiguous vessels has been reported by Pine, Grogan and Hewitt (91), but the actual mechanism of wall breakdown was not elucidated.

The observation that the bacterium moves only in a downward direction from the inoculated petiole and that no upward movement occurs in the vessels of the stem until approximately 96 h after inoculation, is essentially similar to the observations made by Pine, Grogan and Hewitt (91). These authors suggested that the bacterium moves downward in the leaf trace until the spiral vessel elements of the traces join the vessels of the main axis lower down in the stem, after which upward movement in the vessels of the stem is rapid.

Apart from the relative ease of movement in vessels, the apparent susceptibility and resistance to bacterial attack shown by the primary walls of vessels and those of parenchyma cells respectively, may account for the rapid vertical and slow horizontal spread observed in the present study and previously reported by others (9, 91, 98). The relationship between the bacterium and the primary wall varies considerably during the process of degradation; in some instances the bacteria penetrate the disorganized wall layers causing them to separate prior to undergoing complete degradation [Plates 30(a), 30(c), 30(d), 32(d), 33(c) and 33(d)], whereas in others the wall is degraded without being penetrated by the bacteria [Plates 30(b), 32(c), 33(a) and 33(b)]. Which of these relationships occurs in any particular instance is possibly related to the stage of development of the vessel

or cell since the primary wall, being formed chiefly during enlargement of the cell, itself undergoes surface enlargement which affects the orientation of the component cellulose microfibrils (25). On the other hand the physical presence of bacteria appears, in some instances, to be unnecessary for degradation of primary wall materials /Plate 34(c)/, so that penetration or non-penetration by the bacteria might be of little significance.

The ability of C. michiganense to invade vesselswith most forms of secondary wall thickening indicates a marked wall degrading capacity of this pathogen. The dissolution of middle lamella material between phloem cells /Plate 40(a)/, the separating of the elements of the phloem /Plates 39(b) and 39(c)/ and the subsequent collapse of the bacterium-filled phloem cells during advanced stages of pathogenesis /Plates 40(b) and 40(c)/, could explain the conclusion reached by some researchers (61, 80, 106, 123) that C. michiganense is primarily a phloem pathogen. In the present study it was found that the xylem vessels are initially invaded, the phloem becoming invaded only during later stages of pathogenesis, after the bacteria have escaped from the infected xylem vessels and spread to the phloem through the intervening parenchymatous ground tissue. Similar results were obtained by Pine, Grogan and Hewitt (91). My findings that much of the phloem tissue is rapidly disrupted, many of the cells collapsing completely only 24 h after apparently first becoming invaded, tend to contradict the statement made by these authors, that the bacteria do not move about freely in the phloem tissue.

The various materials observed in the spaces between separating cells /Plates 35(c), 35(d), 37(c), 38(b), 38(c), 40(b) and 40(c)/ could be either host degradation products or bacterial products which, according to Bloch (6), are difficult to separate in slowly proceeding defence reactions that involve many host cells. In vessels and,

apart from degenerating cytoplasm, within cells, the major amount of degraded material consists of host cell wall products, as in many of the electron micrographs it is still attached to either the remaining primary wall residues /Plates 29(c), 30(c), 31(a), 32(a), 34(a), 37(b), 37(c) and 37(c) - inset/, or to the secondary thickenings /Plates 30(a), 30(b), 30(c), 30(d), 31(a), 32(d), 34(a), 34(b) and 34(c)/ as a reticulate network of fibrillar material. Additional proof for the host origin of this material is the apparent ability of the bacteria to degrade it further /Plates 29(c), 30(c), 32(d) and 34(b)/.

As mentioned in the introduction to this chapter there are two theories concerning the wilt mechanism of Corynebacterium species. These are the mechanical vessel plugging theory and the toxic action theory in which substances, produced by the bacterium, damage host cell membranes.

Generally where vessel plugging has been suggested as a contributory factor to wilting in Corynebacterium-incited plant diseases, the organisms under consideration have been C. insidiosum (13, 56, 109, 117), C. sepedonicum (109, 117) or C. flaccumfaciens (128) rather than C. michiganense. However, Wellhausen (124) reported the vessels of C. michiganense-inoculated maize, which is a non-host, to be plugged with bacterial slime, and Patino-Mendez, as cited by Strobel and Hess (118), concluded that, since difficulty was experienced in drawing water through C. michiganense-infected tomato plants, the wilt mechanism may involve plugging of the vessels. Apart from these two references a search of the literature revealed no research paper implicating vessel plugging as the mechanism of wilt in C. michiganense-infected plants. It is perhaps significant that in the two most comprehensive light microscope investigations on the pathological histology of tomato plants infected with C. michiganense

(9, 91) no mention is made of vessel plugging.

Apart from a few vessels in which small amounts of some debris occurred among the bacteria [Plate 29(a)], or in which the bacterial cells appeared to be surrounded by capsular material [Plates 31(d) and 31(e)], or in which occasional tyloses occurred [Plates 31(a) and 31(b)], no vessel plugging material or structures were present in sufficient quantities to account for the wilting seen in the present investigation. The absence of large amounts of plant degradation products, bacterial extracellular material, or dense masses of bacterial cells, in the vessels, indicates that in bacterial canker of tomato vessel plugging is apparently not a major factor in the wilt mechanism; particularly as large amounts of polysaccharide are thought to be necessary to produce wilting (20). As wilting of the test plants occurred after 144 h, at which time few vessels contained large numbers of bacteria, it seems unlikely that plugging of vessels with bacterial cells is a major contributing factor to wilting.

Rai and Strobel (94) are also of the opinion that the wilt mechanism in C. michiganense-infected tomato plants does not involve vessel plugging. They suggest that wilting is due to the action of a membrane-damaging toxin as the amount of toxic material taken up by their experimental tomato cuttings (46,5 to 58,0 µg) was too small to cause vessel plugging and report that electron microscopic examination of diseased plant material showed no plugging of vessels. However, as no electron micrographs were published comparison with the present work is not possible. Electron micrographs of unidentified, non-conducting cells from tomato stems infected with C. sepedonicum (118) show damage to the bounding and internal membrane systems of chloroplasts and mitochondria, and the disruption of the plasma membrane which, according to the authors, is caused by the toxin produced by this organism.

Since this thesis is essentially a comparative ultrastructural investigation of the effects of three bacterial vascular pathogens on the conducting tissues of their respective hosts, no attempt was made, at this stage, to investigate the possible involvement of toxic substances on the membrane system of cells in non-vascular tissue. Disorganization of some membranous material, which could possibly be due to toxic action, was observed in phloem cells /Plates 39(c), 40(b) and 40(c)/ and in xylem parenchyma cells adjacent to both invaded /Plates 29(a), 29(b), 29(c) and 34(a)/ and non-invaded /Plate 31(a)/ vessels. However, as already mentioned, the nature of the present study does not permit definite ascription of this damage to the action of a toxin produced by the pathogen.

In addition to its disruptive action on cell membranes the toxin produced by C. sepedonicum is reported to affect the structure of cell walls, the distinct pattern of layering, observed in the walls of healthy cells, being destroyed (118). However, in view of the complete dissolution of primary wall material in xylem vessels /Plates 32(d), 33(d), 36(a), 36(b) and 36(c)/, and in some instances possibly of secondary wall material also /Plate 34(a)/, it is unlikely that the wall destruction associated with the bacterial canker disease of tomato is due to the action of a toxin produced by the pathogen.

Thus it appears that C. michiganense depends largely on possession of a very active enzyme system for its pathogenicity. The organism is able to degrade completely most, if not all, plant cell wall components. As the primary wall materials are degraded most rapidly it would seem that the organism possesses a particularly active complement of cellulases and/or hemicellulases. The apparent dissolution of secondary thickened walls as well as middle lamella materials suggests the possible additional action of lignanolytic

and pectinolytic enzymes. It is conceivable that the combined action of these enzymes is responsible for the complete vascular tissue breakdown and consequential wilting, that are such characteristic features of advanced stages of bacterial canker disease in tomato.

GENERAL DISCUSSION AND SUMMARY

Xanthomonas campestris, Pseudomonas solanacearum and Corynebacterium michiganense are all xylem invading bacterial pathogens, but show marked differences in the mechanism of their pathogenicity.

In the black rot disease of cabbage incited by X. campestris the bacteria act on the primary walls at sites between the spiral thickenings. Complete dissolution of the primary wall in some interspiral regions enables the bacteria to pass into adjacent vessels. Within invaded vessels the bacteria are embedded in a matrix of fibrillar beaded material. Separation of the spiral thickening from the primary wall is accomplished by a 'shredding' of the latter, a phenomenon not observed in healthy tissue. Such shredding, which occurs initially on the exposed wall layer results in swelling of the primary wall residue and release of masses of fibrillar material similar to that which surrounds the bacteria.

Complete disappearance of primary wall material is not as commonly observed in this disease, or in bacterial wilt incited by P. solanacearum, as in bacterial canker, incited by C. michiganense. In X. campestris-infected cabbage a granular residue, composed apparently of a lignic component of the vessel primary wall usually remains. The secondary thickenings are not noticeably degraded except occasionally at their bases. In addition to the fibrillar material a reticulate substance, which appears to be composed largely of host material, possibly a mixture of disorganised cellulose and lignin microfibrils, completely or partially plugs some of the vessels in infected leaf veins.

The plugs conceivably act as a host defence mechanism since they form in seemingly non-invaded vessels at sites where bacterial action in contiguous vessels has reached an advanced stage. Evidence for

the host origin of the plugging material is the apparent ability of the bacterium to degrade it partially. In the black rot disease the bacteria, which are restricted initially to the xylem vessels of the leaf veins, require a somewhat extended period of multiplication before they break out from the vessels.

Pseudomonas solanacearum, the causal agent of bacterial wilt of tomato is initially less strictly confined to the xylem vessels than either X. campestris or C. michiganense. This pathogen was found to degrade vessel wall materials to a much lesser extent than the other two organisms investigated. Following root inoculations the bacterium entered only the cells adjacent to and surrounding the large vessels. After a period of bacterial multiplication these cells are stimulated to produce tyloses which balloon out into the adjacent vessels. The bacteria then pass into the tyloses. Subsequently these disrupt releasing bacteria into the vessels where they multiply rapidly with concomitant formation of large amounts of extracellular slime.

The numbers of bacteria and the amount of their seemingly viscid slime increase to such an extent that in certain regions, particularly in the root vessels, the bacterial cells become so highly compressed that they show distortion. Eventually the lumina of the vessels are completely filled with masses of bacteria and their slime. The increasing pressure exerted, together with bacterial enzyme action on the wall materials, cause the vessels to become disrupted and bacteria to be released into the surrounding tissues where they cause lysigenous cavities. A noteworthy feature of this disease is the diversity of substances which seem to play a rôle in plugging the invaded vessels. Perhaps of particular interest in connection with the wilt mechanism is the occurrence of a thick layer of electron-dense material overlying the pit membranes between invaded vessels

or between invaded vessels and adjacent parenchyma cells. This material, which is not observed in healthy tissue, could conceivably prevent lateral movement of water and nutrients from the invaded vessels thereby causing death of surrounding xylem parenchyma tissue.

Corynebacterium michiganense like X. campestris, but unlike P. solanacearum, is strictly confined to the xylem vessels during early stages of pathogenesis. Of the three pathogens investigated the organism responsible for bacterial canker of tomato appears to be the most active in host cell wall degradation. Bacterial action on the vessel wall material results in complete derangement of the wall structure and eventual disappearance of the primary wall allowing free movement of bacteria, particularly between contiguous vessels.

Another major difference between C. michiganense and the other two bacterial pathogens investigated is the apparent ability of this bacterium to degrade actively the secondary thickening bars in some vessels. The amount of general tissue damage is much greater in bacterial canker than in the other two diseases investigated; possibly a reflection of greater enzyme activity by this organism which appears to possess all the enzymes necessary for complete dissolution of plant cell walls. At no stage of pathogenesis did the number of bacteria in the vessels become as large as that observed in vessels of tomato plants infected with P. solanacearum.

A noteworthy feature of bacterial canker is the almost complete absence of vessel plugging that is so characteristic of the other two diseases investigated. Spread of bacteria in the intercellular spaces of non-conducting tissue occurs earlier and is much more extensive in this disease than in either black rot or bacterial wilt, and enables the bacteria to enter the phloem tissues, which are rapidly destroyed. C. michiganense appears to attack mainly the stem tissues of the host, the vessels in the roots being invaded rarely.

On the other hand P. solanacearum seems to have an affinity for the root tissue and occurs in much greater numbers in the vessels of the roots than in the vessels of the stem.

In the course of this study it became apparent that the wilt mechanism of the three pathogens differed. Although a general wilting of the plant is not a characteristic symptom of the black rot disease of cabbage incited by X. campestris, localized wilting and water stress are important in lesion development (120). Results of the present study indicate that the water stress is due to plugging of the xylem vessels with bacterial slime or host breakdown products, or a mixture of both.

Wilting in P. solanacearum-infected tomato plants appears to be due mainly to occlusion of the vessels, particularly those of the roots, with masses of bacterial cells and their copious slime together with host degradation products. These observations confirm the results obtained by Husain and Kelman (51). Other factors probably contributing to wilting are the layer of dense material deposited over the pit membranes in invaded vessels and the occlusion of vessels by tyloses.

Of the three diseases investigated bacterial canker is the only one in which (i) vessel plugging appears to be of little significance in the wilt syndrome, (ii) there is some indication that action of toxin(s) produced by the pathogen contributes to wilting. However, it is evident that the rapid and almost complete destruction of the vessel walls and subsequent loss of integrity of the xylem tissue is the major cause of wilting.

REFERENCES

1. ARK, P.A. (1944). Studies on bacterial canker of tomato. Phytopathology 34, 394 - 400.

2. AUGER, J.G., SHALLA, T.A. & KADO, C.I. (1974). Pierce's disease of grapevines: Evidence for a bacterial etiology. Science 184, 1375 - 1377.

3. BASU, P.K. (1966). Conditions for symptomatological differentiation of bacterial canker, spot, and speck on tomato seedlings. Canadian Journal of Plant Science 46, 525 - 530.

4. BECKMAN, C.H. (1964). Host responses to vascular infection. Annual Review of Phytopathology 2, 231 - 252.

5. BECKMAN, C.H., BRUN, W.A. & BUDDENHAGEN I.W. (1962). Water relations in banana plants infected with Pseudomonas solanacearum. Phytopathology 52, 1144 - 1148.

6. BLOCH, R. (1953). Defence reactions of plants to presence of toxins. Phytopathology 43, 351 - 354.

7. BRYAN, M.K. (1915). A nasturtium wilt caused by Bacterium solanacearum. Journal of Agricultural Research 4, 451 - 457.

8. BRYAN, M.K. (1928). Bacterial canker of tomatoes. United States Department of Agriculture Circular 29, 4p.

9. BRYAN, M.K. (1930). Studies on bacterial canker of tomato. Journal of Agricultural Research 41, 825 - 851.

10. BUDDENHAGEN, I.W. & KELMAN, A (1964). Biological and physiological aspects of bacterial wilt caused by Pseudomonas solanacearum. Annual Review of Phytopathology 2, 203 - 230.

11. BUDDENHAGEN, I.W. & TAKATA, G. (1969). Ultrastructural changes of host and parasite in Pseudomonas solanacearum-infected banana roots. Phytopathology 59, 1020 (Abstr.).

12. CASS SMITH, W.P. & GOSS, O.M. (1946). Bacterial canker of tomatoes. Journal Department of Agriculture Western Australia 23, 147 - 156.

13. CHO, Y.S., WILCOXSON, R.D. & FROSHEISER, F.I. (1973). Differences in anatomy, plant-extracts, and movement of bacteria in plants of bacterial wilt resistant and susceptible varieties of alfalfa. Phytopathology 63, 760 - 765.

14. COOK, A.A., LARSON, R.H. & WALKER, J.C. (1952). Relation of the black rot pathogen to cabbage seed. Phytopathology 42, 316 - 320.

15. COPLIN, D.L., SEQUEIRA, L. & HANSON, R.S. (1972). Virulence of biochemical mutants of Pseudomonas solanacearum. Phytopathology 62, 1107 - 1108.

16. COREY, R.R. & STARR, M.P. (1957). Colony types of Xanthomonas phaseoli. Journal of Bacteriology 74, 137 - 140.

17. CURTIS, L.C. (1944). The influence of guttation fluid on pesticides. Phytopathology 34, 196 - 205.

18. DE HERRERA, E.C. & JURADO, O.G. (1974). Ultrastructural changes produced in Vicia faba and Phaseolus vulgaris inoculated with Pseudomonas viridiflava. Phytopathologische Zeitschrift 81, 354 - 363.

19. DICKEY, R.S. & NELSON, P.E. (1967). Pseudomonas caryophylli in carnation. III. Effect of certain environmental factors on development of the pathogen in the host. Phytopathology 57, 1353 - 1357.

20. DIMOND, A.E. & WAGGONER, P.E. (1953). On the nature and role of vivotoxins in plant diseases. Phytopathology 43, 229 - 235.

21. DOWSON, W.J. (1949). Gram-positive bacterial plant pathogens: Corynebacterium. In Manual of bacterial plant pathogens. Adam and Charles Black, Longon p. 68 - 71.

22. DRECHSLER, C. (1919). Cotyledon infection of cabbage seedlings by Pseudomonas campestris. Phytopathology 9, 275 - 282.

23. DUECK, J., ZEYEN, R.J. & KENNEDY, B.W. (1972). Ultrastructural observations of soybean leaves affected by bacterial toxemia. Canadian Journal of Botany 50, 529 - 531.

24. DYE, D.W. (1960). Pectolytic activity in Xanthomonas. New Zealand Journal of Science 3, 61 - 69.

25. ESAU, K. (1960). Anatomy of Seed Plants. John Wiley and Sons, Inc. New York.

26. FLIEGE, H.F. (1974). Elektronenoptische Untersuchungen zum Auftreten rickettsien - ähnlicher Bakterien in Wurzeln von Erica graulis Salisb. Zeitschrift für Pflanzenkrankheiten und Pflanzenschutz 81, 765 - 767.

27. FOX, R.T.V., MANNERS, J.G. & MYERS, A. (1971). Ultrastructure of entry and spread of Erwinia carotovora var. atroseptica into potato tubers. Potato Research 14, 61 - 73.

28. GOHEEN, A.C. NYLAND, G. & LOWE, S.K. (1973). Association of a rickettsialike organism with Pierce's disease of grapevines and alfalfa dwarf and heat therapy of the disease in grapevines. Phytopathology 63, 341 - 345.

29. GOODMAN, R.N. (1972). Electrolyte leakage and membrane damage in relation to bacterial population, pH, and ammonia production in tobacco leaf tissue inoculated with Pseudomonas pisi. Phytopathology 62, 1327 - 1331.

30. GOODMAN, R.N. & BURKOWICZ, A. (1970). Ultrastructural changes in apple leaves inoculated with a virulent or an avirulent strain of Erwinia amylovora. Phytopathologische Zeitschrift 68, 258 - 268.

31. GOODMAN, R.N. & PLURAD, S.B. (1969). Ultrastructural modifications in tobacco undergoing the hypersensitive reaction caused by Erwinia amylovora and Pseudomonas pisi. Phytopathology 59, 1028.

32. GOODMAN, R.N. & PLURAD, S.B. (1971). Ultrastructural changes in tobacco undergoing the hypersensitive reaction caused by plant pathogenic bacteria. Physiological Plant Pathology 1, 11 - 15.

33. GOTO, M. & OKABE, N. (1959). Studies on cellulolytic enzymes of phytopathogenic bacteria: Part 4. On the nature of cellulose in the lesions of black rot of cauliflower (Xanthomonas campestris) and citrus canker (Xanthomonas citri). Report Faculty of Agriculture Shizuoka University 9, 21 - 23.

34. GOTO, M. & OKABE, N. (1960). Studies on the cellulolytic enzymes of phytopathogenic bacteria: Part 3. Some experiments on the mechanism of decomposition of cellulose or its derivatives due to cellulases. Report Agricultural Research Branch Shizuoka University Bulletin 10, 27 - 31.

35. GRIEVE, B.J. (1941). Studies in the physiology of host parasite relations. I. The effect of Bacterium solanacearum on the water relations of plants. Proceedings of the Royal Society Victoria 53, 268 - 299.

36. GROGAN, R.G. & KENDRICKS, J.B. (Sr.) (1953). Seed transmission, mode of overwintering and spread of bacterial canker of tomato caused by Corynebacterium michiganense. Phytopathology 43, 473 (Abstr.).

37. HARRIS, H.A. (1940). Comparative wilt induction by Erwinia tracheiphila and Pseudomonas stewarti. Phytopathology 30, 625 - 638.

38. HAYWARD, A.C. (1964). Characteristics of Pseudomonas solanacearum. Journal of Applied Bacteriology 27, 265 - 277.

39. HESS, W.H. & STROBEL, G.A. (1969). Ultrastructural investigations of tomato stems treated with the toxic glycopeptide of Corynebacterium sepedonicum. Phytopathology 59, 12 (Abstr.).

40. HILDEBRAND, D.C. (1971). Pectate and pectin gels for differentiation of Pseudomonas spp. and other bacterial plant pathogens. Phytopathology 61, 1430 - 1436.

41. HOAGLAND, D.R. & ARNON, D.I. (1950). The water-culture method for growing plants without soil. (Revised by D.I. Arnon). California Agricultural Experiment Station Circular, 347.

42. HODGSON, R., PETERSON, W.H. & RIKER, A.J. (1949). The toxicity of polysaccharides and other large molecules to tomato cuttings. Phytopathology 39, 47 - 62.

43. HOPKINS, D.L. & MOLLENHAUER, H.H. (1973). Rickettsia-like bacteria associated with Pierce's disease of grapes. Science, 179, 298 - 300.

44. HUANG, P. (1974). Ultrastructural modification by and pathogenicity of Erwinia amylovora in apple tissues. Ph.D.Thesis University of Missouri, Columbia. (Dissertation Abstracts International Vol. 35(a), B series, March 1974).

45. HUANG, P. & GOODMAN, R.N. (1970). Morphology and ultrastructure of normal rod shaped and filamentous forms of Erwinia amylovora. Journal of Bacteriology 102, 862 - 866.

46. HUANG, J. & GOODMAN, R.N. (1972). Alterations in structural proteins from chloroplast membranes of bacterially induced hypersensitive tobacco leaves. Phytopathology 62, 1428 - 1434.

47. HUANG, J., HUANG, P. & GOODMAN, R.N. (1974). Ultrastructural changes in tobacco thylakoid membrane protein caused by bacterially induced hypersensitive reaction. Physiological Plant Pathology 4, 93 - 98.

48. HUANG, P., HUANG, J. & GOODMAN, R.N. (1975). Resistance mechanisms of apple shoots to an avirulent strain of Erwinia amylovora. Physiological Plant Pathology 6, 283 - 287.

49. HUSAIN, A. & KELMAN, A. (1956). Mode of pathogenesis of Pseudomonas solanacearum. Phytopathology 46, 16.

50. HUSAIN, A. & KELMAN, A. (1957). Presence of pectic and cellulolytic enzymes in tomato plants infected by Pseudomonas solanacearum. Phytopathology 47, 111 - 112.

51. HUSAIN, A. & KELMAN, A. (1958). Relation of slime production to mechanism of wilting and pathogenicity of Pseudomonas solanacearum. Phytopathology 48, 155 - 165.

52. HUSAIN, A. & KELMAN, A. (1958). The role of pectic and cellulolytic enzymes in pathogenesis by Pseudomonas solanacearum. Phytopathology 48, 377 - 386.

53. HUSAIN, A. & KELMAN, A. (1959). Tissue is disintegrated. In Plant Pathology, Vol. 1, Ed. by J.G. Horsfall & A.E. Dimond. Academic Press, New York.

54. HUTCHINSON, C.M. (1913). Rangpur tobacco wilt. Memoirs Department of Agriculture India, Bacteriology Service 1, 67 - 83.

55. JERMYN, M.A. & ISHERWOOD, F.A. (1956). Changes in the cell wall of the pear during ripening. Biochemical Journal 64, 123 - 132.

56. JONES, F.R. & McCULLOCH, L. (1926). A bacterial wilt and root rot of alfalfa caused by Aplanobacter insidiosum. Journal of Agricultural Research 33, 493 - 521.

57. KELMAN, A. (1953). The bacterial wilt caused by Pseudomonas solanacearum, a literature review and bibliography. North Carolina Agricultural Experiment Station Technical Bulletin 99, 194p.

58. KELMAN, A. (1954). The relationship of pathogenicity in Pseudomonas solanacearum to colony appearance on a tetrazolium medium. Phytopathology 44, 693 - 695.

59. KELMAN, A. (1969). How bacteria damage crops. Connecticut Experiment Station Bulletin 708, 128 - 154.

60. KELMAN, A. & COWLING, E.B. (1965). Cellulolytic enzymes of Pseudomonas solanacearum in relation to pathogenesis. Phytopathology 55, 148 - 155.

61. KENDRICK, J.B. Jr. & WALKER, J.C. (1948). Predisposition of tomato to bacterial canker. Journal of Agricultural Research 77, 169 - 186.

62. KITAJIMA, E.W., BAKARCIC, M. & FERNANDEZ-VALIELA, M.V. (1975). Association of Rickettsia-like Bacteria with Plum leaf scald disease. Phytopathology 65, 476 - 479.

63. KLEMENT, Z. (1965). Method of obtaining fluid from the intercellular spaces of foliage and the fluids' merit as substrate for phytobacterial pathogens. Phytopathology 55, 1033 - 1034.

64. KNÖSEL, D. & GARBER, E.D. (1967). Pektolytische und cellulolytische Enzyme bei Xanthomonas campestris (Pammel) Dowson. Phytopathologische Zeitschrift 59, 194 - 202.

65. KNÖSEL,D. & GARBER, E.D. (1968). Separation of pectolytic and cellulolytic enzymes in culture filtrates of phytopathogenic bacterial species by starch gel zone electrophoresis. Phytopathologische Zeitschrift 61, 292 - 298.

66. KONTAXIS, D.G. (1962). Leaf trichomes as avenues for infection by Corynebacterium michiganense. Phytopathology 52, 1306 - 1307.

67. KUNZ, R. (1952). Die Wirkangsweise von Bacterium solanacearum E.F.S., den Erreger der tropischer Schleimkrankheit des Tabaks, auf Solanum lycopersicum L. Phytopathologische Zeitschrift 20, 89 - 112.

68. LARSON, R.H. (1944). The ring rot bacterium in relation to tomato and eggplant. Journal of Agricultural Research 69, 309 - 325.

69. LAYNE, R.E.C. (1967). Foliar trichomes and their importance as infection sites for Corynebacterium michiganense on tomato. Phytopathology 57, 981 - 985.

70. LAYNE, R.E.C. & RAINFORTH, J.R. (1966). A new symptom of bacterial canker resulting from systemic infection of tomato fruits and its implications in dissemination and seed transmission. Canadian Journal of Plant Science 46

71. LEACH, J.G., LILLY, V.G., WILSON, H.A. & PURVIS, M.R. Jr. (1957). Bacterial polysaccharides: the nature and functions of the exudate produced by Xanthomonas phaseoli. Phytopathology 47, 113 - 120.

72. LELLIOTT, R.A. (1966). The plant pathogenic coryneform bacteria. Journal of Applied Bacteriology 29, 114 - 118.

73. LE NORMAND, M., COLENO, A., GOURRET, J.P. & FERNANDEZ-ARIAS, H. (1971). Etude de la graisse du haricot et de son agent: Pseudomonas phaseolicola (Burk.) Dowson: I. Ultrastructure de la bacterie "in situ" et des modifications induites dans e'hote sensible. Annals of Phytopathology 3, 391 - 400.

74. LEPPARD, G.G., COLVIN, J.R., ROSE, D. & MARTIN, S.M. (1971). Lignofibrils on the external cell wall surface of cultured plant cells. Journal of Cell Biology 50, 63 - 80.

75. LESSERMANN, D. & RUDOLPH, K. (1970). Die Bildung von Ribosomen - Helices unter dem Einfluss des Toxins von Pseudomonas phaseolicola in Blattern von Mangold (Beta vulgaris L.). Zeitschrift Pflanzenphysiologie 62, 108 - 115.

76. MARAMOROSCH, K., PLAVSIC-BANJAC, B., BIRD, J. & LIU, L.J. (1973). Electron microscopy of ratoon stunted sugar cane: micro-organisms in xylem. Phytopathologische Zeitschrift 77, 270 - 273.

77. MEIER, D. (1934). A cytological study of the early infection stages of the black rot of cabbage. Bulletin of the Torrey Botanical Club 61, 173 - 190.

78. MOLL, J.N. (1974). Citrus greening disease. Ph.D.Thesis University of Natal, Pietermaritzburg, Natal.

79. MOLLENHAUER, H.H. & HOPKINS, D.L. (1974). Ultrastructural study of Pierce's disease bacterium in grape xylem tissue. Journal of Bacteriology 119, 612 - 618.

80. MUSHIN, R. (1938). Studies in the physiology of plant pathogenic bacteria: The food requirements of a xylem invader, Bacterium solanacearum E.F. Sm. and of a phloem invader Aplanobacter michiganense E.F. Sm. Australian Journal of Experimental Biology and Medical Science 16, 323 - 329.

81. NASUNO, S. & STARR, M.P. (1967). Polygalacturonic acid transeliminase of Xanthomonas campestris. Biochemical Journal 104, 178 - 185.

82. NELSON, P.E. & DICKEY, R.S. (1966). Pseudomonas caryophylli in carnation. II. Histological studies of infected plants. Phytopathology 56, 154 - 163.

83. NELSON, P.E. & DICKEY, R.S. (1970). Histopathology of plants infected with vascular bacterial pathogens. Annual Review of Phytopathology 8, 259 - 280.

84. NYLAND, G., GOHEEN, A.C., LOWE, S.K. & KIRKPATRICK, H.O. (1973). The ultrastructure of a rickettsia-like organism from a peach tree affected with Phony disease. Phytopathology 63, 1275 - 1278.

85. O'BRIEN, T.P. & THIMANN, K.V. (1967). Observations on the fine structure of the oat coleoptile. III. Some aspects of the vascular system. Protoplasma 63, 443 - 478.

86. PAQUIN, R., LACHANCE, R.A. & COULOMBE, L.J. (1960). The production of pectic enzymes by Corynebacterium sepedonicum. Canadian Journal of Microbiology 6, 435 - 438.

87. PEGG, G.F. & SEQUEIRA, L. (1966). Stimulation of aromatic biosynthesis in tobacco plants during the initial phase of infection by Pseudomonas solanacearum. Phytopathology 56, 894.

88. PEGG, G.F. & SEQUEIRA, L. (1968). Stimulation of aromatic biosynthesis in tobacco plants infected by Pseudomonas solanacearum. Phytopathology 58, 476 - 483.

89. PERRY, R.L., MOLLENHAUER, H.H. & BOWEN, H.H. (1974). Electron photomicroscopy verification of Pierce's disease on grape plants from Texas. Plant Disease Reporter 58, 780 - 782.

90. PETZOLD, H., MARWITZ, R. & KUNZE, L. (1973). Elektronenmikroskopische Untersuchungen über intrazelluläre rickettsienähnliche Bakterien in triebsucht kranken Äpfeln. Phytopathologische Zeitschrift 78, 170 - 181.

91. PINE, T.S., GROGAN, R.G. & HEWITT, W.B. (1955). Pathological anatomy of bacterial canker of young tomato plants. Phytopathology 45, 267 - 271.

92. RAI, P.V. & STROBEL, G.A. (1967). Phytotoxins of Corynebacterium. Phytopathology 57, 1008 (Abstr.).

93. RAI, P.V. & STROBEL, G.A. (1969). Phytotoxic glycopeptides produced by Corynebacterium michiganense. I. Methods of preparation, physical and chemical characterization. Phytopathology 59, 47 - 52.

94. RAI, P.V. & STROBEL, G.A. (1969). Phytotoxic glycopeptides produced by Corynebacterium michiganense. II. Biological properties. Phytopathology 59, 53 - 57.

95. REYNOLDS, E.S. (1963). The use of lead citrate at high pH as an electron-opaque stain in electron microscopy. Journal of Cell Biology 17, 208 - 213.

96. RIES, S.M. (1971). Chemical and biological properties of a phytotoxic glycopeptide from Corynebacterium insidiosum. Ph.D. Thesis Montana State University, Bozeman. Dissertation Abstracts 32, 657-B.

97. ROTH, I. (1961). Physiological aspects of injury caused by Xanthomonas campestris in vascular tissue. Bulletin of the Research Council of Israel 10, 271 - 274.

98. ROTHWELL, A. (1971). Bacterial canker of tomato caused by Corynebacterium michiganense (Smith) Jensen. Rhodesia Agricultural Journal 68, 75 - 78.

99. SEQUEIRA, L. (1964). Origin of indoleacetic acid in tobacco plants infected by Pseudomonas solanacearum. Phytopathology 54, 907 (Abstr.).

100. SEQUEIRA, L. (1965). Origin of indoleacetic acid in tobacco plants infected by Pseudomonas solanacearum. Phytopathology 55, 1232 - 1236.

101. SEQUEIRA, L. (1973). Hormone metabolism in diseased plants. Annual Review of Plant Physiology 24, 353 - 380.

102. SEQUEIRA, L. & KELMAN, A. (1962). The accumulation of growth substances in plants infected by Pseudomonas solanacearum. Phytopathology 52, 439 - 448.

103. SIGEE, D.C. & EPTON, H.A.S. (1975). Ultrastructure of Pseudomonas phaseolicola in resistant and susceptible leaves of French bean. Physiological Plant Pathology 6, 29 - 34.

104. SMITH, E.F. (1910). A new tomato disease of economic importance. Science 31, 794 - 796.

105. SMITH, E.F. (1911). Black rot of cruciferous plants. In Bacteria in Relation to Plant Diseases, Vol. 2, pp. 300 - 334. Carnegie Institute, Washington, D.C.

106. SMITH, E.F. (1914). The Grand Rapids Tomato Disease - Aplanobacter michiganense E.F.S. In Bacteria in Relation to Plant Diseases, Vol. 3, pp. 161 - 165. Carnegie Institute, Washington, D.C.

107. SMITH, E.F. (1914). Brown rot of Solanaceae, In Bacteria in Relation to Plant Diseases, Vol. 3, pp.174 - 219. Carnegie Institute, Washington, D.C.

108. SMITH, W.K. (1958). A survey of the production of pectic enzymes by plant pathogenic and other bacteria. Journal of General Microbiology 18, 33 - 41.

109. SPENCER, J.F.T. & GORIN, P.A. (1961). The occurrence in the host plant of physiologically active gums produced by Corynebacterium insidiosum and Corynebacterium sepedonicum. Canadian Journal of Microbiology 7, 185 - 188.

110. STAPP, C. (1965). Die Bakterielle Schleimfäule und ihr Erreger Pseudomonas solanacearum. Zentralblatt für Bakteriologie Parasitenkunde infektionskrankheiten und Hygiene 119, 166 - 190.

111. STARR, M.P. (1959). Bacteria as plant pathogens. Annual Review of Microbiology 13, 211 - 238.

112. STAUB, T. & WILLIAMS, P.H. (1972). Factors influencing black rot lesion development in resistant and susceptible cabbage. Phytopathology 62, 722 - 728.

113. STAUB, T. & WILLIAMS, P.H. (1972). Fluorescing materials associated with vein blackening and necrosis in leaves of black rot-resistant cabbage. Phytopathology 62, 858 - 865.

114. STRIDER, D.L. (1969). Bacterial canker of tomato caused by Corynebacterium michiganense - A literature review and bibliography. North Carolina Agricultural Experiment Station Technical Bulletin, No. 193. 110pp.

115. STRIDER, D.L. (1970). Tomato seedling inoculations with Corynebacterium michiganense. Plant Disease Reporter 54, 36 - 39.

116. STROBEL, G.A. (1967). Purification and properties of a phytotoxic polysaccharide produced by Corynebacterium sepedonicum. Plant Physiology 42, 1433 - 1441.

117. STROBEL, G.A. (1971). The biological activity of phytotoxic bacterial glycopeptides pp.69-70. In Proceedings of the Third International Conference on Plant Pathogenic Bacteria. ed. H.P. Maas Geesteranus Wageningen, 1972.

118. STROBEL, G.A. & HESS, W.M. (1968). Biological activity of a phytotoxic glycopeptide produced by Corynebacterium sepedonicum. Plant Physiology 43, 1673 - 1688.

119. STROBEL, G.A., TALMADGE, K.W. & ALBERSHEIM, P. (1972). Observations on the structure of the phytotoxic glycopeptide of Corynebacterium sepedonicum. Biochemica et Biophysica Acta 261, 365 - 374.

120. SUTTON, J.C. & WILLIAMS, P.H. (1970). Relation of xylem plugging to black rot lesion development in cabbage. Canadian Journal of Botany 48, 391 - 401.

121. SUTTON, J.C. & WILLIAMS, P.H. (1970). Comparison of extracellular polysaccharides of Xanthomonas campestris from culture and from infected cabbage leaves. Canadian Journal of Botany 48, 645 - 651.

122. WAINWRIGHT, S.H. & NELSON, P.E. (1972). Histopathology of Pelargonium species infected with Xanthomonas pelargonii. Phytopathology 62, 1337 - 1347.

123. WALKER, J.C. & KENDRICK, J.B. (1948). Plant nutrition in relation to disease development. IV. Bacterial canker of tomato. American Journal of Botany 35, 186 - 192.

124. WELLHAUSEN, E.J. (1938). Infection of maize with Phytomonas flaccumfaciens, P. insidiosa, P. michiganensis, P. campestris, P. panici and P. striafaciens. Phytopathology 28, 475 - 482.

125. WILSON, E.E. & MAGIE, A.R. (1964). Systemic invasion of the host plant by the tumor-inducing bacterium, Pseudomonas savastanoi. Phytopathology 54, 576 - 579.

126. WINDSOR, I.M. & BLACK, L.M. (1973). Evidence that Clover Club Leaf is caused by a Rickettsia-like organism. Phytopathology 63, 1139 - 1148.

127. WORLEY, J.F. & GILLASPIE, A.G. Jr. (1975). Electron microscopy *in situ* of the bacterium associated with ratoon stunting disease in Sudangrass. *Phytopathology* 65, 287 - 295.

128. ZAUMEYER, W.J.(1932). Comparative pathological histology of three bacterial diseases of bean. *Journal of Agricultural Research* 44, 605 - 632.

129. ZOLLER, B.G. & KOSUGE, T. (1972). Effect of soil amendments on the generation time of *Xanthomonas campestris* in cabbage guttation fluid and on lesion development in the host. *Phytopathology* 62, 800 (Abstr.).